

Organic Bioelectronics: Using Highly Conjugated Polymers to Interface with Biomolecules, Cells, and Tissues in the Human Body

Stuart G. Higgins,* Alessandra Lo Fiego, Ijeoma Patrick, Adam Creamer, and Molly M. Stevens*

Conjugated polymers exhibit interesting material and optoelectronic properties that make them well-suited to the development of biointerfaces. Their biologically relevant mechanical characteristics, ability to be chemically modified, and mixed electronic and ionic charge transport are captured within the diverse field of organic bioelectronics. Conjugated polymers are used in a wide range of device architectures, and cell and tissue scaffolds. These devices enable biosensing of many biomolecules, such as metabolites, nucleic acids, and more. Devices can be used to both stimulate and sense the behavior of cells and tissues. Similarly, tissue interfaces permit interaction with complex organs, aiding both fundamental biological understanding and providing new opportunities for stimulating regenerative behaviors and bioelectronic based therapeutics. Applications of these materials are broad, and much continues to be uncovered about their fundamental properties. This report covers the current understanding of the fundamentals of conjugated polymer biointerfaces and their interactions with biomolecules, cells, and tissues in the human body. An overview of current materials and devices is presented, along with highlighted major *in vivo* and *in vitro* applications. Finally, open research questions and opportunities are discussed.

charge carriers such as electrons, holes or ions. Scientists have been building these interfaces for hundreds of years, since Galvani's early experiments with frog legs.^[1] In the past three decades a wide range of organic materials have been found to conduct charge carriers in a manner similar to metals or inorganic semiconductors (e.g., silicon). Highly conjugated polymers are one such class of materials. Overlapping π - π molecular orbitals found within these polymers combine to facilitate the movement of charge carriers, enabling the fabrication of electrical devices such as electrodes and transistors. Unlike their inorganic counterparts, the disordered nature of these polymeric systems, mediated by weak van der Waals and electrostatic interactions, mean they are highly sensitive to material morphology, and their local electrostatic and chemical environment. By virtue of these electrical properties, conjugated polymers have attracted attention as a transduction material for biosensing both inside and outside of the human body.

Similarly, their desirable mechanical and chemical properties, which can be easily modified using organic chemistry, have led researchers to investigate their use as tissue and cell scaffolds. Here, we discuss recent developments using conjugated polymers as bioelectronic interfaces both *in vivo* and *in vitro*, before summarizing the current research challenges.


1. Introduction

1.1. Overview

Bioelectronic interfaces are devices that sense and stimulate biological systems (cells, tissue, organs) using materials that have charge transport properties, as a result of the movement of

Dr. S. G. Higgins, A. Lo Fiego, I. Patrick, Dr. A. Creamer, Prof. M. M. Stevens
Department of Bioengineering
Imperial College London
London SW7 2AZ, UK
E-mail: stuart.higgins@imperial.ac.uk; m.stevens@imperial.ac.uk

Dr. S. G. Higgins, A. Lo Fiego, I. Patrick, Dr. A. Creamer, Prof. M. M. Stevens
Department of Materials
Imperial College London
London SW7 2AZ, UK

 The ORCID identification number(s) for the author(s) of this article can be found under <https://doi.org/10.1002/admt.202000384>.

Dr. S. G. Higgins, A. Lo Fiego, I. Patrick, Dr. A. Creamer, Prof. M. M. Stevens
Institute of Biomedical Engineering
Imperial College London
London SW7 2AZ, UK

A. Lo Fiego
Centre for Neurotechnology
Imperial College London
London SW7 2AZ, UK

I. Patrick
Centre for Processable Electronics
Imperial College London
London SW7 2AZ, UK

DOI: 10.1002/admt.202000384

Conjugated polymers as bioelectronic interfaces

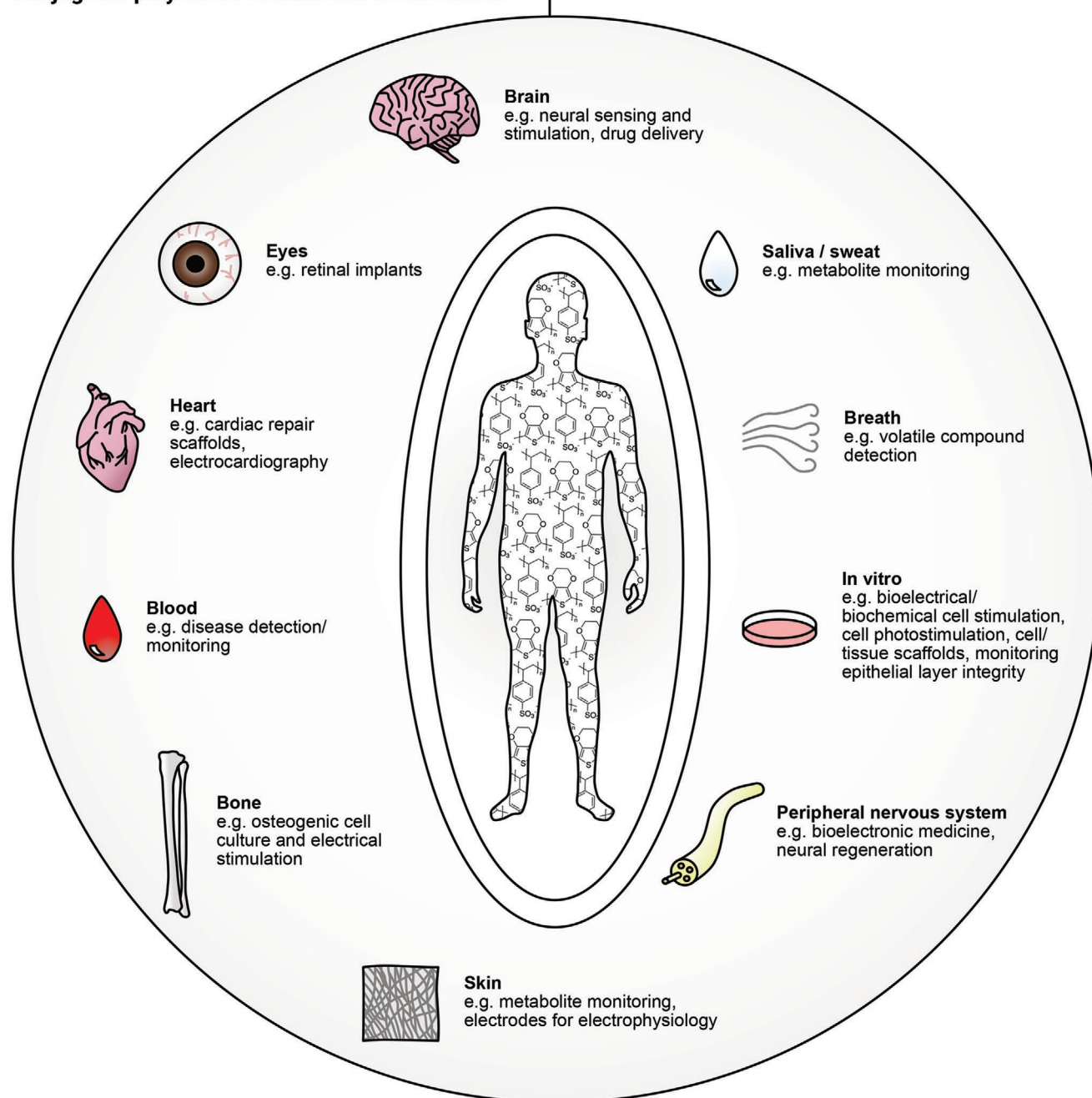


Figure 1. Applications of conjugated polymers as organic bioelectronic interfaces with the human body.

Figure 1 illustrates where highly conjugated polymers are being used for interfacing different aspects of human physiology. These applications broadly range from in vivo (sensing and stimulating specific cells, tissues, and organs) to in vitro applications (biosensing of analytes in liquid biopsies and modeling human physiology in cell culture). Comparatively few devices have been tested in vivo in humans, reflecting the current state of the material and device development,^[2] as well as the regulatory framework surrounding medical devices, hence we highlight the most relevant examples here.

This report focuses mostly on developments from roughly the past five years, with reference to prior seminal works or reviews as appropriate. It is written for readers who wish to see a broad overview of the ways conjugated polymers are being used to interface with the human body, with enough relevant theory to allow them to engage with the arguments and results presented. Where more specific reviews for a given topic exist, we have signposted them in the appropriate locations. We focus exclusively on interfaces that use highly conjugated polymers to interface an aspect of human physiology, where the polymer's

primary proposed use relies on its electronic properties. For example, we do not discuss organic small molecule devices, conjugated polymer nanoparticles for imaging or optical biosensing,^[3–5] biomimicking neuromorphic designs,^[6–8] hydrogen-bond mediated bioprotonics,^[9–11] or polymers for nonelectronic/ionic driven drug delivery.^[12] We also include a brief discussion of the origin of bioelectricity itself, as this is fundamental to the motivation and application of many organic bioelectronic interfaces.

1.2. Summary of Motivations

Researchers are motivated to use conjugated polymers due to the combination of their intrinsic and extrinsic material properties. Conjugated polymers can be sensitive to both electronic and ionic-based charge carriers.^[13,14] This makes them inherently well-suited to developing devices that transduce the ion-based signals of biological organisms into the electronic signals used by the majority of modern measurement and stimulation devices. This is an advantage over metals and inorganic semiconductors, which are generally impermeable to ions.^[15] Devices fabricated from conjugated polymers can often be controlled with high precision using voltage gradients and/or electronic current injection. For example, precise changes in electrical current can result in the delivery of correspondingly precise quantities of drugs from polymer devices.^[16] The semiconducting properties of some conjugated polymers make them well suited to building devices such as transistors, which can act as amplifiers, transducing small voltage changes into large changes in current.^[17,18]

Conjugated polymers can be chemically altered to tailor material properties, for example, from hydrophobic to hydrophilic.^[19] Decades of research has helped develop structure–property relationships between the polymer molecular structure and its optoelectronic properties.^[20–23] Insoluble conjugated polymer backbones can be modified with hydrophilic sidechains, which allow the formation of semiconducting and conducting inks, facilitating solution-processing fabrication techniques.^[24,25]

Thin films or engineered scaffolds of highly conjugated polymers can be tailored to have similar mechanical moduli to biological tissue.^[26] In vivo, the mechanical mismatch between the implanted device and local tissues can result in the formation of a foreign-body response, where the body effectively tries to isolate and exclude the implanted device through an inflammatory response.^[27,28] This can often result in the formation of scar tissue around devices which effectively insulate them from the biological system.^[29] At a cellular level, cells directly sense the mechanical nature of their microenvironment through complex mechanotransduction machinery.^[30] Minor changes in material stiffness or surface properties can result in profound changes in cellular phenotype.^[31] Hence, the ability to tune these properties is important for cell sensing and cell stimulating applications. Conjugated polymers, modifiable both intrinsically through chemical synthesis and extrinsically through subsequent material processing, are well-suited to the development of cell and tissue stimulating interfaces.

A wide-range of manufacturing techniques can be used to process conjugated polymers into devices, ranging from

cleanroom-based manufacture, to desktop printing technologies, and more.^[32] The ability to rapidly upscale devices made from conjugated polymers using graphic arts technologies such as gravure or inkjet printing has long been a key motivation for their use.^[24,25,33] These manufacturing approaches lend themselves well to the production of affordable, electronic, point-of-care diagnostic tests, that fulfil the requirements set out by the diagnostics research community.^[34,35]

Conjugated polymers are not only patternable in 2D, but also via 3D printing methods.^[36] Highly conjugated polymers can be patterned onto flexible plastics, glass, paper,^[37,38] or incorporated directly into composite gel systems.^[39] They can be drawn into fibers, nanofibers, or used to coat existing fibers which can subsequently be woven into organic electronic fabrics.^[40–42] The variety of intrinsically weak bonding interactions present between adjacent polymer chains can be harnessed through a variety of approaches to form “self-healing” systems,^[43,44] namely where a previously cut or damaged material can reform their initial network.

2. Fundamental Mechanisms

2.1. Bioelectricity in Living Organisms

2.1.1. Bioelectricity Originates from the Separation of Charge Carriers Across Membranes

Bioelectricity refers to the presence of potential gradients (voltages) and the movement of charge carriers (the flow of current) within living organisms. These endogenous electric fields exist at the organelle, cellular, tissue, and organism level (**Figure 2**).^[47] They originate from charge carrier gradients, established by the diffusion or active transport of charge across membranes. This transport is mediated by a range of structures including ion channels, ion pumps, gap junctions, and specialized receptor/transporter molecules.^[48] The machinery that regulates the movement of charged species is itself regulated by the potential gradient. For example, the opening of voltage-gated calcium channels, allows the influx of calcium ions, which in turn activate calcium sensing molecules such as calcineurin, a protein phosphatase capable of activating transcription factors. The emergent behavior of this nonlinear feedback system is complex and still being understood.^[49,50] For the interested, we recommend a number of reviews for a more in-depth discussion of the current state of understanding of these mechanisms.^[48,51,52]

In addition to fundamental bioelectronic gradients, there are specialized classes of electrically excitable (also referred to as electrogenic) cells, which are capable of rapidly manipulating ionic gradients across their membranes to facilitate signal transmission. Changes in the adjacent local ionic environment result in a significant depolarization of an excitable cell (i.e., the interior of the cell loses negative charge). This can trigger a cascade of voltage-gated ion channels to open, resulting in a wave of changing membrane potential that propagates rapidly along the cell body.

Measuring single cell membrane potentials remains a challenging task. The gold standard in electrophysiology is the

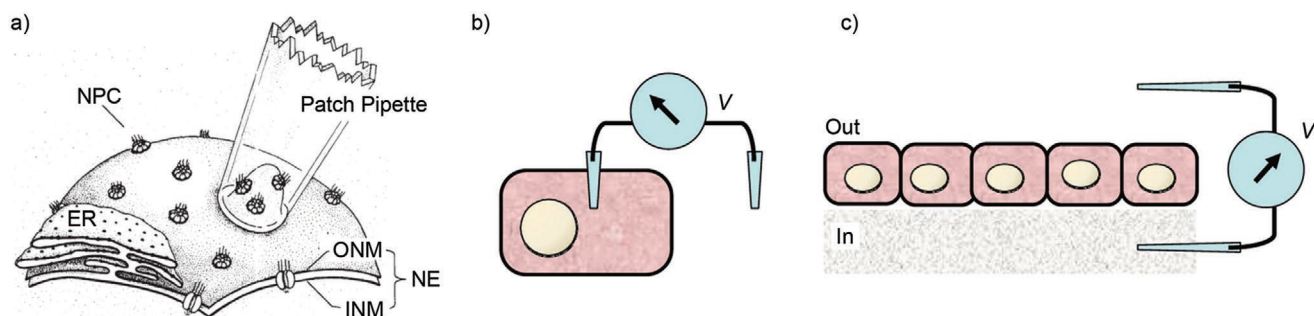


Figure 2. Endogenous bioelectric gradients occur on different length scales within living organisms. a) Potentials occur across the nuclear envelope (NE). Illustration shows measurement using patch clamp technique, nuclear pore complexes (NPC), endoplasmic reticulum (ER), outer nuclear membrane (ONM), and inner nuclear membrane (INM). Adapted with permission.^[45] Copyright 2013, John Wiley & Sons. b) Potentials occur across the cell membrane. c) Transepithelial potentials occur across epithelial layers. (b,c) Reproduced with permission.^[46] Copyright 2012, Elsevier.

patch clamp technique,^[53] which involves introducing an electrolyte-filled micropipette into the cell membrane (Figure 2a). While attempts have been made to incorporate conjugated polymers into micropipettes for biochemical sensing,^[54] the majority of organic bioelectronic biointerfaces are currently only capable of stimulating single cells, with the patch clamp approach used to monitor single cell membrane potentials.^[55–57] The sensing biointerfaces reported here typically measure the superposition of many simultaneously changing cell potentials. This includes transepithelial (or transendothelial) potentials (e.g., used to sense the integrity of cell layers),^[58,59] or organ level potentials (e.g., for monitoring cardiac or neuronal electrophysiology).^[60,61]

2.1.2. Bioelectricity Influences Cell and Tissue Development and Regeneration

Bioelectronic gradients play a key role in regulating the development of tissues and organs.^[51,62] The resting membrane potential of cells has been linked to their potency (a measure of the ability of a cell to differentiate into different cell types). Some stem-like cells show greater polarization of their resting membrane potential than highly differentiated cell types.^[48] Cell membrane potential has also been linked to cell cycle stage, with mitotic cells more depolarized than nondividing, quiescent cells.^[63] Manipulating the bioelectronic environment can result in profound changes in cell, tissue, and organ behavior post-transcription, that is distinct from the underlying genomic or transcriptomic states.^[48,64] This is seen to be particularly valuable in the fields of regenerative medicine, where there is scope for more localized interventions that promote healing behaviors.

Bioelectronic gradients are observed in wound sites. Damage to cells comprising an epithelial layer allows ions to move freely across an otherwise tightly regulated barrier, resulting in a local reduction in potential at the wound site relative to undamaged regions (Figure 3).^[52] Much remains unknown, but the resulting potentials and current flows appear to be actively regulated. Different cell types can migrate along electric fields (referred to as galvanotaxis or electrotaxis), contributing to the wound healing process.^[51,52,66] Within the field of regenerative medicine, there are multiple approaches to electrical

stimulation. These methods have been used to heal bone fractures (Figure 4),^[67,68] induce regenerative healing responses,^[69] and have been proposed for a range of other applications.^[47] Ultimately, the complexity and influence of bioelectric signals is a major motivation for developing better bioelectronic interfaces.

2.1.3. Charge Transport in Conjugated Polymers

2.1.4. Charge Transport in Conjugated Polymers Originates from Overlapping π -Orbitals

Conjugated polymers consist of an extended π -molecular orbital network along the polymer backbone. This is made possible by hybridization of S and P orbitals (forming sp hybrids), resulting in unhybridized p_z orbitals above and below the plane of the polymer. These orbitals can then overlap, forming an extended π -bonding network of occupied and unoccupied states (bonding and antibonding, respectively). Increasing the extent of conjugation typically increases the number of available states.^[70] A π -conjugated system contains many of these molecular orbitals, creating a range of allowed energy states for electrons (Figure 5).

For a polymer such as polyacetylene (which comprises a backbone of alternating carbon–carbon single and double bonds),

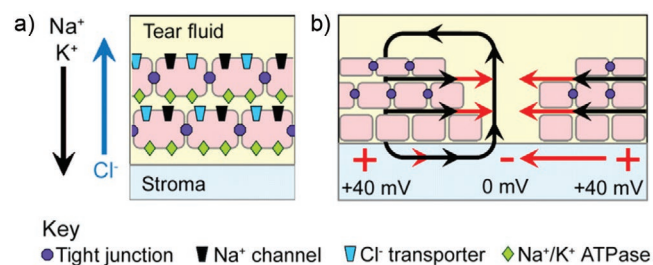


Figure 3. Formation of electric field gradients at wound sites. Example shown is for a mammalian epithelium model. a) Normally tight junctions between cells restrict the movement of ions and ion transporting channels. b) Disruption of the epithelium results in the formation of electric field gradient and the movement of ions oriented toward the wound. Adapted with permission.^[65] Copyright 2009, The Company of Biologists Ltd.

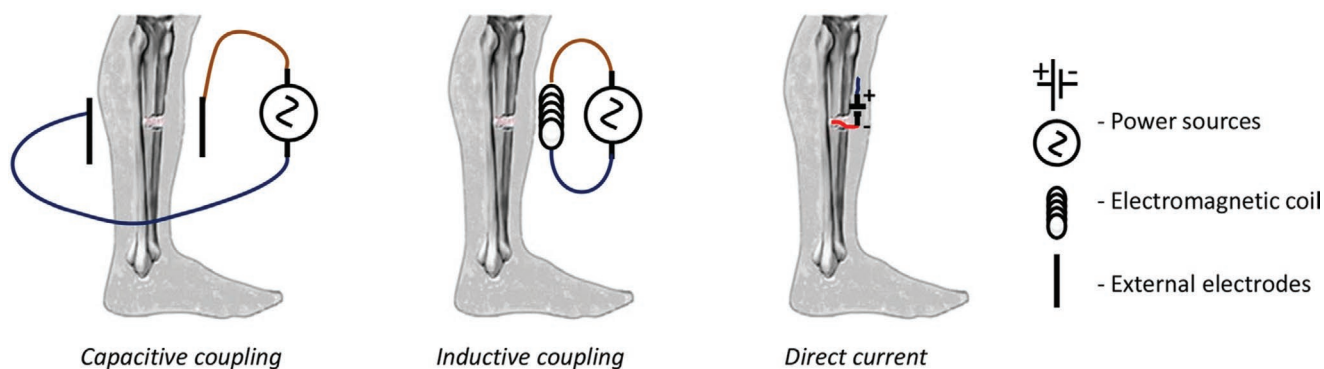


Figure 4. Summary of clinically used electrical stimulation devices for bone healing, based on capacitive coupling, inductive coupling, or direct current injection. Reproduced under the terms of CC-BY 4.0 license.^[68] Copyright 2020, The Authors, published by Springer Nature.

the high degree of π -conjugation creates a near-continuum of permitted electron states. Due to fundamental electronic instabilities (an effect known as Peierls distortion) the continuum of electronic states is separated by a region of forbidden energy states (a bandgap). The permitted states on either side of this

bandgap are referred to as the highest-occupied molecular orbital (HOMO) or lowest-occupied molecular orbital (LUMO). The formation of these permitted states, and the transition of electrons between them, are why conjugated polymers have interesting optical and electrical properties.^[71]

Overlapping π -orbitals give conjugated polymers semiconducting properties

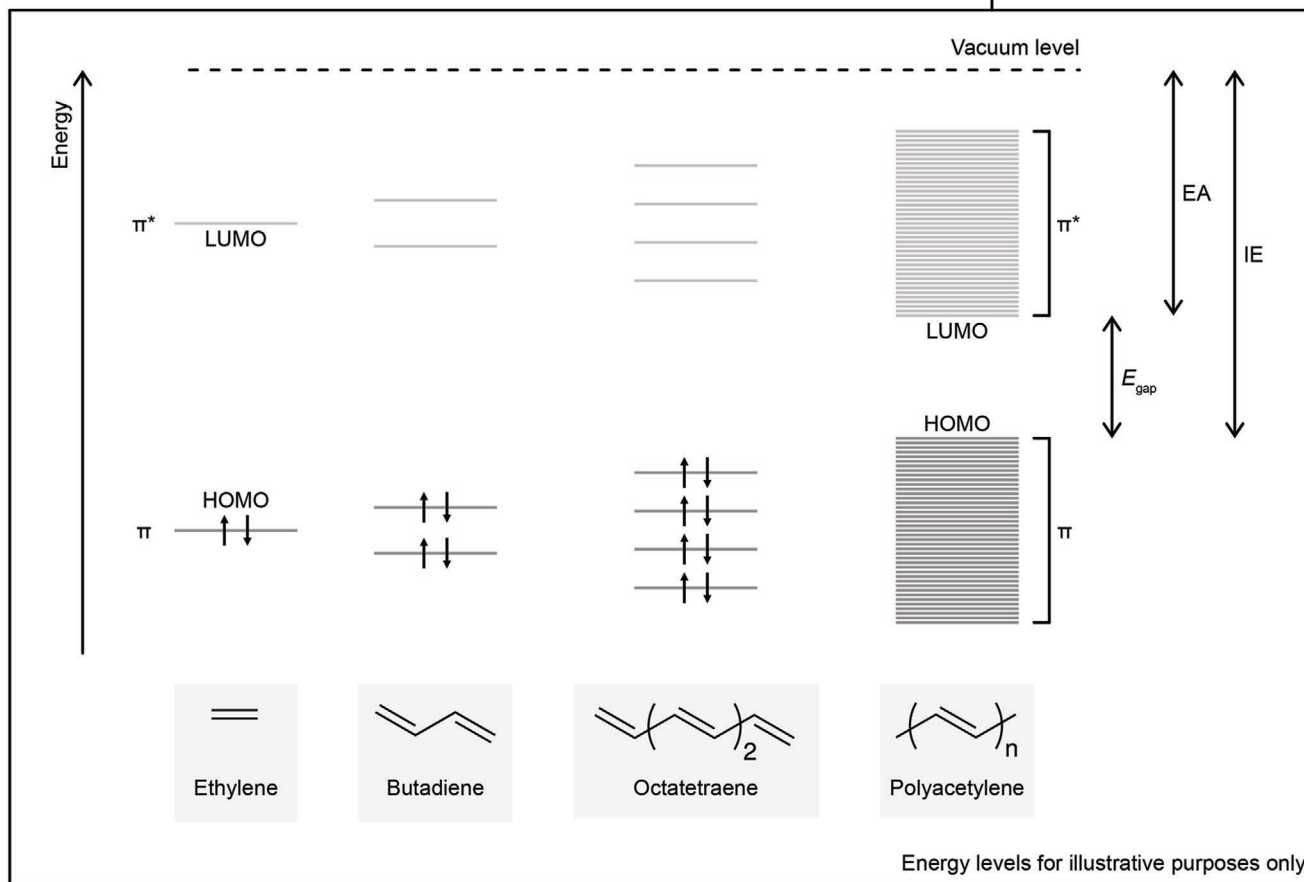


Figure 5. Increasing polymer repeat units increases the overlap of consecutive molecular orbitals, resulting in a larger number of available electron energy states.^[72,73] In an ideal conjugated polymer, this results in the formation of two continua of states (in real materials structural and energetic disorder disrupts this idealized behavior).^[74] Arrows on states indicate population of electrons in spin up (\uparrow) and spin down states (\downarrow) (not shown for the HOMO of polyacetylene for the sake of clarity). Key optoelectronic figures of merit, including the electron affinity (EA), ionization energy (IE), and bandgap (E_{gap}) are indicated. Note: energy levels are for illustrative purposes only, and do not accurately represent the energetic states of the molecules.

Electrons reside in the HOMO, but under certain circumstances can be introduced into the LUMO. Once in the LUMO, electrons can move through delocalized regions of the polymer or “hop” to another delocalized region on an adjacent polymer chain. This behavior facilitates charge transport through the material.^[75] Depending on the molecular structure of the polymer and how it has been processed, it may not be the movement of a specific electron per se that acts as the charge carrier. Instead, it may be an absence of charge referred to as a hole. A hole is not a real particle but can be mathematically and conceptually treated as a positive charge carrier.^[76] Hence, the movement of holes through a material will also establish a flow of electrical current. Conjugated polymers in which electrons are the dominant charge carrier are referred to as n-type semiconductors, those with hole dominant transport are referred to as p-type. Some polymers show mixed p- and n-type conductivity and are referred to as ambipolar. Most reported conjugated polymers are p-type semiconductors, in part due to the energy levels for electron (vs hole) transport relative to charge traps within the material.^[77] Charge traps strongly influence material behavior, as there is evidence to suggest all semiconducting conjugated polymers are intrinsically ambipolar, but under normal material processing conditions charge trapping prevents n-type transport.^[78]

2.1.5. Conjugated Polymers Require Doping to Become Conducting Polymers

In their idealized pristine form, conjugated polymers effectively behave as semiconductors.^[70,79] For example, pure poly(3,4-ethylenedioxythiophene) (PEDOT) is a semiconductor.^[80,81] Different mechanisms increase the free charge carrier density and hence conductivity. Charge carriers can be generated optically, as happens in organic photodiodes or organic photovoltaic devices.^[82] They can be injected into the film under the influence of an externally applied electric field, as seen in organic field-effect transistors.^[17] In most reported bioelectronic interfaces chemical or electrochemical doping methods are used.^[71,83,84] Doping refers to the addition or removal of electrons from a semiconductor to change the free charge carrier density. In this context, it is often used interchangeably by those with a chemistry background with the terms oxidation and reduction. Chemical doping includes approaches such as the vapor deposition of highly electron accepting molecules onto a polymer film that acts to p-type dope (or oxidize) the polymer backbone.^[85] Electrochemical doping is found in electrochemical transistors, where an electrode connected to the polymer film is used to inject or remove charge. The displaced charges are compensated by the ingress of counterions from an electrolyte also in contact with the polymer.^[71,80] Conjugated polymers that can be highly doped to form stable materials are referred to as conducting polymers, with the increase in charge carriers giving some polymers metal-like conductivities.^[83,86,87]

While doping is understood to be responsible for achieving high conductivities, considerable research efforts continue to be devoted to understanding the charge transport mechanisms of pristine and doped systems.^[83,84,88,89] The presence of both ionic and electronic currents in conjugated polymer–polyelectrolyte systems further complicates interpretation, with many ongoing

attempts to accurately model this behavior.^[89–92] Tybrandt et al. recently proposed a two-phase model based on drift-diffusion equations.^[89] They argue that doping in conjugated polymer–polyelectrolyte systems should be considered as a combination of separate electronic and ionic charge carrier processes, and not as a redox process as often described in the literature. Further complicating matters, morphological and energetic disorder, along with chemical contaminants, can cause the formation of charge trap states within conjugated polymer films.^[93,94] Disorder and charge trapping can significantly impact the effective material conductivity,^[23,73,93,95,96] making it challenging to analytically model electronic device behavior and fabricate functionally identical devices. Adding a variety of additives has been shown to partly overcome some of these limitations in both electrochemical,^[97] and field-effect devices.^[98] However, the complexity of competing mechanisms, plus an incomplete theoretical understanding, often means that devices based on the same underlying polymer show vastly different charge transport characteristics depending on their synthesis, processing, and operating conditions.^[73,95]

2.2. Interactions between Conjugated Polymers and Biological Systems

2.2.1. Electrostatic and Electrochemical Interactions of Biomolecules with Conjugated Polymers Permit the Transduction of Binding Events

Biomolecules such as metabolites, nucleic acids, and proteins can interact with conjugated polymers through electrostatic and electrochemical mechanisms. In a device such as an electrolyte-gated organic field-effect transistor (EGOFET), the biomolecule effectively alters the strength of the electric field that is responsible for injecting electrical charge into the conjugated polymer. Modulating the amount of charge present in the film modulates the amount of current that can flow, resulting in a transduction of the biomolecule binding event into a change in electrical current.^[99,100]

While biorecognition elements can be incorporated directly into polymer sidechains,^[38,101] they are challenging to conjugate without overly disrupting the underlying charge transport.^[102] Instead, they are often conjugated either to an intermediate coating or layer,^[103,104] or to metal electrodes that form part of the device.^[99,105,106] Depending on the application, biorecognition elements can include antibodies,^[107–109] nucleic acid sequences,^[110,111] and enzymes.^[112–114]

Biosensors can also take advantage of biochemical reactions, as is often seen in organic electrochemical transistors (OECTs).^[100] In enzyme-based electrochemical approaches, a target biomolecule may interact with an enzyme immobilized to the surface of a conjugated polymer (or electrically connected electrode). A common example is glucose oxidase (an enzyme that catalyzes the oxidation of glucose), which can be immobilized directly onto conjugated polymer films.^[112] Different charge transport mechanisms exist, but in the simplest form hydrogen peroxide is produced by the reaction, which is subsequently detected when reduced at a polymer/electrode surface. More recent approaches aim to improve

the detection performance by incorporating a chain of redox couples between the glucose oxidase and the electrode to mitigate the diffusion of hydrogen peroxide away from the sensor surface.^[115]

There are many other permutations of device operation and much remains to be understood about the underlying device physics.^[116–118] For an in depth and quantitative discussion of these electrostatic and electrochemical mechanisms, see the recent reviews from Torsi and colleagues.^[100,102]

2.2.2. Conjugated Polymer Coated Surfaces Can Influence Cell Interactions

Cell–material interactions depend strongly on material surface topography, mechanical properties, surface chemistry, and the presence or absence of other biomolecules.^[30,119] The process of cell adhesion is mediated initially by weakly acting physisorption and chemisorption processes,^[120] and ultimately by transmembrane proteins, referred to collectively as cell adhesion molecules.^[121,122] In vivo, cells may bind either to each other or to the extracellular matrix, a complex mixture of molecules secreted by cells. Cells can form similar bonds with conjugated polymers if the material has sufficient equivalent binding sites. However, even in the absence of these sites, the spontaneous physisorption of proteins to a material surface from the supporting cell media, or the secretion of extracellular matrix by cells can indirectly facilitate cell binding. Hence, relying on the surface energy of a given polymer surface as a proxy for cell attachment may be misleading.^[120] If a cell can bind, the relative stiffness of the material impacts the degree of force transmitted from outside to inside the cell via its cytoskeleton, influencing fundamental cell behaviors such as gene expression, motility, and differentiation.^[123]

Strategies for promoting cell adhesion to conjugated polymers include incorporating bioactive ligands,^[124] such as peptide mimicking sequences,^[125–127] or lysines,^[128] into sidechains. Other approaches include tailoring the polymer backbone or sidechains to alter the hydrophobic/hydrophilic nature of the polymer surface,^[129] patterning extracellular proteins onto the polymer surface,^[31,130,131] or using physical gas and vapor deposition techniques to add electronegative species such as fluorine.^[132] When working with extracellular matrix proteins, layer thickness, and proteolytic degradation may present additional challenges.^[126] For more comprehensive reviews of cell–polymer adhesion, see the reviews of Hackett et al.,^[133] and Chen et al.^[120]

Modifying polymer sidechains or the surface of polymeric films is likely to alter polymer solubility or vary the degree of energetic disorder in the system, which in turn can affect charge transport. Tailoring biointerfaces is a juggling act within a wide parameter space. In the case of tissue scaffolds, where cells are grown in a 3D matrix of the conjugated polymer,^[59,134,135] the choice of processing (e.g., hydrogel, freeze-dried scaffold, etc.) influences the stiffness experienced by the cell which can impact cell proliferation and differentiation.^[136] All these effects are highly cell type dependent, so care must be taken to optimize for each given application.

The intimacy between cell and material can strongly dictate electronic sensing parameters such as signal-to-noise ratio.^[137] Minimizing the gap between cell and material reduces the amount of intermediate electrolyte helping to maximize the measured signal.^[72]

The oxidation state of some conjugated polymers has been shown to influence the proliferation and propagation of cells in culture,^[130,138–140] although some studies suggest this behavior is cell type dependent.^[141] Changes to the degree of polymer doping can also affect the surface chemistry of the polymer films. This change in surface energy can promote (or reverse) the physisorption of proteins from the cell culture media, which in turn affects cell adhesion.^[139,142,143] Amorini et al. recently proposed that films of an electropolymerized conjugated polymer act as “nanosponges.”^[57] Electrically induced changes to the oxidation state result in the influx or outflux of counterions from the cell media. This affects film swelling and the local ionic environment, triggering depolarization of the cell membrane. Interestingly, they noted that this effect was cell line dependent (**Figure 6**).

2.2.3. Care Must Be Taken to Minimize Foreign-Body Reactions in Conjugated Polymer–Tissue Interfaces

Conjugated polymers have been used both in vitro to promote the organization of cells into tissues,^[124] and in vivo to interface tissues in the body.^[60,145] Materials are effectively encoded with a multitude of stimuli thanks to their intrinsic and extrinsic properties.^[119] These stimuli can trigger inflammatory and foreign body responses within the body as it attempts to remove and encapsulate nonnative material (**Figure 7**).^[28] This is a major concern in biointerfaces such as neural implants, where encapsulation of the electrode can degrade interface performance and ultimately require the device to be surgically removed.^[144,146] While the material properties of conjugated polymers are nominally better-suited to mitigating this response, careful engineering is still required. For example, a conjugated polymer polymerized in rat hippocampi in vivo triggered an inflammatory response, causing a gradual reduction of electrode performance.^[147,148] Recently, interest has grown in incorporating conjugated polymers into hydrogels to overcome this challenge.^[149] Liu et al. compared the inflammatory response of a neural interfacing conjugated polymer hydrogel electrode, to that of a sham control and a more rigid plastic cuff electrode.^[39] They reported a relative reduction in inflammatory response, which they attributed to the lower Young’s modulus of their material system (**Figure 8**).

A general challenge facing conjugated polymer–tissue interfaces is the convolution of mechanical and electrical properties.^[59] For example, electrically stimulating a fibrous tissue scaffold coated with the conducting polymer mixture polypyrrole:DBS results in the influx and egress ions, causing a mechanical actuation.^[150] The cross-interaction of parameters often necessitates a more empirical approach to interpreting the interface behavior. While many reports have demonstrated conjugated polymers as tissue scaffold materials,^[151] much remains to be explored about their underlying mechanisms.

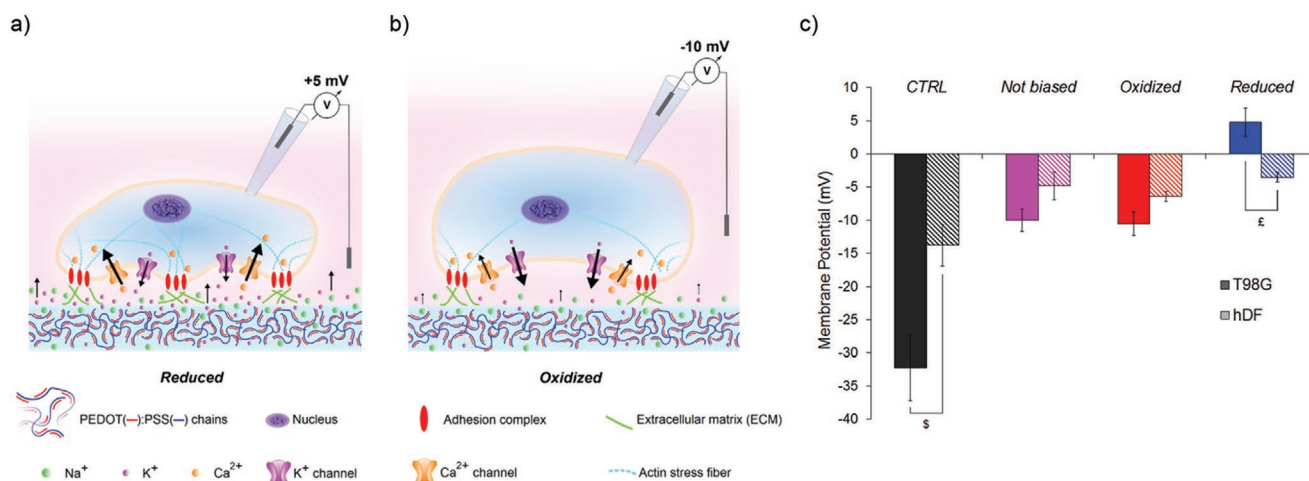


Figure 6. Proposed model for the movement of ions and cellular response for cells seeded upon PEDOT:PSS in a) reduced and b) oxidized states. c) Cell membrane potentials, as measured using a patch-clamp technique, for two different cell types as seeded on PEDOT:PSS under different oxidative states. Solid bars represent glioblastoma multiforme (T98G) cells, striped bars represent human dermal fibroblast (hDF) cells. Adapted with permission.^[57] Copyright 2017, American Chemical Society.

3. Materials

3.1. Overview of Conjugated Polymers used in Organic Bioelectronic Interfaces

Figure 9 and Table 1 summarize prevalent conjugated polymer structures used in organic biointerfaces. Often these polymers have multiple derivatives, including copolymer and/or sidechain variants.^[117,179–181] Polyacetylene is provided for reference as the prototype conjugate polymer; its low stability in ambient conditions has limited its adoption.^[182] Polyacetylene, polypyrrole, polyaniline, and PEDOT are typically used in a highly doped state, hence are often referred to as conducting polymers in the literature. PEDOT is rarely reported in isolation, instead the majority of reports use PEDOT with polystyrene sulfonate (PEDOT:PSS), which together form an intimately doped conductive colloidal dispersion. The polythiophene derivative poly(3-hexylthiophene)

(P3HT), along with a wide range of conjugated donor–acceptor copolymers,^[26,117,180] are typically referred to as semiconductors. However, the distinction is somewhat arbitrary, and many of these systems can be highly doped to achieve modest conductivity.^[183] For example, P3HT can be both solution-doped using chlorauric acid,^[184] or vapor-phase doped using strongly accepting materials such as 2,3,5,6-Tetrafluoro-7,7,8,8-tetracyanoquinodimethane (F4-TCNQ),^[185] to yield solid-state films with conductivities of around 70 and 50 S cm⁻¹, respectively (cf. PEDOT:PSS with maximum conductivities of >6000 S cm⁻¹ reported).^[186]

Few n-type conjugated polymer organic bioelectronic interfaces exist. Polymers based on the naphthalene-1,4,5,8-tetracarboxylic-diimide-bithiophene monomer unit have been demonstrated (Figure 9h), albeit with relatively low electron mobility. Researchers continue to optimize these systems, for example, Savva et al. recently found that blending an NDI-T2 based polymer with an intentionally poor solvent (acetone) and

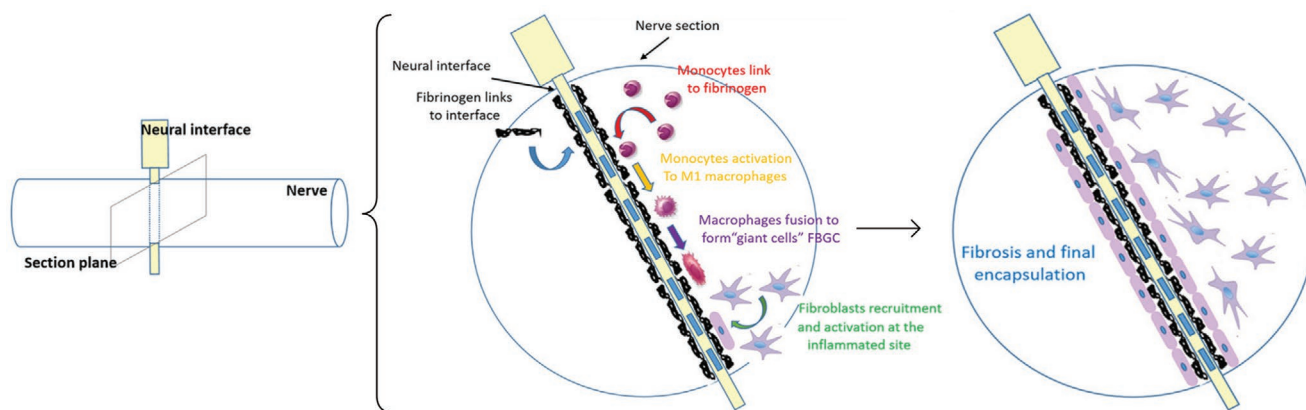


Figure 7. Implanted neural interfaces (along with other biomedical implants) can trigger a foreign body response, causing the recruitment of macrophages and the formation of glial scar cells that effectively encapsulate and insulate the implant. Adapted under the terms of CC-BY 4.0 license.^[144] Copyright 2017, Lotti, Ranieri, Vadalà, and Di Pino, published by Frontiers.

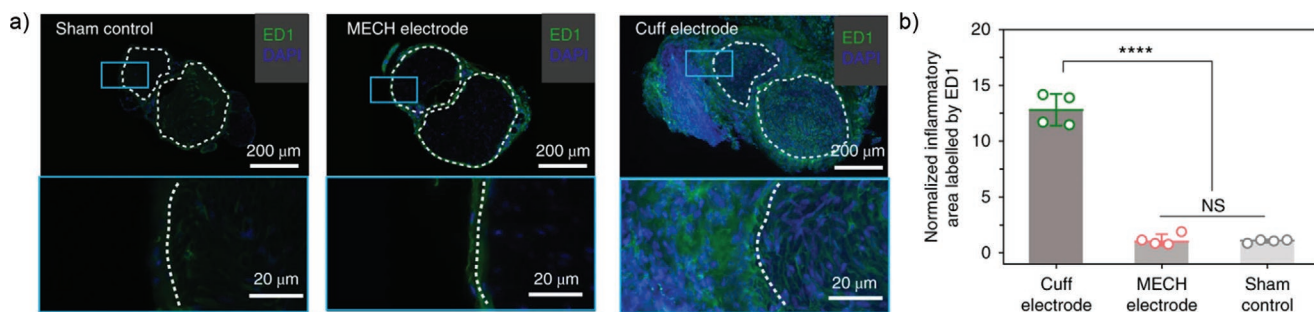


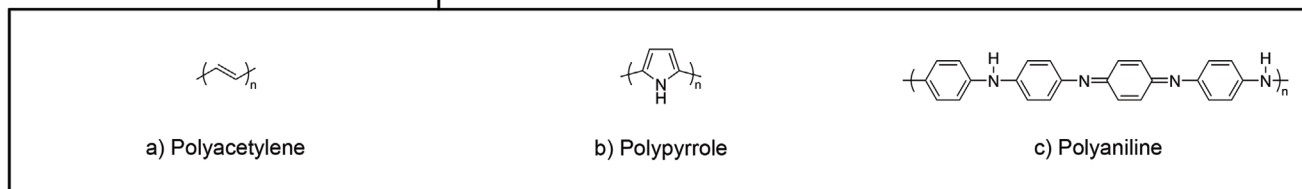
Figure 8. Comparison of the inflammatory response of an implanted PEDOT:PSS based conductive hydrogel (micropatterned electrically conductive hydrogel, MECH), as compared to a sham control and a cuff electrode (flexible polyethylene terephthalate with a thin film of gold). Devices were wrapped around the sciatic nerve of a mouse model for 6 weeks. a) Optical images of cross-section of sciatic nerve labeled for inflammatory biomarkers (ED1). Inset shows zoomed view of nerve bundle interface. b) Normalized inflammatory area for different treatment conditions. **** $P < 0.0001$, N.S. not significant. Adapted with permission.^[39] Copyright 2019, Springer Nature.

chloroform resulted in a threefold improvement in transconductance of OECTs and hence an improvement in glucose biosensing.^[187]

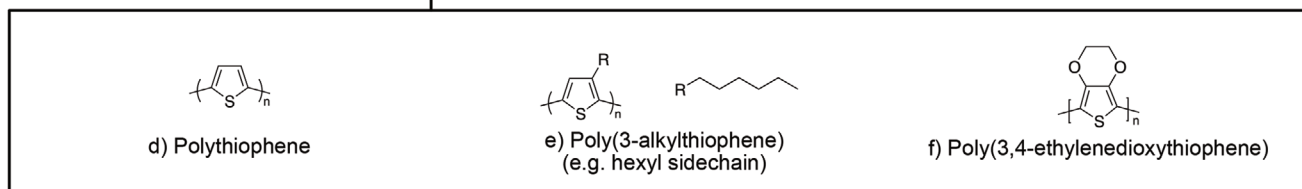
Glycolated thiophene-based polymers have attracted attention for improving the performance of OECTs.^[188–190]

Nielsen et al. varied the monomeric composition of homopolymer and copolymer backbones based on 2,2'-bithiophene (2T) and benzo[1,2-b:4,5-b']dithiophene (BDT) and observed large changes in material conductivities, as measured in an OECT configuration (Figure 10).^[188] Giovannitti et al. explored the

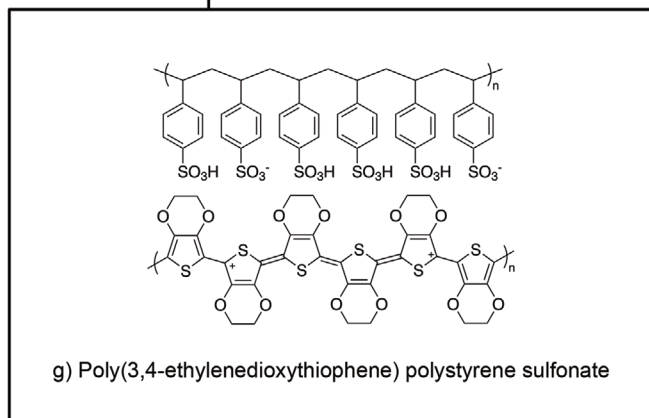
Exemplar conjugated polymers



Polythiophene and derivatives



PEDOT:PSS



n-type conjugated polymer

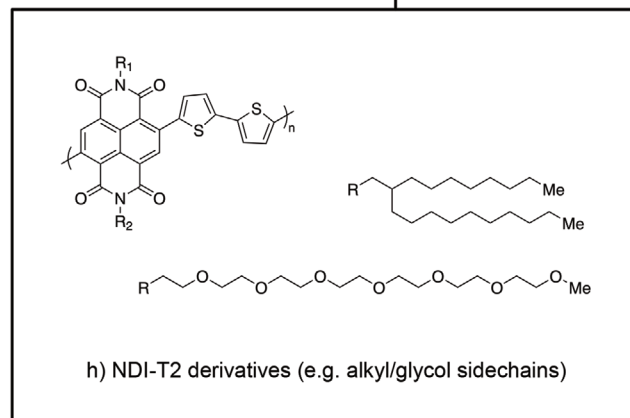


Figure 9. Overview of commonly used conjugated polymers for bioelectronic interfaces and reference structures. See Table 1 for corresponding polymer information. a–f) Structures redrawn from reference [70]; g) from reference [152]; h) from reference [153].

Table 1. Examples of conjugated polymers used (or proposed) as bioelectronic interface materials.

Figure notation	Acronym	Full name	Application
a)	PA	Polyacetylene	See note ^{a)}
b)	PPy	Polypyrrole	Influencing cell culture, ^[138,154–161] electrode coating, ^[162] tissue engineering, ^[131,150,163] biosensing ^[40]
c)	PANI	Polyaniline	Influencing cell culture, ^[161,164] electrode coating, ^[165] tissue engineering, ^[135,145,166,167] biosensing ^[165,168]
d)	PT	Polythiophene	See note ^{a)}
e)	P3AT ^{b)}	Poly(3-alkylthiophene)	Optical biosensing, ^[169] influencing cell culture, ^[130] optoelectronic stimulation, ^[56,170,171] biosensing, ^[111,172–176] lipid bilayer interfacing. ^[177]
f)	PEDOT	Poly(3,4-ethylenedioxythiophene)	See note ^{a)}
g)	PEDOT:PSS ^{c)}	Poly(3,4-ethylenedioxythiophene) polystyrene sulfonate	Ubiquitous—see references cited throughout this report
h)	NDI-T2 ^{d)}	Naphthalene-1,4,5,8-tetracarboxylic-diimide-bithiophene derivatives (e.g., p(gNDI-gT2))	Lipid bilayer interfacing, ^[178] biosensing ^[153]

^{a)}Provided for reference purposes, material is infrequently used directly and/or derivatives are more prevalent; ^{b)}A hexyl sidechain is used in the examples provided; ^{c)}PEDOT:PSS is a dispersion of two different polymers; ^{d)}Refers to base repeat unit, a number of variants and/or notations of this polymer exist.

impact of sidechain modification on similar thiophene derivatives, showing that glycolation and alkylation can be used to tune ion ingress into a polymer film, and hence alter OECT performance.^[189] Glycolated polymers have been successfully used to fabricate OECTs to perform electrophysiological measurements on humans.^[191]

Another class of derivatives that has attracted recent attention are crown-ether incorporating polythiophenes.^[193,194] Wustoni et al. demonstrated ion-sensitive OECTs which, with the appropriate calibration, were capable of distinguishing between sodium and potassium ion concentrations in a human serum sample.^[192] They incorporated crown ethers directly into the polymer backbone along with sufficient EDOT repeat units to minimize steric hindrance (Figure 11). Ion-sensitive devices can also be fabricated by incorporating ion selective membranes onto the conjugated polymer layer.^[176,195,196]

3.2. PEDOT:PSS as an Exemplar Conjugated Polymer

3.2.1. The Formation of Polarons and Bipolarons Make PEDOT:PSS Conductive

First developed in 1988,^[182,197] the polymeric dispersion of PEDOT:PSS has become ubiquitous in the organic bioelectronic literature for its favorable properties: relatively good ambient stability, solution-processability as a colloidal suspension in water, and high conductivities (typically on the order of 10^3 S cm^{-1}).^[73,198] While the underlying physics of the PEDOT:PSS is an area of intense discussion in the literature,^[14,88,96,118] much is already known that can help inform our understanding of the real-world conductivities observed in biomaterials.

The p-type doped (oxidized) form of PEDOT is stabilized by the presence of sulfonate counterions from the PSS.^[80] Doping

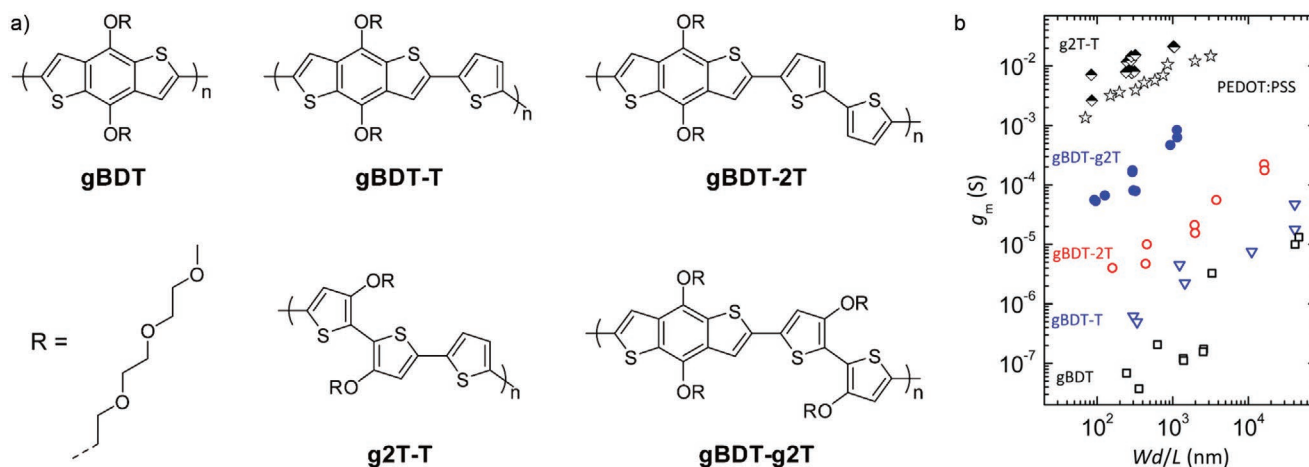


Figure 10. a) Glycolated variants of thiophene-derived homo and copolymers and b) their corresponding performance in an OECT device. The higher the transconductance value (g_m) for given device dimensions (Wd/L) the better the effective amplification of the OECT. The plot indicates the polymer notated g2T-T gives optimal electrical performance, in this configuration exceeding that of PEDOT:PSS. Adapted under the terms of CC-BY 4.0 license.^[188] Copyright 2016, American Chemical Society.

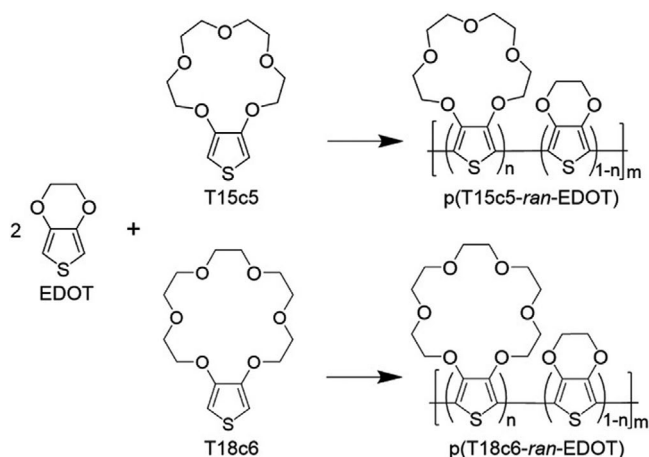


Figure 11. Crown ethers can be incorporated into thiophene based polymers in order to create ion-sensitive OEETs. Reproduced with permission.^[192] Copyright 2019, Wiley-VCH.

generated holes interact with the local polymer structure, deforming it slightly. This results in the formation of additional energy states between the existing HOMO and LUMO.^[87] The combination of the hole and the structural deformation it induces can be considered as a new charge carrier, a polaron (aka radical cation).^[87] In this context, polarons are charge carriers that represent the combined movement of charge and charge-induced deformation through the polymer system. Two polarons can become bound together, referred to as a bipolaron (two charge carriers plus the distortions they impact on the local polymer environment, considered as one combined quasiparticle) (Figure 12).

In PEDOT:PSS, as with some other conjugated polymers,^[199] the formation of polarons and bipolarons is responsible for the observed conductivity of the material.^[87] This conductivity can vary anywhere between 0.1 and $>6000 \text{ S cm}^{-1}$ depending on the processing and additives used,^[73,186] (cf. the conductivity of gold which is $\approx 10^5 \text{ S cm}^{-1}$ at room temperature).^[200] The relative position of polaron and bipolaron energy states in PEDOT:PSS remains an area of discussion. Figure 13 shows recent results from Zozoulenko et al., who used density-functional theory to estimate the position of the polaron and bipolaron states within the bandgap.^[88] Electron transitions between these states help explain the characteristic absorption peaks of PEDOT:PSS, which are typically used during material characterization as evidence of polaron and bipolaron formation.

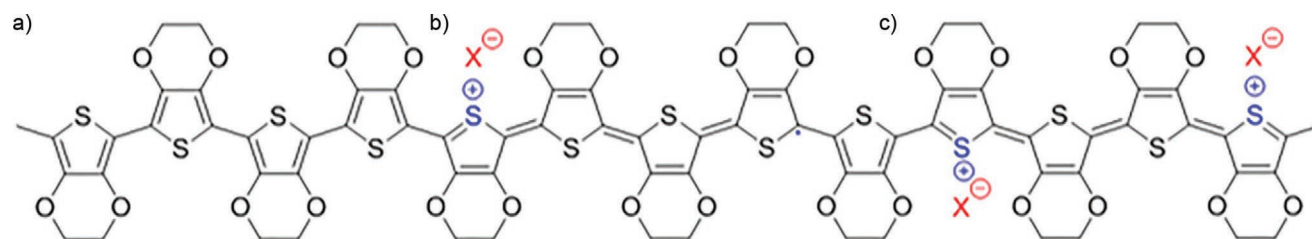


Figure 12. Illustration of the different states of PEDOT: a) neutral state, b) polaron formation, and c) bipolaron formation. Reproduced with permission.^[73] Copyright 2020, Elsevier.

3.2.2. There Are Many Alternative Doping Strategies for PEDOT

PEDOT:PSS is an imperfect material system. The dispersion of colloidal PEDOT particles surrounded by PSS can limit the formation of intimate stacking and connections between adjacent PEDOT chains, influencing charge transport and necessitating the introduction of additives to improve conductivity.^[201–203] The fixed nature of the PSS counterion means the PEDOT polymer cannot achieve a fully neutral state, impacting the on–off ratio of devices.^[180] The complexity of the material makes it a challenging model system to probe charge transport behaviors.^[80] Alternative counterions to PSS have been explored as a method of overcoming these limitations.^[204] These include small molecular dopants,^[142,205] other polyelectrolytes,^[206] and naturally occurring biomaterials such as chondroitin sulphate,^[207] and DNA.^[208] The requirement for stable doping is a key concern for the development of any new material system based on PEDOT. Any biointerface design, where the intention is to create a conductive material, must incorporate an effective doping strategy that is stable under physiological conditions. Many small molecule dopants, such as F4-TCNQ, are toxic and therefore may not be appropriate to incorporate into in vivo devices. For a comprehensive summary of dopants tested with PEDOT (although not necessarily in a biointerfacing context), we recommend other recent reviews.^[73,209]

Self-doped conjugated polymers are an alternative to introducing an external counterion. A charged group, such as an alkyl sulfonate is added as a sidechain to the conjugated polymer backbone in order to form a conjugated polyelectrolyte,^[210] an approach previously demonstrated as a means for electrically controlling cell adhesion.^[211] To date, this has resulted in films with relatively low conductivities compared to PEDOT:PSS, however recently Yano et al. reported a self-doped PEDOT variant they call S-PEDOT, with an electrical conductivity of over 1000 S cm^{-1} .^[201] They found the conductivity is highly dependent on the concentration of the S-EDOT monomer during polymerization, which in turn impacts crystallite formation in thin films (Figure 14). In general, the conjugated polyelectrolyte approach is not limited to PEDOT and has also been demonstrated in OEETs fabricated from a polyelectrolyte derivative of polythiophene.^[212]

3.3. Stretchable, Self-Healing, and Biodegradable Conjugated Polymer Systems

Pure conjugated polymer films can be brittle, tearing or cracking under strain.^[26] Improving the mechanical properties

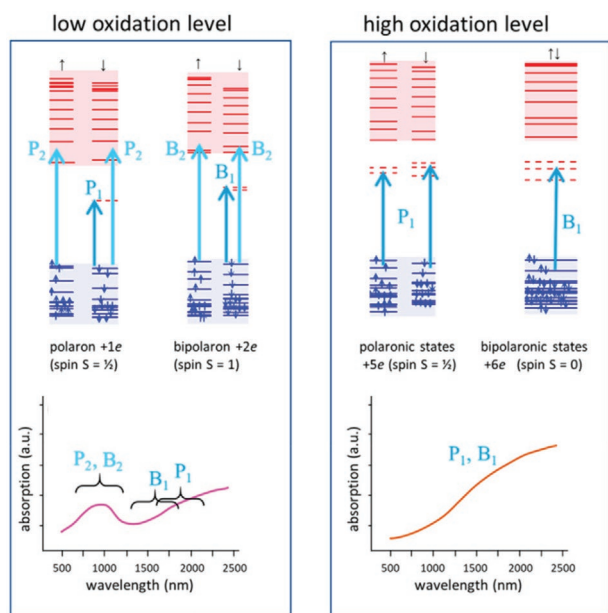


Figure 13. Density-functional theory (DFT) based modeling of the polaronic and bipolaronic states in PEDOT from Zozoulenko et al. The authors argue that prior pre-DFT models have failed to properly interpret the optoelectronic properties. The schematic shows the formation of intermediate energy states within the bandgap, that correspond to the characteristic patterns of absorption seen in PEDOT derived systems. Adapted with permission.^[88] Copyright 2019, American Chemical Society.

of conjugated polymer systems has focused on developing either intrinsically stretchable polymers,^[213–215] composites,^[43,216–218] or conjugated polymer hydrogels.^[39,219] Patterning materials with designs that compensate for motion are another approach, as developed for flexible thin film metal electrodes.^[220] The goal is to sustain the electrical properties of the conjugated polymer while under strain, an essential requirement for organic bioelectronic interfaces in vivo. Bao and colleagues have reported a number of developments in these areas.^[26,39,213,214,221] Xu et al. confined conjugated polymer chains inside an

elastomer, allowing the electrical properties of the material to be maintained even under strain.^[26] They applied this approach to multiple conjugated polymer systems and successfully fabricated organic field-effect transistors from each.

An emerging area of research is the development of biodegradable conjugated polymers, enabling the concept of transient bioelectronic interfaces.^[221,222] An in-depth discussion of developments in both stretchable and degradable conjugated polymers is beyond the scope of this report, but for a full discussion we recommend a number of recent reviews in this area.^[43,149,215,221,223,224]

4. Device Architectures

4.1. Overview of Devices that Incorporate Conjugated Polymers

Figure 15 and **Table 2** illustrate the wide range of device architectures and applications used as organic biointerfaces. They can be broadly categorized as: electrodes, where the conjugated polymer serves either directly to transfer charge or electrostatically couple with a system; 3D scaffolds and devices, where the polymer is patterned to create an environment for cell culture, or into nonplanar form factors such as fabrics; transistor architectures, where the addition of electrodes adjacent to the conjugated polymer film facilitates both charge injection and removal, and voltage probing; ion delivery devices, which take advantage of the dual ionic-electronic conductivity of many conjugated polymers; and photostimulation architectures, a relatively new research area which takes advantage of the optically active properties of conjugated polymers. Examples of these devices are given in Sections 5 and 6.

4.2. Specific Device Considerations

4.2.1. Transistor Architectures

Transistor architectures such as EGO-FETs, OECTs, and OFETs typically have the advantage of in situ amplification compared

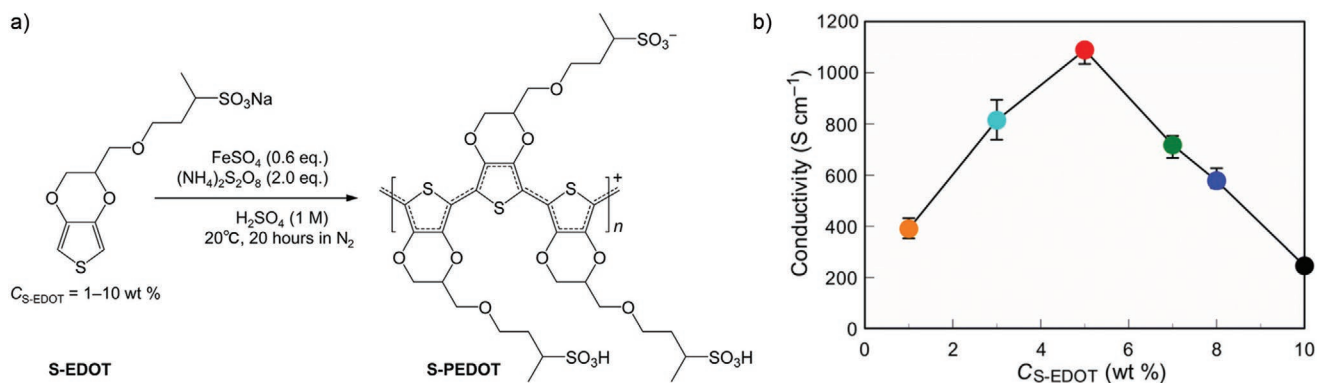
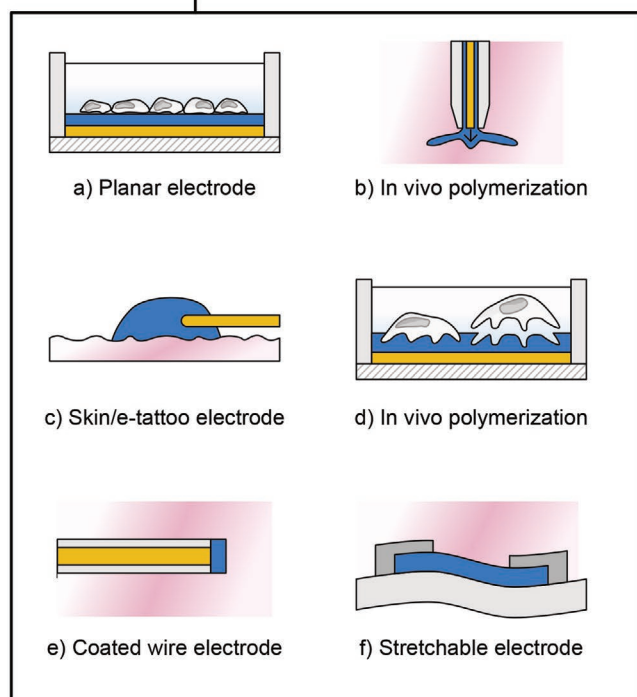
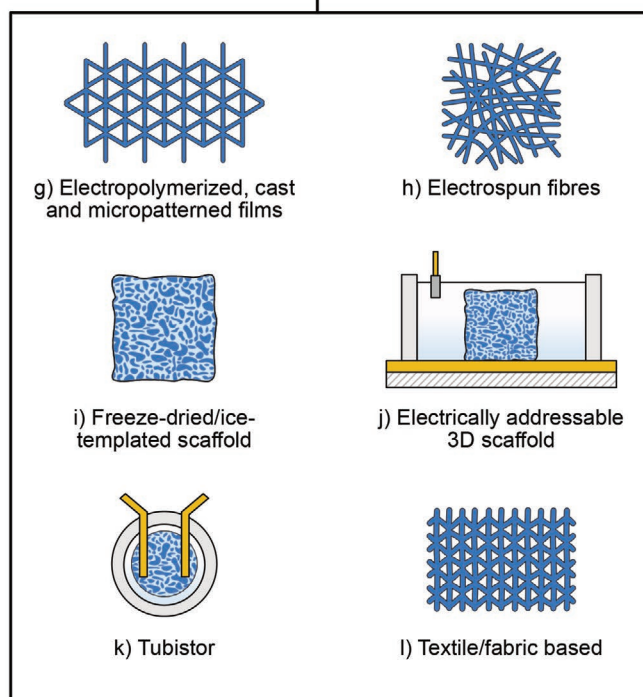


Figure 14. a) Self-doping polymer S-PEDOT as reported by Yano et al. b) The authors found that tuning the concentration of the S-EDOT monomer gave conductivities greater than 1000 S cm⁻¹. Adapted with permission.^[201] Copyright 2019, The Authors, some rights reserved; exclusive licensee American Association for the Advancement of Science. Distributed under a Creative Commons Attribution NonCommercial License 4.0 (CC BY-NC).

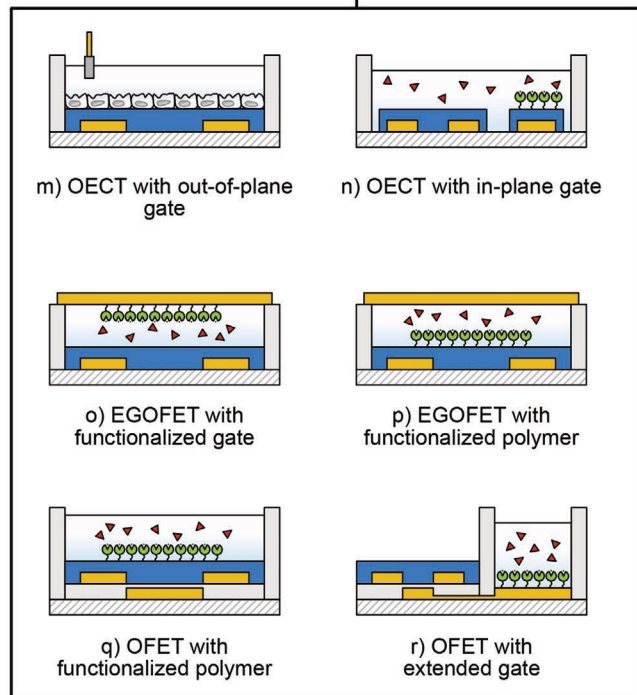
Electrodes



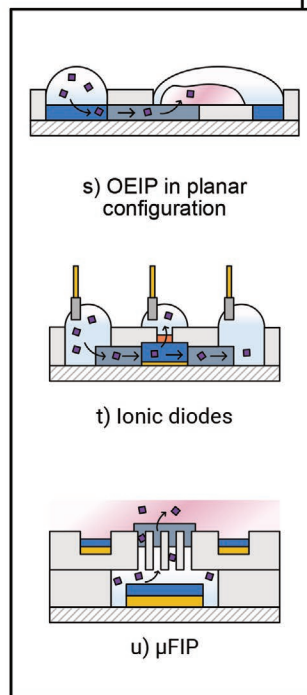
3D scaffolds/devices



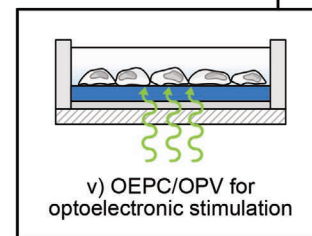
Transistor architectures



Ion delivery devices



Photostimulation



- Spacer/container
 - Tissue
 - Water/electrolyte
 - Ion exchange membrane
 - Metal electrode
 - Substrate
 - Conjugated polymer
- Illustrations not to scale

Figure 15. Illustrations of device architectures fabricated from conjugated polymers and used as organic bioelectronic interfaces. See Table 2 for descriptions and references.

to simpler electrode designs. Motivations include: label-free operation (i.e., analytes can bind directly to the device and be detected without the need for an additional molecular label);

the direct transduction of binding events into a quantitative electrical readout; and the option to self-calibrate devices immediately prior to testing, providing a relative baseline for each

Table 2. Table of different device architectures used with conjugated polymers for organic bioelectronic interfacing, see Figure 15 for illustrations.

Figure notation	Description	Acronym	Application area
a)	Planar electrode	–	Microelectrode arrays, ^[60,225–227] cell interfacing, ^[126,140,159,160,205,207,211,228–230] transepithelial sensing, ^[231] neural interfacing, ^[232–234] biosensing, ^[165,235] retinal prosthesis, ^[236] iontophoresis ^[237]
b)	In vivo polymerization	–	Neural interfacing ^[147,238]
c)	Skin electrode/e-tattoo	–	Electrophysiology measurements ^[42,239–242]
d)	In vitro polymerization	–	Cell interfacing ^[238]
e)	Coated wire electrode	–	Electrophysiology stimulation and measurement ^[243–245]
f)	Stretchable/hydrogel electrode	–	Neural interfacing, ^[39,216,246] cell culture, ^[217,219] tissue scaffold ^[247–250]
g)	Electropolymerized, cast and micropatterned films	–	Tissue scaffold, ^[145] cell culture ^[130,141,163,251]
h)	Electrospun fibers	–	Cell scaffold, ^[127,131,164,252] optoelectronic cell stimulation, ^[171] tissue scaffold ^[166]
i)	Freeze-dried/ice-templated scaffold	–	Cell scaffold, ^[139,253] tissue scaffold ^[254,255]
j)	Electrically addressable 3D scaffold	–	Cell scaffold ^[59]
k)	Tubistor	–	Cell monitoring/cell scaffold ^[134]
l)	Textile/fabric based	–	Electrophysiology, ^[256] biosensing ^[40,196,257]
m)	Organic electrochemical transistor with out-of-plane gate electrode	OEET	Transepithelial sensing, ^[9,58,258–260] biosensing, ^[61,106,177,187,261] electrophysiology ^[61,262–264]
n)	Organic electrochemical transistor with in-plane gate electrode	OEET	Biosensing, ^[112–114,153,192,265–269] transepithelial sensing, ^[270,271] neural interfacing ^[272,273]
o)	Electrolyte-gated organic field-effect transistor with functionalized gate electrode	EGOFET	Biosensing ^[108,175,274–277]
p)	Electrolyte-gated organic field-effect transistor with functionalized conjugated polymer	EGOFET	Biosensing, ^[172,174,176,278,279] cell interfacing ^[280]
q)	Organic field-effect transistor with functionalized conjugated polymer	OFET	Biosensing ^[281,282]
r)	Organic field-effect transistor with functionalized extended/floating gate electrode	OFET	Biosensing ^[105,107,110]
s)	Organic electronic ion pump in planar configuration	OEIP	Tissue interfacing, ^[283–286] cell interfacing, ^[287] peptide modeling, ^[288] capillary-based ion delivery ^[289]
t)	Ionic diodes (e.g., addressable refillable ion delivery array)	ARIDA	Neurotransmitter delivery ^[290,291]
u)	Microfluidic ion pump	μFIP	Drug delivery in vivo ^[16,292]
v)	Organic electrolytic photocapacitors (or organic photovoltaics)	OEPC (or OPV)	Optoelectronic cell stimulation, ^[55,56,170,293,294] optoelectronic tissue stimulation, ^[56,295] retinal prosthesis ^[296,297]

individual transistor. Despite the miniaturization of organic transistors being many decades behind that of the silicon industry,^[298] dense arrays of organic transistors can be patterned onto a variety of substrates, suitable for applications that require large numbers of sensors such as spatially resolved tissue monitoring,^[60] or multiplexed biosensing.^[299–301]

Voltage gradients and current flows in aqueous environments run the risk of electrolysis of water.^[302,303] This often necessitates operating devices at low voltages (<|1 V|). EGOFETs benefit from the formation of sub-nanometer electrical double layers at the gate–electrolyte and electrolyte–semiconductor interfaces, which can generate large capacitances in the range of 20–500 μF cm⁻².^[304,305] These double layers serve to lower device operating voltages as well as increasing the sensitivity of the device to changes at either interface.^[100] Other approaches, such as the use of high-*k* or thin dielectrics,^[306] also help to

provide sufficient signal amplification at low operating voltages. Organic electrochemical transistors take advantage of the penetration of ions to form a volumetric capacitance which can yield high device transconductances at relatively low voltages compared to field-effect devices.^[80]

Potentiometric-based biosensor designs need to consider the impact of electrostatic shielding of the analyte by ions in the supporting electrolyte. This is characterized by the Debye length (a measure of the distance of electrostatic influence of a charged species). If the Debye length is excessively large, the analyte may become screened from the biorecognition element.^[278] Workarounds include varying the density of the biorecognition element on the conjugated polymer surface and tuning the ionic strength of the electrolyte,^[307] or taking advantage of Donnan equilibria,^[278] discussed in greater detail below.

4.2.2. Iontronic Devices

Iontronic devices, such as organic electronic ion pumps (OEIPs) take advantage of the permeability of many conjugated polymers to ions. The movement of ions through conjugated polymer electrodes and ion selective membranes can be controlled using an external electrical stimulus.^[308] OEIPs can deliver small positively charged molecules with high spatial and temporal resolution. The electrically driven nature of the device allows the release rate and dose to be finely controlled, and ions are transported independently through the material, minimizing tissue perturbation that can arise from the codelivery of excess liquid.^[287,309,310] Scaling planar OEIP architectures can result in prohibitively high voltage requirements.^[16] A number of alternative architectures have been proposed to overcome this issue, including ionic diodes,^[290,291,311] and the integration of microfluidics.^[16,292]

4.2.3. General Considerations

In any biosensor care must be taken to avoid nonspecific interactions, where nontarget molecules bind to the sensing surface yielding a false positive signal. Approaches include: using serum,^[174,312] or hydrophilic polymers,^[172] to block nonspecific binding sites; applying glycolated self-assembled monolayers;^[161,261] or adding antifouling groups to the polymer sidechain.^[133]

The ability to sterilize devices is also critical for any biomedical application. Exposed conjugated polymer surfaces should be able to sustain industry accepted sterilization procedures. Relatively little research has been conducted in this area, however two studies have examined the impact of autoclave and gamma-ray sterilization on PEDOT:PSS and polypyrrole, respectively.^[313,314]

5. In Vivo Applications

5.1. Skin

Skin contact electrophysiology encompasses electroencephalography (EEG), electrooculography (EOG), electrocardiography (ECG), and electromyography (EMG). Electrodes placed on the

surface of the body record the electrical activity of specific cells, tissues or organs for monitoring or diagnostic purposes. Metal-based electrodes require the application of aqueous conductive gel to promote adhesion and lower impedance at the interface with the skin.^[315] In addition to time-consuming preparation and discomfort, the gel dries with time causing signal instability and hampering long-term recording. Leleux et al. demonstrated dry PEDOT:PSS electrodes with similar performance to gel-assisted gold electrodes (**Figure 16a**).^[242] Combining these electrodes with an ionic gel allowed the electrodes to maintain a low impedance contact with skin over 3 days compared to 20 h for conventional systems.^[315]

Incorporating OEETs into skin interfaces provides in situ amplification, improving device signal-to-noise ratios.^[272] OEETs have been used for EEG,^[262,316] EOG,^[262] and ECG recording.^[263] However, hair at the interface can interfere with skin contacts, often requiring removal before electrodes can be applied. Approaches to overcome this include a photocurable PEDOT formulation that can be applied onto the skin and around existing hair (**Figure 16b**).^[240] A less invasive option is “tattoo electronics.”^[220,239] Inkjet-printed PEDOT:PSS electrodes on commercial decal transfer paper are transferred onto the skin as temporary tattoos (**Figure 16c**). These ultra-conformable and imperceptible electrodes are able to perform EMG recording,^[241] and can withstand hair growth through the tattoo.^[239] ECG signal recording has been demonstrated,^[239] and this approach has shown promise for long-term EEG monitoring devices.^[317]

Conjugated polymer interfaces can be used for active drug delivery through the epidermal barrier via iontophoresis.^[318] Zhang et al. used a PEDOT:PSS anode to transfer $MnCl_2$ solution from a PDMS reservoir into the vitreous humor of a rabbit eye. Their device sits under the eyelid in contact with the sclera, but requires a counter electrode on the ear and a copper wire connection to the external electronics.^[237] The integration of bio-fuel cells into a iontophoretic patch offers a self-powered, wireless alternative. The device is well-tolerated in vivo,^[319] opening the way for long-term, noninvasive, and effective delivery of hydrophilic and charged molecules through the skin.

Sweat monitoring is another area of interest, thanks to the use of relatively noninvasive patches.^[196,257,265] Keene et al. have demonstrated how ion-selective OEETs can be used to monitor ammonium and calcium ions from the sweat of volunteers wearing a forearm patch (**Figure 17**).^[195]



Figure 16. Three different approaches for conjugated polymer-based skin interfaces. a) PEDOT:PSS coated electrodes. Reproduced with permission.^[242] Copyright 2014, Wiley-VCH. b) On skin light-cured PEDOT:PSS electrodes. Adapted under the terms of CC-BY 4.0 license.^[240] Copyright 2018, The Authors, published by Springer Nature. c) Tattoo-style PEDOT:PSS electrodes, using temporary transfer paper. Adapted with permission.^[42] Copyright 2018, IOP Publishing.

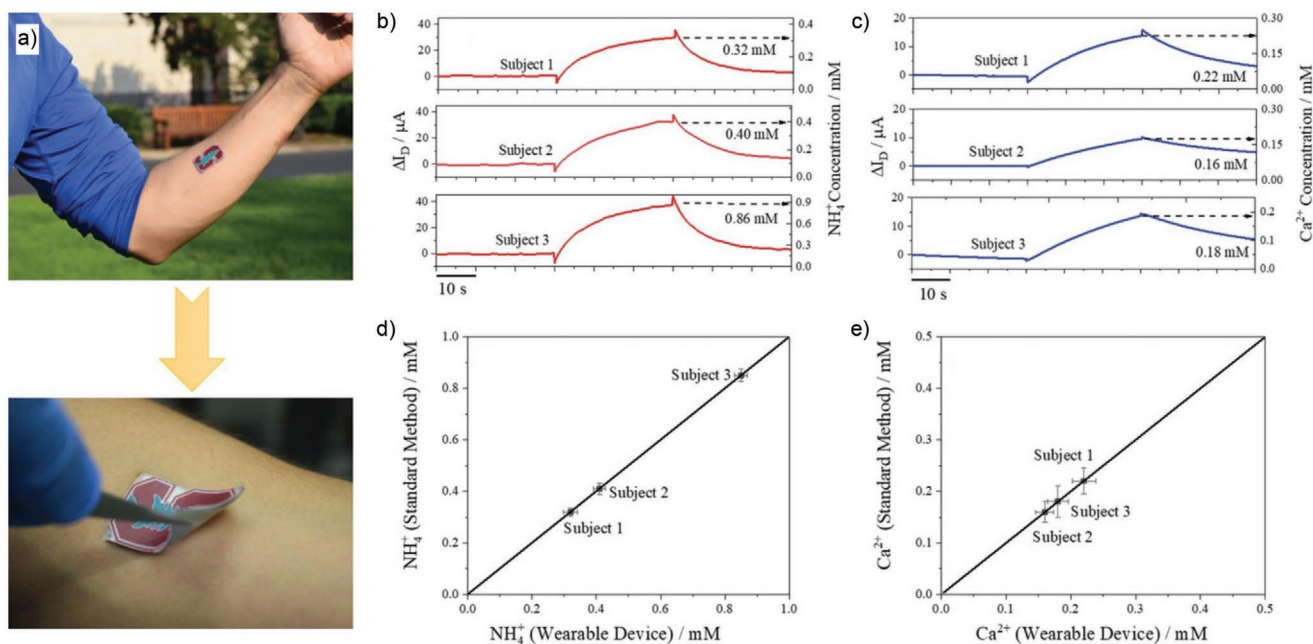


Figure 17. Wearable patch with ion sensing OECT for sweat monitoring. a) Photographs of patch as worn by volunteer. Change in device current (ΔI_D) as a function of time for b) ammonium and c) calcium ion measurements. Device response compared with standard methods for d) ammonium and e) calcium ions. Reproduced with permission.^[195] Copyright 2019, Wiley-VCH.

5.2. Nervous System

Neural interfaces enable communication between the nervous system and external electrical equipment. They can provide electrical stimulation to restore or modulate neural activity,^[39,283] record activity for diagnostic and monitoring purposes,^[60,225] or act as an input for prosthetic limb control systems.^[320] High spatial resolution is desirable for both stimulating and recording applications. This implies a reduction of the electrode dimensions, which typically translates into increased electrode impedance and thus lower signal-to-noise ratios and safe charge injection limits.^[321,322] Conjugated polymer electrodes can be engineered to form lower impedance interfaces than equivalently sized metal electrodes,^[323] thanks in part to their high charge storage capacity.^[302] Neural interfacing covers a vast array of topics, below we highlight selected major results. For a general discussion we recommend a number of recent reviews.^[324–326]

5.2.1. Central Nervous System: Brain and Spinal Cord

Electrocorticography (ECoG), the recording of electrical activity directly from the exposed surface of the brain, enables intraoperative monitoring of brain surgery and is an emerging tool for brain–machine interfaces and real-time functional brain mapping fields. Khodagholy and colleagues have presented numerous reports demonstrating the benefits of a highly conformable and flexible ECoG array, based on PEDOT:PSS coated electrodes (**Figure 18**).^[60,225,327] The first proof of principle in vivo dates back to 2011, when this array was used to record drug induced sharp-wave events, mimicking epileptic spikes, from

the somatosensory cortex of rats.^[327] In 2015, an improved version of the same array, with neuron-sized-density electrodes, was used to record both local field potentials (LFPs) and action potentials from the cortex of two patients undergoing brain surgery.^[60] More recently, Khodagholy et al. have demonstrated how this system can aid fundamental neuroscience, such as investigations into the consolidation of memories.^[225] Others have reported similar approaches, including Ganji et al. who used a conjugated polymer-based ECoG array to measure evoked cognitive activity in humans with high spatial resolution.^[233] ECoG arrays are not restricted to simple electrodes; OECTs can be incorporated directly into sensing surfaces, providing in situ amplification with reduced signal-to-noise ratios. This approach has been used to record both induced and spontaneous epileptiform activity in rats.^[328] PEDOT:PSS based electrodes have also been explored for transcranial electrical stimulation and monitoring, where the electrodes are placed onto the skull or scalp, rather than directly onto the brain.^[234]

While planar neural interfaces allow surface measurements, penetrating neural probes are required to measure subcortical brain activity. Williamson et al. reported a neural probe, consisting of three OECTs and a PEDOT:PSS electrode.^[283] The probe is inserted in the hippocampus with an ultrathin SU-8 shuttle, delaminating once in situ as a result of water absorption. While some insertion damage was noted, no significant glial scar formation was observed in the month following implantation. A recent example by Xie et al. used a similar array of OECTs mounted on an insertable shank for in vivo detection of dopamine from the brain of a rat model.^[273]

Localized, controlled and tunable delivery of molecules to the nervous system is highly valuable for both basic research and therapeutic treatment. Local delivery of drugs solves issues

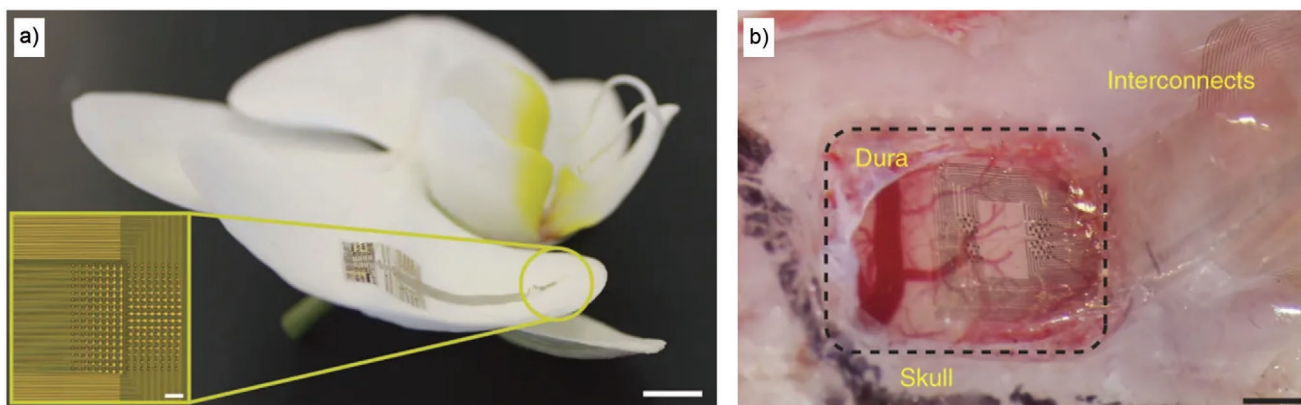


Figure 18. NeuroGrid neural interface by Khodagholy et al. The PEDOT:PSS electrode coating was found to decrease the impedance mismatch between electrode and tissue. a) Photograph showing interface placed onto an orchid petal. Scale bar is 5 mm. Inset is optical image of electrode array, scale bar is 100 μm . b) Photograph of NeuroGrid on surface of rat somatosensory cortex, scale bar is 1 mm. Adapted with permission.^[60] Copyright 2015, Springer Nature.

such as limited crossing of the blood brain barrier, poor dosage control due to systemic metabolism and side effects due to off-target action.^[16,329] Organic electronic ion pumps have been adopted for this purpose. Jonsson et al. delivered γ aminobutyric acid (GABA, a neurotransmitter) into the subarachnoid space of the spinal cord. This successfully reduced pain response in a rat model, with no observable side effects, even at the higher GABA dosage.^[329] GABA delivery via a planar OEIP has also been used also to suppress epileptiform activity in hippocampal living slices.^[285] Microfluidic ion pumps (μFIPs) use a microfluidic channel to transport a drug to miniaturized OEIPs adjacent to the point of delivery. This permits lower operating voltages, faster delivery, and a larger quantity of drug to be pumped.^[16,292,330] A μFIP integrated with PEDOT:PSS sensing electrodes was used to monitor and modulate the epileptiform activity in rat hippocampus through GABA administration (Figure 19).^[330] A similar system in an ECoG probe configuration has been used for the monitoring and treatment of cortical epileptic focal seizures.^[292]

5.2.2. Peripheral Nervous System

Peripheral nerve interfaces have been explored extensively for functional electrical stimulation and for the control of prosthetic limbs.^[331] More recently they have found application in bioelectronic medicine, where the electrical modulation of nerve activity is used to treat pathological conditions.^[332–334] The anatomical structure of the peripheral nervous system is a challenge for bioelectronic interfaces. Peripheral nerves undergo relatively huge mechanical strain as a result of limb motion,^[335] with underlying nerve fibers sheathed in several fatty layers that permit fascicles (bundles of axons) to slide past each other.^[336] Peripheral nerves can comprise hundreds or thousands of clusters of individual axons, presenting a formidable obstacle to the spatiotemporal resolution of nerve impulses.^[337] To date, a wide-range of nonorganic bioelectronic interfaces have attempted to tackle this challenge (Figure 20).

Schönle et al. used a PEDOT:PSS coated commercial flexible cuff electrode to modulate heart rate and blood pressure

in a rat model, through the stimulation of the aortic depressor nerve.^[338] Similarly, an array of PEDOT:PSS-coated electrodes was used to modulate cardiac activity in rats via stimulation of the vagus nerve.^[232] PEDOT:pTS (PEDOT doped with p-toluenesulfonic acid) coated electrodes have been used to facilitate real time monitoring of neural activity of sheep model vagus nerves via electrical impedance tomography, yielding

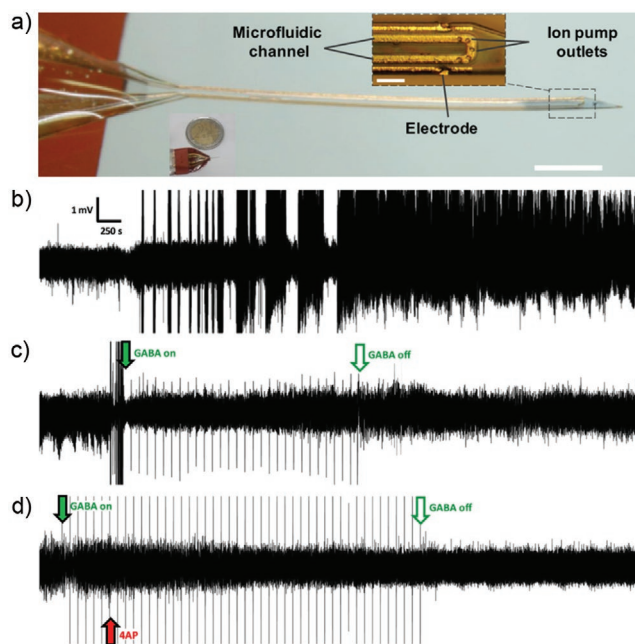
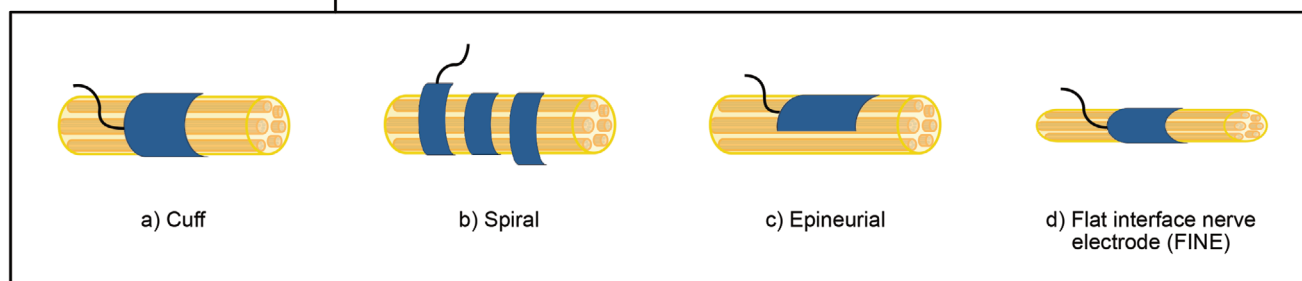


Figure 19. A microfluidic ion pump (μFIP) based on PEDOT:PSS was inserted into the brain of a mouse epilepsy model and used to suppress seizure activity. a) Photograph of device, scale bar is 1 mm; inset shows optical image of device tip, scale bar is 100 μm . b) Measured electrophysiological activity during induced seizure. c) Suppression of seizure activity after onset by enabling μFIP . d) Suppression of the onset of the seizure by pre-emptive drug delivery via μFIP . Reproduced with permission.^[330] Copyright 2018, The Authors, some rights reserved; exclusive licensee American Association for the Advancement of Science. Distributed under a Creative Commons Attribution NonCommercial License 4.0 (CC BY-NC).

Extraneural electrodes



Intraneural electrodes

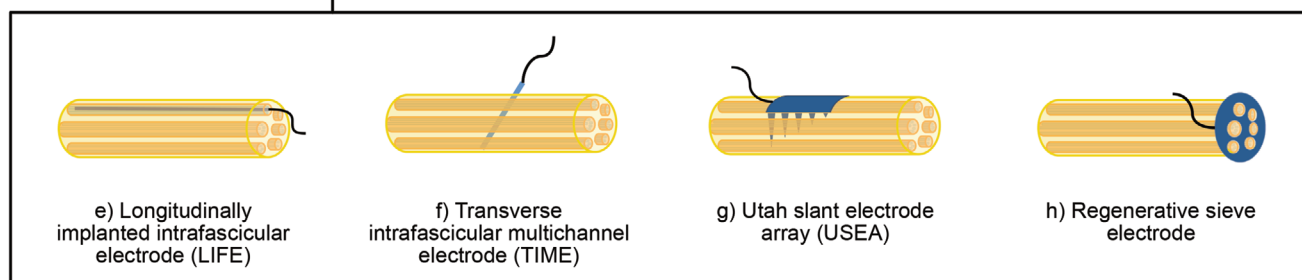


Figure 20. Existing neural electrode designs, some of which are starting to be adopted for conjugated polymer interfaces. a) Insulating sheet with exposed electrodes sites encircling the nerve bundle. b) Flexible platinum ribbon with open helical design to minimize mechanical trauma. c) Strips of insulating material with exposed electrode sites, sutured to the epineurium. d) Cuff designed to flatten the nerve making central fascicles more accessible, at the expense of nerve functionality. e) Insulated microwire with exposed electrode sites, longitudinally threaded within a fascicle. f) Insulated strip with exposed electrode sites, transversally threaded through several fascicles. g) Arrays of microelectrodes of increasing length, individually interfacing different axons. h) Insulating sieve with platinum coated holes, sutured at the end of a cut nerve, to form a conduit for axon regrowth.

better performance than platinum and iridium oxide based electrodes.^[339]

As discussed above, hydrogel or ionic liquid based conjugated polymer systems are one approach to create peripheral nerve interfaces with desirable mechanical properties.^[39,213] Decataldo et al. also demonstrated how polyethylene glycol could be incorporated into a PEDOT:PSS film during electropolymerization to tune the flexibility of a conductive interface used for chronic renal nerve recordings in a rat model (Figure 21).^[216]

5.2.3. Eyes and Ears

Retinal prostheses (artificial eye implants) aim to improve the quality of life for people living with visual impairments caused by a lack of photoreceptor cells, but who retain underlying retinal neurons.^[340] Electrical stimulation of these neurons can result in limited restoration of visual perception.^[341] High spatial resolution is crucial to achieve a viable visual acuity and conjugated polymers aid the miniaturization and density of the electrode arrays used for retinal stimulation.^[340] PEDOT-based coatings have been shown to improve the charge transfer properties of platinum electrodes both in suprachoroidal,^[342] and subretinal,^[236] locations in animal models, leading to more defined electrically evoked potentials in the visual cortex.

Electrode arrays alone require interconnections and power supply, a nontrivial requirement for organs such as the eye. These constraints can be overcome by exploiting photovoltaic

materials, able to generate a current in response to light stimulation.^[343] An organic photovoltaic patch was used to restore light sensitivity in a rat model of retinitis pigmentosa (a genetic disorder that results in the progressive loss of photoreceptors). The patch was fabricated via the sequential spin-coating of PEDOT:PSS and P3HT on a silk fibroin substrate, which was then laser cut and implanted into a subretinal position.^[297,344] The patch resulted in mild and transient inflammation and

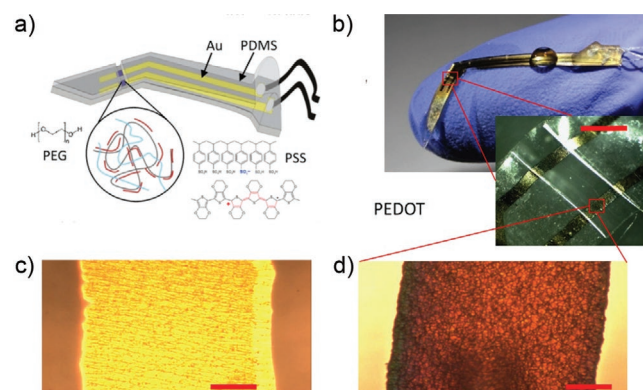


Figure 21. Polyethylene glycol (PEG) is incorporated during the electropolymerization of PEDOT:PSS to create a stretchable electrode for neural interfacing. a) Illustration of interface. b) Photographs of device, scale bar is 500 μm . c) Optical image of gold fiberconnect, scale bar is 50 μm . d) Optical image of PEDOT:PSS/PEG electrode, scale bar is 50 μm . Adapted under the terms of CC-BY 4.0 license.^[216] Copyright 2019, The Authors, published by Springer Nature.

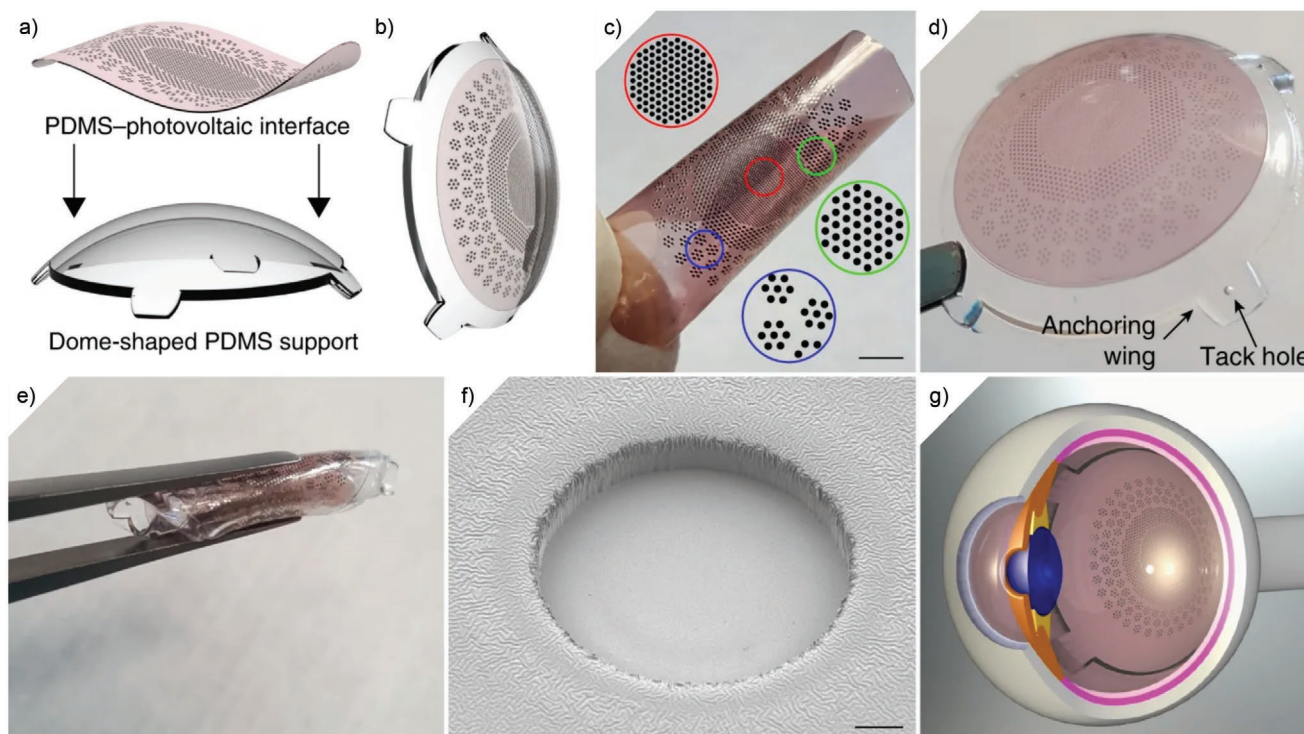


Figure 22. The POLYRETINA concept, as reported by Ferlauto et al. A PDMS scaffold supports an area of photovoltaic sites, comprising an indium tin oxide anode, PEDOT:PSS, P3HT:PCBM (a common photovoltaic conjugated polymer-small molecule blend) and an aluminum or titanium cathode. a,b) Illustration of device. c) Photograph of fabricated device, highlighted regions indicate different pixel densities in different locations. Scale bar is 2.5 mm. d,e) Further photographs. f) Scanning electron microscopy image of a single photovoltaic pixel, scale bar: 10 μm . g) 3D model illustrating device after epiretinal placement. Adapted under the terms of a CC-BY 4.0 license.^[296] Copyright 2018, The Authors, published by Springer Nature.

both tissue and device were intact and functional six-months post implantation. This concept has also been used with an organic photovoltaic bulk-heterojunction device architecture, using a blend of P3HT with a small conjugated molecule, [6,6]-phenyl-C61-butyric acid methyl ester (PCBM) (a common organic solar cell material system). Ferlauto et al. fabricated an epiretinal array of 2215 photovoltaic pixels, now approaching *in vivo* validation (Figure 22).^[296]

Cochlear implants are a well-established treatment pathway for sensorineural hearing loss, however, foreign body reactions result in complications and implant failure.^[345] Conjugated polymer electrodes have been investigated as an approach to minimize mechanical mismatch and deliver protective growth factors. Richardson et al. found polypyrrole:pTS coated electrodes could be combined with neurotrophin-3 (a protein observed to promote neuronal survival) to produce a cochlear implant that proactively supported the survival of spiral ganglion neurons, helping to restore auditory response in a deafened guinea pig model.^[162] Similarly, Chikar et al. used an electrode coating combining PEDOT and an arginylglycylaspartic acid (RGD peptide)-alginate hydrogel to improve the electrical performance of a cochlear implant and deliver a different neurotrophin to spiral ganglion neurons for up to two weeks postimplantation.^[244] Simon et al. demonstrated an iontronic approach, using a planar OEIP architecture to deliver glutamate (a neurotransmitter), selectively stimulating nerve cells in the cochlear of a guinea pig model.^[284]

5.3. Heart and Muscles

Tian et al. used PEDOT:pTS capped microwire electrodes as part of a larger implant into rat muscle, delivered through a syringe. The device also combined microfluidic channels for drug delivery and could be used for electromyographic recording and functional stimulation.^[243]

Lee et al. used an ultraconformable circuit design to fabricate planar ultraconformable arrays (Figure 23). The design consisted of an active matrix of OFETs, a technology originally developed for flat panel displays. Each sensing OEET is electrically addressed using an OFET that provides both *in situ* amplification and facilitates very high electrode densities while helping to mitigate the challenge of electrically addressing large numbers of sensors simultaneously. They demonstrated this concept by using an electrode array to perform electromyographic recording from the moving muscle, with negligible mechanical interference.^[61]

Cardiac patches and injectable conductive hydrogels can act as a conductive bridge across the fibrotic scar formed after a myocardial infarction, restoring cell-to-cell electrical communication and thus effective coordinated beating.^[135] Research in this area has focused on both polyaniline,^[135,145,250] and polypyrrole systems.^[247–249] Mawad et al. reported a cardiac patch consisting of polyaniline polymerized on a chitosan substrate.^[135] Phytic acid was immobilized into the film as a dopant, via ionic interactions with both the polyaniline and chitosan.

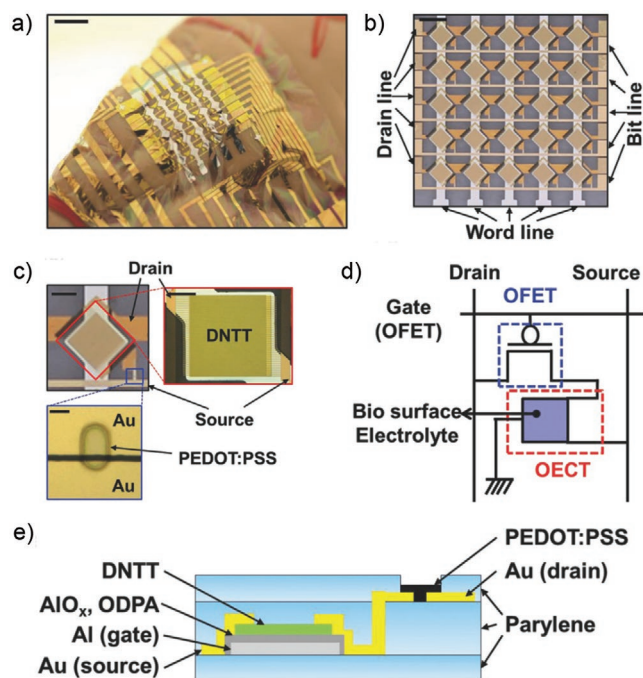


Figure 23. Ultraconformable sensing array by Lee et al. Each sensor consists of a sensing OEET, coupled to an OFET that acts both as an amplifier and allows the high-density array to be addressed. The OEET uses PEDOT:PSS as the active material; the OFET uses dinaphtho[2,3-b:2',6'-f]thieno[3,2-b]thiophene, which is a semiconducting conjugated small molecule. a) Photograph of sensor array, scale bar is 0.5 cm. b) Top-view of sensor array, scale bar is 2 mm. c) Optical images of sensor components (top-left scale bar is 0.5 mm, top-right scale bar is 0.2 mm, bottom scale bar is 5 μm). d) Circuit diagram of single cell. e) Device cross-section. Reproduced with permission.^[61] Copyright 2016, Wiley-VCH.

Only a mild fibrotic reaction was observed and no mechanical interference with the heart contraction or arrhythmia was induced, while conductivity was maintained for up to two weeks.^[135] Successfully securing cardiac patches to a beating heart while simultaneously not impairing muscle function is a major challenge in this area. Kapnisi et al. tackled this problem by taking the same polyaniline–chitosan material system and laser patterning it with an auxetic design.^[145] The auxetic patch exhibited a negative Poisson's ratio, meaning the material expands laterally in response to a longitudinal strain force, as

opposed to the more common contraction behavior (Figure 24). They secured the patch using a photoactivated small molecule dye (rose bengal) that facilitated sutureless binding to the heart. The resulting conductive patch allowed normal heart function, presenting a pathway toward conjugated polymer based cardiac patches for treating myocardial infarction.

6. In Vitro Applications

6.1. Cell Stimulation

6.1.1. Electrical Stimulation of Excitable Cells

Polypyrrole, polyaniline, and PEDOT:PSS guided nerve growth has been studied extensively, with interfaces permitting enhanced control over neurite outgrowth and orientation.^[154,164,346] Zhang et al. electrically stimulated cells cultured on polypyrrole, demonstrating that this could reduce the effect of specific gene knockouts that otherwise impair neurite growth (Figure 25).^[159] In another study, increased populations of neurons with higher elongation and longer neurites were also observed in cross-linked PEDOT:PSS scaffolds after an electrical stimulus.^[130] Neurite outgrowth was enhanced in cells cultured on a polypyrrole substrate containing two different neurotrophins. The combination of electrical stimulation and dual neurotrophin release resulted in greater neurite outgrowth than unstimulated or single neurotrophin releasing materials.^[156] Electrically stimulated mouse retinal progenitor cells cultured on polypyrrole were also shown to express significantly higher levels of the early photoreceptor marker cone rod homeobox, more pronounced neuronal morphologies and larger cell bodies than the controls.^[158]

Cardiac muscle contraction is triggered by the propagation of electrical signals through electrically excitable cells. Vascular smooth muscle cells stimulated on polypyrrole were observed to exhibit increased proliferation and expression of muscle phenotype marker proteins.^[155] Human pluripotent stem cells cultured on polypyrrole-coated poly(lactic-co-glycolic acid) fibers demonstrated an increased expression of cardiac markers both with and without electrical stimulation,^[150] suggesting the polypyrrole itself provided some innate benefit to cell culture. Conductive polypyrrole–polycaprolactone films were observed to increase the speed of calcium wave propagation and promote cellular attachment compared to the pure

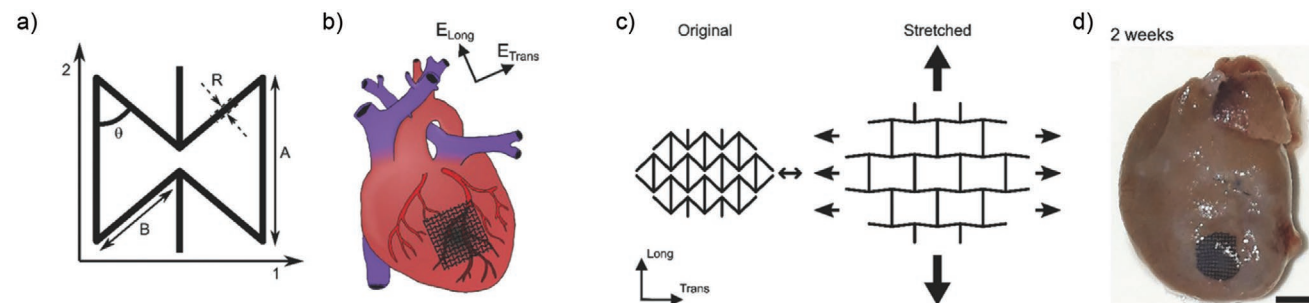


Figure 24. An auxetic cardiac patch fabricated from polyaniline on a chitosan substrate. a–c) The bowtie design means the patch expands in the transverse axis when stretched in the longitudinal one, accommodating the beating motion of the heart. d) After two weeks in vivo in a rat model, the patch remained well attached. Scale bar is 4 mm. Adapted under terms of CC-BY 4.0 license.^[145] Copyright 2018, The Authors, published by Wiley-VCH.

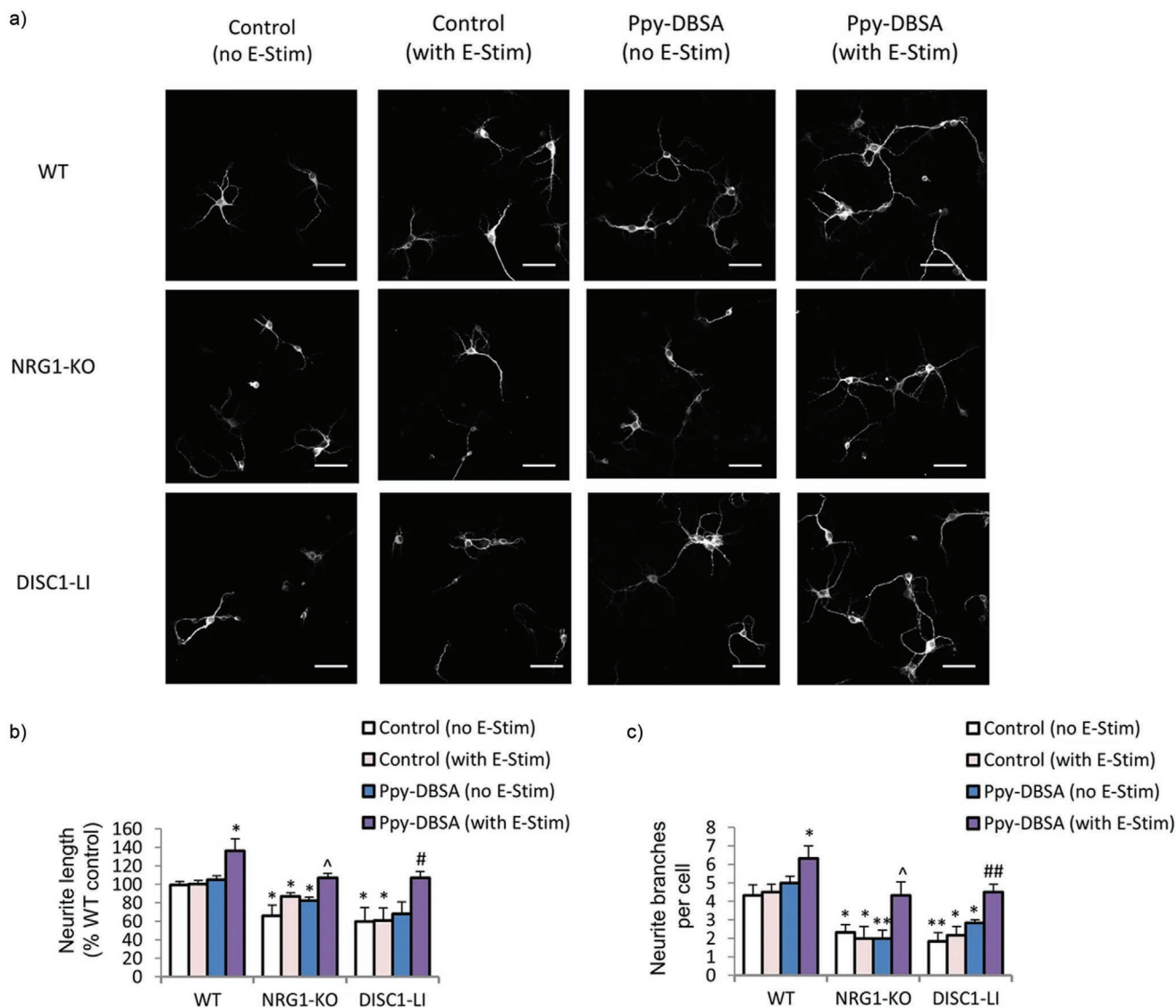


Figure 25. Zhang et al. cultured primary pre-frontal cortical neurons on a polypyrrole film (doped with dodecyl benzene sulfonic acid, DBSA) and subjected them to either electrical stimulation or not. a) Comparison between cells from wild type (WT), and two genetically impaired mouse lines (NRG1-KO and DISC1-LI) showed that electrical stimulation on polypyrrole resulted in cells with b) longer neurites and c) a greater number of branches per cells than equivalent controls. (a) Scale bars represent 50 μm . b,c) Error bars represent standard error of the mean. Adapted under the terms of CC-BY 4.0 license.^[159] Copyright 2017, The Authors, published by Springer Nature.

polycaprolactone film.^[163] Similarly, the beating behavior of cardiomyocyte cultures has been electrically synchronized on electrospun polyaniline/poly(lactic-co-glycolic acid) fibers,^[166] and modulated on a crystalline PEDOT:PSS substrate.^[347]

6.1.2. Electronic Stimulation of Osteogenic Cells

Conjugated polymers have been used in two contexts as bone interfaces: as porous, cytocompatible tissue scaffolds suitable for hosting osteogenic cells;^[254,255] and as interfaces for electrically promoting cell differentiation and growth.^[157,230,253,348] Guex et al. used ice-templated PEDOT:PSS scaffolds for culturing a preosteogenic precursor cell line (MCT3-E1).^[254] The

porous, interconnected nature of the material supported 3D cell culture and permitted the long term culture and differentiation of precursor cells into osteoblasts (bone synthesizing cells). The same osteogenic cell line cultured on 2D polypyrrole films coated on interdigitated electrodes was investigated by Liu et al.^[348] They applied a range of different electrical pulsing regimes to cells via the polypyrrole interface and found different stimulation regimes evoked different levels in a range of osteoblast biomarkers, as observed in other similar studies too.^[157] While much remains to be understood, the empirical effects of electrical stimulation of bone tissue are widely recognized outside the field of organic bioelectronics,^[67] suggesting there is significant scope to develop bone organic bioelectronic interfaces further.

6.1.3. Photostimulation via Conjugated Polymer Devices

Optical stimulation has potential as a simple, noninvasive technique to modulate cellular behavior with high spatial and temporal selectivity. Light can excite charge carriers between the HOMO and LUMO energy states of conjugated polymers, an effect used in organic photodetectors and organic photovoltaics.^[82] Hence, conjugated polymer layers, in close contact with a cell, can convert light into an electrical or thermal stimulus. A number of reports have emerged in this area,^[56,170,171,293,295,297,343,349] including using nonpolymeric organic conjugated small molecules,^[55,350] with work ongoing to understand the precise mechanisms of photostimulation.

Benfenati et al. stimulated primary cultured rat neocortical astrocytes by, in effect, placing cells into a solar cell architecture.^[293] Cells were cultured on top of the conjugated polymer layer comprising P3HT and PCBM. Cells cultured on the P3HT:PCBM substrates and irradiated with laser light, showed membrane depolarization over the course of 50 s of illumination, compared to cells on a control substrate, where under illumination the membrane potential remained broadly constant. The authors hypothesized that the excess charge generated by the photovoltaic layer results in the local acidification of the cell media at the conjugated polymer interface, triggering calcium ion channels to open. Later studies, involving some of the same researchers have identified either capacitive effects (where an anode is present) or photothermal effects as other likely mechanisms.^[170,295] Similar recent studies by Głowacki and colleagues have also suggested a capacitive coupling mechanism.^[55,294] Martino et al. investigated human embryonic kidney (HEK-293) cells cultured on P3HT thin films, and observed either membrane depolarization or hyperpolarization under different illumination conditions.^[170] Feyen et al. employed a similar approach to hyperpolarize hippocampal neurons, resulting in the silencing of the evoked action potentials in hippocampal slices.^[295]

Recently, Lodola et al. investigated endothelial colony forming cells on P3HT, observing increased activation of a calcium-related ion channel (TRPV1) after photoexcitation of the polymer film (Figure 26).^[349] Control experiments using non-conjugated photoresist films led the researchers to conclude that photothermal effects were not the primary mechanism of channel activation. Instead, they postulate that the P3HT film acts as a photocatalyst in the formation of reactive oxygen species at the film–media interface. As a side note: organic

semiconductor-based photocatalysts, including conjugated polymer films, are being widely explored within the wider optoelectronic community.^[351]

Wu et al. found that patterned P3HT films, self-assembled nanofibers, and electrospun microfibers could be used to influence neurite extension and length in primary neuronal cultures (PC12).^[171] Using a calcium sensitive fluorescent dye they identified a light-triggered influx of calcium into neuronal cells cultured on P3HT. The authors proposed that this approach has potential in the development of new optically driven neural interfaces and regenerative devices.

6.2. Cell Monitoring

6.2.1. Monitoring Transepithelial Electrical Resistance

Transepithelial/transendothelial electrical resistance can be used as a measure of epithelial (or endothelial) layer integrity in drug screening assays.^[352] A number of organic bioelectronic impedance-based electrode,^[229] and OECT approaches have been reported.^[58,258,259,353]

In a recent example, Koutsouras et al. used a cell layer cultured on a permeable filter, suspended in electrolyte above a PEDOT:PSS coated electrode (Figure 27).^[231] They were able to analytically model the impact of cell layer growth on impedance measurements, extracting both resistive and capacitive contributions of the cell membrane. The same principle can be applied to OECTs with cells cultured directly onto the conjugated polymer surface, with a variety of examples from Owens and colleagues.^[258–260,270,271,353] The total device impedance is measured by modulating the OECT gate voltage, which, depending on the device impedance, results in a modulation of current in the conjugated polymer layer. In this way, Rivnay et al. were able to determine both the transepithelial resistance and capacitance of a layer of epithelial cells (MDCK II).^[259] The same group also applied this approach to a range of nonbarrier and intermediate barrier forming tissue cell types, noting increasing transepithelial resistance as expected.^[270] Combining this approach with enzyme-based OECT sensing allowed the simultaneous monitoring of the transepithelial resistance and the production of metabolites from a layer of MDCK II cells.^[353] In all cases, device dimensions have a significant impact on the sensitivity of devices.^[58,231,354]

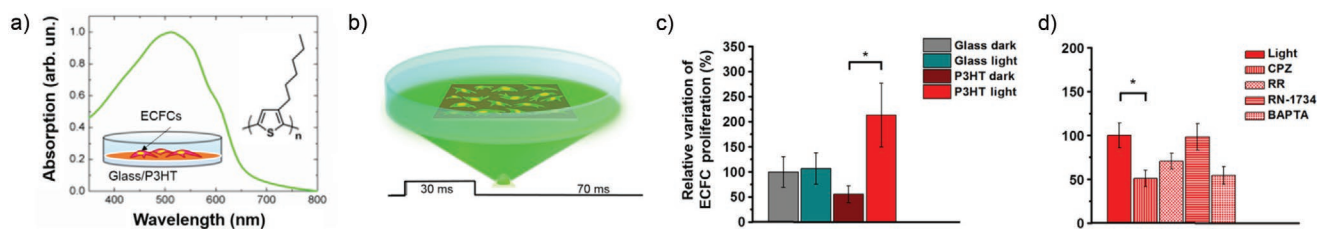


Figure 26. Optoelectronic stimulation of endothelial colony forming cells (ECFCs) cultured on a P3HT film. a) Absorption behavior of P3HT and schematic of experimental setup. b) Illumination protocol for cells. c) Relative proliferation of cells on glass and P3HT substrates in light and dark situations. d) Using different drugs to identify the activation of the TRPV1. Reproduced with permission.^[349] Copyright 2019, The Authors, some rights reserved; exclusive licensee American Association for the Advancement of Science. Distributed under a Creative Commons Attribution NonCommercial License 4.0 (CC BY-NC).

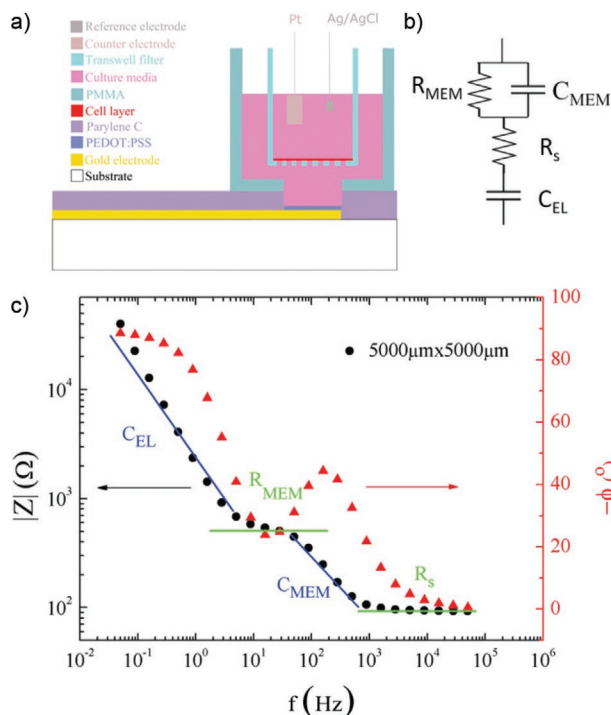


Figure 27. Extracting cell membrane resistance (R_{MEM}) and capacitance (C_{MEM}) from an electrochemical impedance spectroscopy measurement across an epithelial cell layer, using a PEDOT:PSS coated electrode. a) Illustration of the experimental setup. b) Equivalent circuit used to model the measured impedance. c) Example impedance measurement showing the fitted regions. Reproduced with permission.^[231] Copyright 2019, The Authors. Published by Wiley-VCH.

6.2.2. Monitoring Cell Attachment and Detachment

Zhang et al. used a dual-gate EGO-FET,^[355] where an additional electrode (a second gate) allows the accumulated charge in the conjugated polymer layer to be modulated semi-independently of the voltage appearing across the biological interface. This approach allowed them to directly measure the attachment and detachment of human mesenchymal stem cells to the conjugated polymer layer.

Owens and colleagues demonstrated in situ 3D cell culture and impedance monitoring, using PEDOT:PSS scaffolds to support MDCK II epithelial cells.^[59] Cell growth within the scaffold was confirmed using electrochemical impedance spectroscopy; after cell seeding an increase in the impedance of the scaffold at low frequencies was observed. The corresponding phase measurements indicated an additional capacitive component as a result of the cell growth on the scaffold. This result was confirmed by detaching the cells from the scaffold and seeing a subsequent reduction in impedance. Pitsalidis et al. extended this concept further by incorporating a PEDOT:PSS scaffold and OECT electrodes into a tube that permits 3D culture with a continuous supply of cell media and nutrients (**Figure 28**).^[134] They demonstrated their platform through the in situ electrical monitoring of epithelial and fibroblast cells. 3D cell culture approaches are particularly advantageous for organ-on-a-chip applications, where

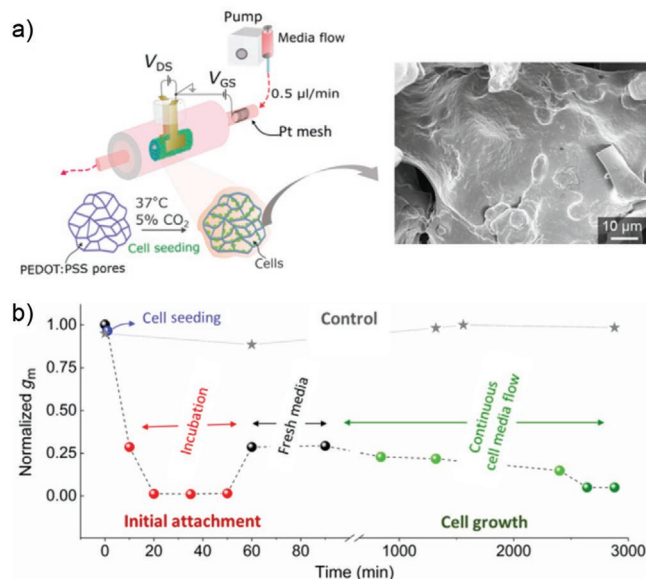


Figure 28. Transistor in a tube “tubistor” concept by Pitsalidis et al. a) Device architecture with inset showing scanning electron microscopy image of epithelial cells on the scaffold after ≈ 2 days of culture. b) Using the normalized transconductance of the OECT (g_m) as a measure of cell activity on the scaffold during culture. Reproduced with permission.^[134] Copyright 2018, The Authors, some rights reserved; exclusive licensee American Association for the Advancement of Science. Distributed under a Creative Commons Attribution NonCommercial License 4.0 (CC BY-NC).

recreating the complexity of tissues or organs in 2D cultures is often impossible.^[356]

6.3. Detecting Biomolecules

6.3.1. Detection of Analytes in Blood

Palazzo et al. demonstrated an approach for overcoming the limitation of electrostatic shielding of a protein analyte. They fabricated an EGO-FET capable of detecting C-reactive protein (CRP) in human blood serum.^[278] CRP is an inflammatory biomarker often used to assess cardiovascular disease, heart attacks, and strokes. A receptor layer was bioconjugated onto a P3HT layer using a phospholipid, streptavidin, biotin, and anti-CRP antibody stack (**Figure 29**). They found that the outermost protein in the stack dominated electronic transduction, despite being further from the semiconducting layer. The authors attributed this to the formation of Donnan’s equilibria within the protein layer, where the charged protein layer is compensated by counterions from the electrolyte, in effect creating a large capacitance that acts in series with the existing gate.^[279] This allows binding event detection at a distance many times further from the transistor channel than the Debye screening length. More recently, researchers from the same group have shown that self-assembled monolayers, attached to the gate electrode of a P3HT driven EGO-FET can also provide single-molecule detection.^[357] Macchia et al. first used a thiol-based self-assembled monolayer to treat the EGO-FET

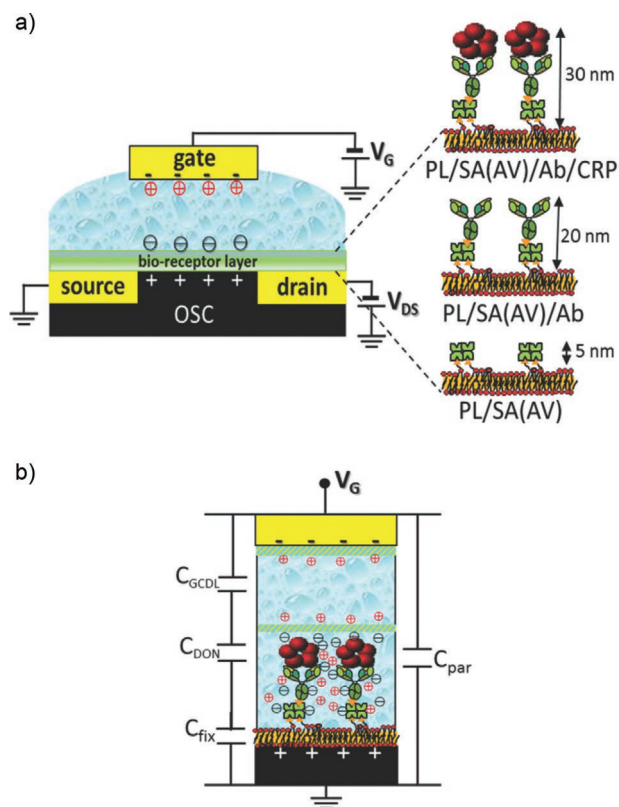


Figure 29. a) Illustration of the bioconjugation approach adopted by Palazzo et al. b) Proposed model for the formation of a Donnan equilibrium (C_{DON}) and its contribution to the overall parallel capacitance of the gate (C_{PAR}). Reproduced with permission.^[278] Copyright 2015, Wiley-VCH.

gate electrode, followed by the binding of relevant antibodies to the monolayer. Using this approach, the authors report a limit of detection of 250×10^{-21} M, or roughly 15 molecules, for measurements of human immunoglobulin G (a common antibody found in blood used as a biomarker for various conditions) spiked into a bovine blood serum sample (Figure 30). They postulate that binding events cause defects in both the antibody biorecognition layer and underlying self-assembled monolayer, which are coupled by hydrogen bonding. A small defect propagates through the monolayers, triggering a larger change in electrode work function than the binding event alone and hence increases amplification. They subsequently used the same platform to detect CRP in saliva,^[274] and the p24 capsid protein,^[276] a biomarker for the early diagnosis of human immunodeficiency virus type-1 (HIV-1).

6.3.2. Detection of Analytes in Saliva, Breath, and Urine

Liquid biopsies of bodily fluids such as saliva, tears and urine, and breath biopsies, use relatively noninvasive collection procedures, which minimize the risk of infection and pain to the user compared to drawing blood.^[358] Pappa et al. demonstrated an OECT array with individual transistors functionalized with enzymes targeting three metabolites (Figure 31).^[112] Enzymes were bioconjugated onto the surface of a PEDOT:PSS gate

electrode via an intermediate self-assembled monolayer (using EDC/NHS chemistry). The array was capable of measuring the levels of glucose, lactate, and cholesterol in saliva samples provided by different volunteers. The work is also an example of multiplexed biosensing, a technique whereby multiple biomarkers are measured simultaneously to increase diagnostic power, while reducing test costs and sample volumes.^[301]

Exhaled breath contains a number of biomolecules.^[359] Conjugated polymers have been widely explored as candidates for gas and vapor sensing within the wider organic electronics community, for example, in electronic nose applications.^[360] Bihar et al. reported a disposable OECT breathalyzer, fabricated by ink-jet printing PEDOT:PSS onto paper (Figure 32).^[266] An alcohol catalyzing enzyme was incorporated in a collagen-based gel and deposited onto the OECT channel. When the device was exposed to ethanol from the breath, a decrease of the transistor current was observed, and the device was capable of detecting the consumption of a single glass of red wine.

Yang et al. demonstrated a conjugated polymer-based textile OECT sensor, capable of detecting metabolites from urine. Their approach is based on nylon fibers coated with metal, PEDOT:PSS, and encapsulation layers, in essence translating the planar OECT architecture into a 3D fiber format. By weaving the fibers together, they were able to create a fabric OECT device, capable of sensing glucose levels in artificial urine samples, prepared with physiological relevant levels of uric acid. The device was integrated into a diaper design, with a smartphone driven wireless interface. Berto et al. demonstrated another approach using a fully printed OECT for urea detection, targeting mass produced, low cost point-of-care sensing.^[267]

6.3.3. Detection of Analytes from Cells

Early diagnosis of cancers significantly improves survival outcomes.^[361] Noninvasive and/or rapid biopsies for cancer are directly applicable to early cancer detection, and for ongoing surveillance and prognostics (detecting recurrence and predicting clinical outcomes).^[362–364] The human epidermal growth factor receptor 2 (HER2) protein is found in breast cancer patients and plays an important role in prognosis. Fu et al. used an OECT-based biosensor combined with a catalytic nanoprobe label to sense HER2 at concentrations of 10^{-14} g mL⁻¹ in phosphate buffered saline solution.^[269] The authors then used their device to differentiate between healthy and cancerous cells, both by incubating cells directly onto the OECT gate, and also by testing the cell lysate. The same technology was used to detect the presence of specific cell surface glycan (mannose) in a human cancer cell line.^[268] Braendlein et al. used an enzyme-based OECT to compare lactate produced from malignant and healthy cells, detecting elevated lactate in cancer cells.^[114]

Dopamine imbalance is responsible for various neurological disorders such as Parkinson's disease. Casalini et al. developed an EGO-FET capable of selectively binding dopamine using a cysteamine and boronic acid-based self-assembled monolayer.^[175] The same research group also demonstrated dopamine sensing in the picomolar range using an organic artificial synapse fabricated from two PEDOT:PSS electrodes

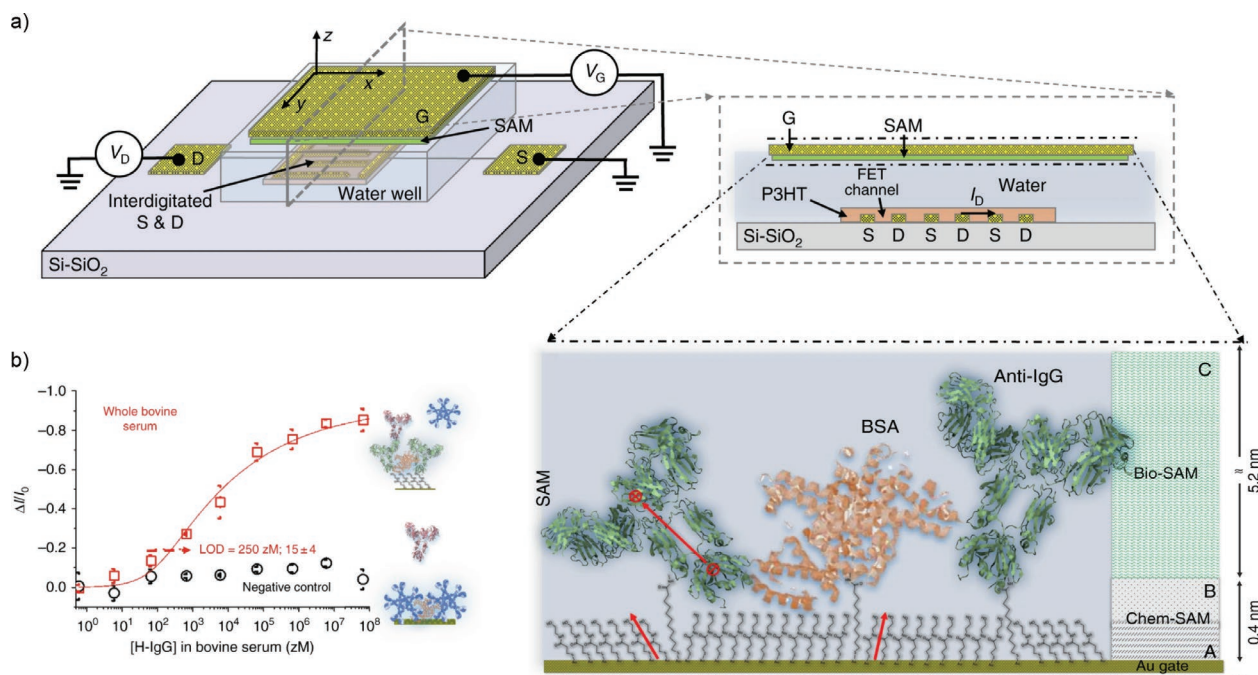


Figure 30. EGOFET sensing architecture as reported by Macchia et al. a) Illustration of device architecture showing location of chemical and biological self-assembled monolayers to the device gate electrode. b) Example of the change in normalized transistor current ($\Delta I/I_0$) as a function of the concentration of human immunoglobulin G spiked into bovine serum. Adapted under the terms of CC-BY 4.0 license.^[357] Copyright 2018 The Authors.

patterned on a PDMS substrate, bridged by an electrolyte (Figure 33).^[365] One electrode is stimulated with a square wave voltage, while the current was recorded at the other electrode. The current signal was systematically shifted during stimulation in a manner that could be fitted with an exponential envelope function. The exponential fit parameters were found to be dependent upon the concentration of dopamine in the electrolyte, allowing a response curve to be calculated. The benefit of this approach was the selective identification of dopamine in the presence of two interfering agents (uric acid and ascorbic acid).

DNA detection has been extensively explored using conjugated polymer-based devices.^[110,111,366–369] Fast, low-cost assays, without the need for sophisticated laboratory facilities and laborious labeling protocols, are desirable. The negatively charged phosphate groups on DNA backbones make it well suited to detection by potentiometric approaches. Lin et al. combined a PEDOT:PSS based OECT with a DNA aptamer probe functionalized gate (aptamers are short sequences of nucleic acids that bind to other specific sequences or other biomolecules).^[367] They were able to reduce the detection limit of their biosensor (for complementary DNA sequences in a buffer solution) from 1×10^{-9} M to 1×10^{-12} M by pulsing the gate electrode during measurements. They propose that electrical pulsing aids the hybridization and reorientation of DNA on the surface. Other approaches include incorporating hairpin-shaped oligonucleotide sequences to form molecular beacons that hybridize to specific target sequences.^[110] White et al. demonstrated a relatively uncommon floating gate organic transistor architecture, with an intermediate electrode that was hybridized with nucleic acid

sequences.^[111] This approach has the advantage of physically separating the biorecognition elements from the other electrodes and providing a high capacitance architecture in a planar format, as opposed to a more complex 3D design.

7. Open Research Questions

Can the long-term electrical stability of conjugated polymers be sustained in vivo? Few long term studies of conjugated polymer stability in vivo exist, however one investigation of chronic neural implants reported that PEDOT:PSS coated electrodes degrade over the course of ≈ 8 weeks.^[245] This effect may be less of an issue for in vitro applications, which experience a less demanding biological environment.^[227,370] Leaching of dopants may also present a challenge in terms of safety and functionality. The effective charge carrier mobility of conjugated polymer systems also varies dramatically depending on the energetic and structural disorder of the local polymer environment, presenting a challenge to maintaining consistent device performance. Developing polymers that inherently minimize torsional disorder along the backbone,^[23,371] along with the appropriate use of additives,^[95,98] to displace the source of charge traps is a possible solution. Similarly, while much remains to be understood about the complex foreign body response to conjugated polymers, many of the characterization tools from the tissue engineering field can provide helpful insight.^[372]

What is the best approach for full integration of conjugated polymer bioelectronic interfaces with measurement and stimulation

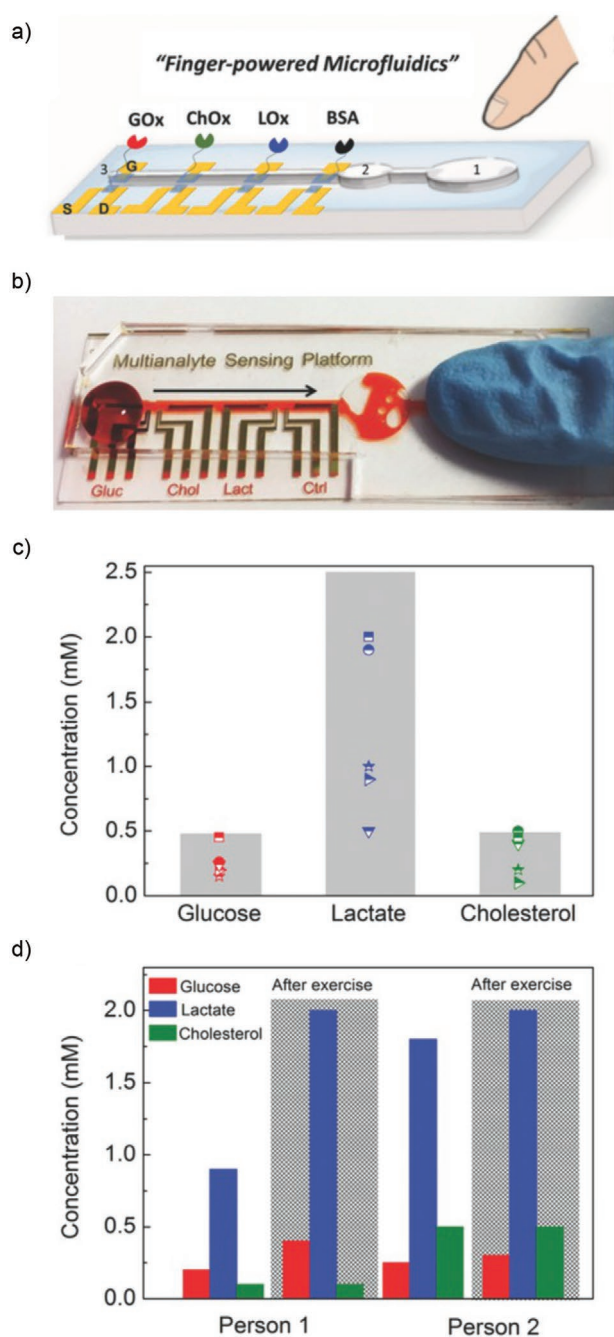


Figure 31. Multiplexed sensing of metabolites in saliva using PEDOT:PSS based OECEs. a) illustration of sensor concept. b) Photograph illustrating fluid flow (fluid stained red for visualization). c) Concentrations of glucose, lactate, and cholesterol as measured in saliva samples provided by three volunteers. d) Change in metabolite concentration levels before and after exercise for two volunteers. Reproduced with permission.^[112] Copyright 2016, Wiley-VCH.

equipment? Interconnects, wiring and external equipment all contribute to a complete medical device and can present a barrier to device adoption. In neural interfaces the strain of the connecting wire can be as problematic as the interface itself.^[336] Systems integration,^[277] the development of more complex

iontronic and electronic circuits,^[308,333,373] miniaturization and the integration of wireless communication systems,^[338,374] may present some solutions.

Are there better strategies for bioconjugating conjugated polymers? While sidechain modification has been used extensively to modify the biological properties of conjugated polymers, it is often observed to be easier to bind biorecognition elements to metallic electrodes or interlayers rather than to the polymer itself. This somewhat defeats the benefit of conjugated polymers, in particular for the case of OFETs, where thin, flexible variants of silicon semiconductor devices arguably offer better performance as in situ amplifiers.^[375–378] Improved conjugation strategies would permit more elegant system designs that fully take advantage of the polymeric approach.

What techniques are best suited to developing 3D conjugated polymer interfaces? Recent results have demonstrated the potential of moving beyond 2D interfaces, in particular for cell and tissue scaffolds, where micro- and nanostructuring have a significant impact on biological response.^[30,119,379] The increased effective surface area created by 3D structuring offers compact, dense signaling surfaces for biosensing applications. Given the range of 3D micropatterning technologies, much scope remains for applying these to the challenge of conjugated polymer interfaces.^[36] However, any devices will have to balance potentially larger interface capacitances and slower ion ingress rates against the speed with which charge can be delivered by the interface.^[322] Greater charge storage may also impact the amount of power required to operate implantable interfaces.

Are homogenous soft mechanical properties always desirable? Neural and tissue interfaces require the aid of shanks or other rigid materials to ensure correct insertion.^[380] Different tissues within the body show a wide range of mechanical stiffnesses, spanning multiple orders of magnitude.^[381] Transient mechanical properties, either to aid interface placement, or in response to changing physiological environments may be required for some applications.

Can organic bioelectronic interfaces provide insight into the wider role of bioelectric gradients within living systems? The application of conjugated polymer organic bioelectronic interfaces in developmental biology is relatively unexplored. Developing new bioelectric gradient models and scaffolds can potentially support studies into the role of bioelectricity and influence fundamental development behaviors.^[48,49]

What more can we understand about the structure–property relationships and charge transport physics of complex, dispersed systems such as PEDOT:PSS? The interplay of morphology, structure, disorder, and charge transport processes present a challenge to developing analytical models of material systems such as PEDOT:PSS. While considerable advances have been made in this area,^[116,382] as noted in a number of reports,^[80,179] much remains to be explored, in particular with respect to the relationship of electronic and ionic transport. Inherent to this is further exploration of the role of dopants within conjugated polymer systems. Better understanding would inform interface design, particularly in terms of material choice, processing conditions, and application environment.

What is the pathway for technology translation? The ultimate motivation for many organic bioelectronic interfaces is to

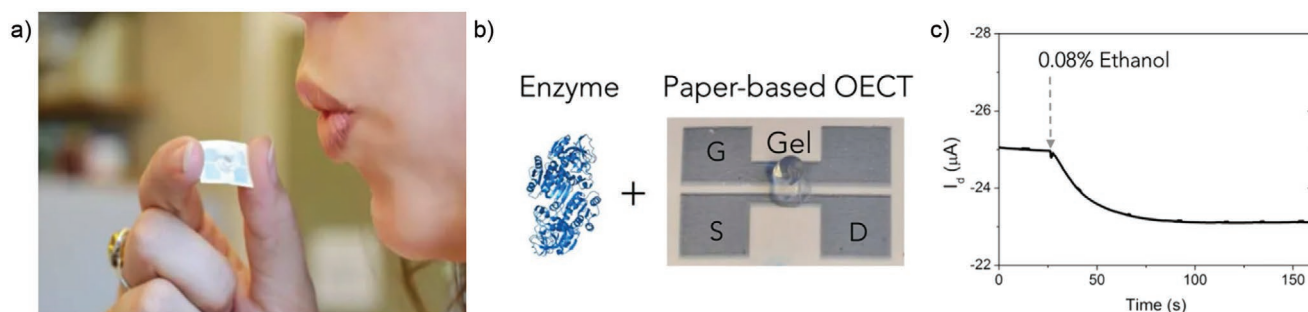


Figure 32. Alcohol-detecting breath sensor based on PEDOT:PSS based OECT from Bihar et al. a) Photograph of device. b) Alcohol dehydrogenase enzyme is immobilized in a gel on the device. c) OECT drain current (I_D) as a function of time after exposure to alcohol in the breath. Adapted under the terms of CC-BY 4.0 license.^[266] Copyright 2016, The Authors, published by Springer Nature.

improve the health outcomes of patients worldwide. Technology translation relies on feasible manufacturing and commercialization pathways. Clinically, progress has been made toward the adoption of PEDOT:PSS based electrodes, through *in vivo*,^[60] and sterilization studies,^[313] although to date few devices have completed the regulatory approval processes.^[383] However, most of the patient-orientated interfaces reported here have yet to be robustly demonstrated in a clinical setting. The challenge of technology translation is not unique to the field of organic bioelectronics, however it remains an important consideration. For biosensing applications this means investigating the feasibility of different architectures both in terms of manufacturing (e.g., compatibility with high throughput manufacturing techniques, devices with a suitable shelf-life), and also usability (e.g., ease of use, minimal required supporting infrastructure). Critically, the design and functionality of a diagnostic test depends strongly upon where it is used.^[35,384] This necessitates a multidisciplinary research approach, involving clinicians and other end-users from an early stage.

8. Closing Remarks

Excitement for organic bioelectronics has arisen from the ability to use conjugated polymers either directly as cell and tissue scaffolds, or by combining them into devices to create electrically addressable biointerfaces. Current prominent application areas include developing biosensing systems, neural interfaces, and tissue scaffolds for controlling and stimulating cell behavior. Organic bioelectronic materials and devices are relevant to applications such as bioelectronic medicine (with the promise of drug-free electrical stimulation-based therapies) and regenerative medicine (where using electronic and ionic transporting materials have the potential to help the body heal itself). In biosensing, organic bioelectronic devices have been shown as well-suited for low-impedance, high-performance electrophysiological sensing, and capable of detecting a wide range of biomarkers in a variety of device architectures. The inherent benefit of interfaces that can natively communicate with both electronic equipment and biological processes is a primary motivation for researchers. The major challenge facing the field is reconciling complex charge transport phenomena with equally complex biological responses. The growing interdisciplinarity between researchers developing materials, and those applying them in bioengineering contexts is key to reaching this goal.

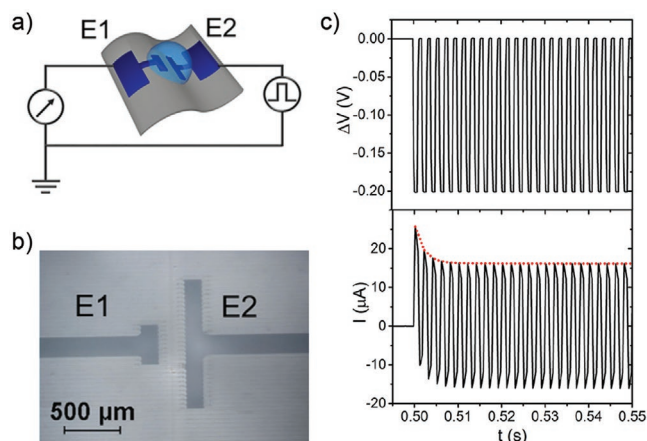


Figure 33. Dopamine sensing using two PEDOT:PSS electrodes bridged by an electrolyte. a) illustration of device architecture and circuit schematic. b) Optical image showing top down view of device and electrodes (E1 and E2). c) Stimulating voltage (ΔV) and observed current response (I) as a function of time. Dotted red line indicates fitted envelope function. The fit parameters of this envelope was found to be proportional to the concentration of dopamine present in the electrolyte. Adapted with permission.^[365] Copyright 2017, American Chemical Society.

Acknowledgements

This article is part of the Advanced Materials Technologies Hall of Fame article series, which recognizes the excellent contributions of leading researchers to the field of technology-related materials science. S.G.H. and M.M.S. acknowledge support from the ERC Seventh Framework Programme Consolidator Grant “Naturale CG” (616417) and a Wellcome Trust Senior Investigator Award (098411/Z/12/Z). S.G.H. acknowledges the many helpful discussions with colleagues within the Stevens Group and with those in the broader organic bioelectronics community, and the support of Dr. Akemi Nogiwa Valdez for extensive proofreading and publishing support. A.L.F. acknowledges the support of the EPSRC Centre for Doctoral Training in Neurotechnology for Life and Health (EP/L016737/1). I.P. acknowledges the support of the EPSRC Centre for Doctoral Training in Plastic Electronic Materials (EP/L016702/1). A.C. and M.M.S. acknowledge support from the Imperial College BHF Centre for Cardiac Regeneration (RM/13/1/30157) and the i-sense EPSRC IRC in Early Warning Sensing Systems for Infectious Diseases

(EP/K031953/1). While every attempt was made to locate recent papers, the authors apologize to any researchers whose work has inadvertently been omitted.

Conflict of Interest

The authors declare no conflict of interest.

Keywords

biointerfacing, biosensing, conducting polymers, conjugated polymers, organic bioelectronics

Received: April 22, 2020

Revised: August 3, 2020

Published online: October 11, 2020

- [1] L. Galvani, *Aloysii Galvani. De Viribus Electricitatis in Motu Musculari Commentarius. Cum Joannis Aldini Dissertatione et Notis. Accesserunt Epistolæ Ad Animalis Electricitatis Theoriam Pertinentes.*, Mutinæ: Apud Societatem Typographicam, Institute of Bologna, Italy **1792**.
- [2] K. Fidanovski, D. Mawad, *Adv. Healthcare Mater.* **2019**, *8*, 1900053.
- [3] A. Creamer, C. S. Wood, P. D. Howes, A. Casey, S. Cong, A. V. Marsh, R. Godin, J. Panidi, T. D. Anthopoulos, C. H. Burgess, T. Wu, Z. Fei, I. Hamilton, M. A. McLachlan, M. M. Stevens, M. Heeney, *Nat. Commun.* **2018**, *9*, 3237.
- [4] C. S. Almeida, I. K. Herrmann, P. D. Howes, M. M. Stevens, *Chem. Mater.* **2015**, *27*, 6879.
- [5] K. Lee, L. K. Povlich, J. Kim, *Analyst* **2010**, *135*, 2179.
- [6] H. Ling, D. A. Koutsouras, S. Kazemzadeh, Y. van de Burgt, F. Yan, P. Gkoupidenis, *Appl. Phys. Rev.* **2020**, *7*, 011307.
- [7] Y. van de Burgt, E. Lubberman, E. J. Fuller, S. T. Keene, G. C. Faria, S. Agarwal, M. J. Marinella, A. Alec Talin, A. Salleo, *Nat. Mater.* **2017**, *16*, 414.
- [8] P. Gkoupidenis, D. A. Koutsouras, G. G. Malliaras, *Nat. Commun.* **2017**, *8*, 15448.
- [9] X. Strakosas, J. Selberg, Z. Hemmatian, M. Rolandi, *Adv. Sci.* **2017**, *4*, 1600527.
- [10] C. Zhong, Y. Deng, A. F. Roudsari, A. Kapetanovic, M. P. Anantram, M. Rolandi, *Nat. Commun.* **2011**, *2*, 1.
- [11] Y. Deng, E. Josberger, J. Jin, A. F. Roudsari, B. A. Helms, C. Zhong, M. P. Anantram, M. Rolandi, *Sci. Rep.* **2013**, *3*, 2481.
- [12] A. Puiggalf-Jou, L. J. del Valle, C. Alemán, *J. Controlled Release* **2019**, *309*, 244.
- [13] J. Rivnay, S. Inal, B. A. Collins, M. Sessolo, E. Stavrinidou, X. Strakosas, C. Tassone, D. M. DeLongchamp, G. G. Malliaras, *Nat. Commun.* **2016**, *7*, 11287.
- [14] M. Berggren, X. Crispin, S. Fabiano, M. P. Jonsson, D. T. Simon, E. Stavrinidou, K. Tybrandt, I. Zozoulenko, *Adv. Mater.* **2019**, *31*, 1805813.
- [15] J. Rivnay, R. M. Owens, G. G. Malliaras, *Chem. Mater.* **2014**, *26*, 679.
- [16] I. Uguz, C. M. Proctor, V. F. Curto, A.-M. Pappa, M. J. Donahue, M. Ferro, R. M. Owens, D. Khodagholy, S. Inal, G. G. Malliaras, *Adv. Mater.* **2017**, *29*, 1701217.
- [17] G. Horowitz, *Adv. Mater.* **1998**, *10*, 365.
- [18] H. Sirringhaus, *Adv. Mater.* **2014**, *26*, 1319.
- [19] J. Mei, Z. Bao, *Chem. Mater.* **2014**, *26*, 604.
- [20] Y. Kim, S. Cook, S. M. Tuladhar, S. A. Choulis, J. Nelson, J. R. Durrant, D. D. C. Bradley, M. Giles, I. McCulloch, C.-S. Ha, M. Ree, *Nat. Mater.* **2006**, *5*, 197.
- [21] A. Wadsworth, H. Chen, K. J. Thorley, C. Cendra, M. Nikolka, H. Bristow, M. Moser, A. Salleo, T. D. Anthopoulos, H. Sirringhaus, I. McCulloch, *J. Am. Chem. Soc.* **2020**, *142*, 652.
- [22] T. Lei, J.-Y. Wang, J. Pei, *Acc. Chem. Res.* **2014**, *47*, 1117.
- [23] D. Venkateshvaran, M. Nikolka, A. Sadhanala, V. Lemaure, M. Zelazny, M. Kepa, M. Hurhangee, A. J. Kronemeijer, V. Pecunia, I. Nasrallah, I. Romanov, K. Broch, I. McCulloch, D. Emin, Y. Olivier, J. Cornil, D. Beljonne, H. Sirringhaus, *Nature* **2014**, *515*, 384.
- [24] S. G. Higgins, B. V. O. Muir, G. Dell'Erba, A. Perinot, M. Caironi, A. J. Campbell, *Adv. Electron. Mater.* **2016**, *2*, 1500272.
- [25] S. Mandal, G. Dell'Erba, A. Luzio, S. G. Bucella, A. Perinot, A. Calloni, G. Berti, G. Bussetti, L. Duò, A. Facchetti, Y.-Y. Noh, M. Caironi, *Org. Electron.* **2015**, *20*, 132.
- [26] J. Xu, S. Wang, G.-J. N. Wang, C. Zhu, S. Luo, L. Jin, X. Gu, S. Chen, V. R. Feig, J. W. F. To, S. Rondeau-Gagné, J. Park, B. C. Schroeder, C. Lu, J. Y. Oh, Y. Wang, Y.-H. Kim, H. Yan, R. Sinclair, D. Zhou, G. Xue, B. Murmann, C. Linder, W. Cai, J. B.-H. Tok, J. W. Chung, Z. Bao, *Science* **2017**, *355*, 59.
- [27] D. Scaini, L. Ballerini, *Curr. Opin. Neurobiol.* **2018**, *50*, 50.
- [28] J. M. Anderson, A. Rodriguez, D. T. Chang, *Semin. Immunol.* **2008**, *20*, 86.
- [29] J. W. Salatino, K. A. Ludwig, T. D. Y. Kozai, E. K. Purcell, *Nat. Biomed. Eng.* **2017**, *1*, 862.
- [30] S. W. Crowder, V. Leonardo, T. Whittaker, P. Papathanasiou, M. M. Stevens, *Cell Stem Cell* **2016**, *18*, 39.
- [31] T. C. von Erlach, S. Bertazzo, M. A. Wozniak, C.-M. Horejs, S. A. Maynard, S. Attwood, B. K. Robinson, H. Autefage, C. Kallepitis, A. del Río Hernández, C. S. Chen, S. Goldoni, M. M. Stevens, *Nat. Mater.* **2018**, *17*, 237.
- [32] V. Subramanian, A. de la Fuente Vornbrock, S. Moles, D. Soltman, H.-Y. Tseng, in *Organic Electronics II*, (Ed: H. Klauk), Wiley-VCH Verlag GmbH & Co. KGaA, Weinheim, Germany **2012**, pp. 235–254.
- [33] Q. Thiburce, A. J. Campbell, *Adv. Electron. Mater.* **2017**, *3*, 1600421.
- [34] D. Mabeey, R. W. Peeling, A. Ustianowski, M. D. Perkins, *Nat. Rev. Microbiol.* **2004**, *2*, 231.
- [35] K. J. Land, D. I. Boeras, X.-S. Chen, A. R. Ramsay, R. W. Peeling, *Nat. Microbiol.* **2019**, *4*, 46.
- [36] R. S. Jordan, Y. Wang, *J. Polym. Sci., Part B: Polym. Phys.* **2019**, *57*, 1592.
- [37] B. Peng, X. Ren, Z. Wang, X. Wang, R. C. Roberts, P. K. L. Chan, *Sci. Rep.* **2015**, *4*, 6430.
- [38] P. Ihalainen, M. Pesonen, P. Sund, T. Viitala, A. Määttänen, J. Sarfraz, C.-E. Wilén, R. Österbacka, J. Peltonen, *Appl. Surf. Sci.* **2016**, *364*, 477.
- [39] Y. Liu, J. Liu, S. Chen, T. Lei, Y. Kim, S. Niu, H. Wang, X. Wang, A. M. Foudeh, J. B.-H. Tok, Z. Bao, *Nat. Biomed. Eng.* **2019**, *3*, 58.
- [40] X. Qing, Y. Wang, Y. Zhang, X. Ding, W. Zhong, D. Wang, W. Wang, Q. Liu, K. Liu, M. Li, Z. Lu, *ACS Appl. Mater. Interfaces* **2019**, *11*, 13105.
- [41] J. Lee, B. L. Zambrano, J. Woo, K. Yoon, T. Lee, *Adv. Mater.* **2020**, *32*, 1902532.
- [42] E. Bihari, T. Roberts, Y. Zhang, E. Ismailova, T. Hervé, G. G. Malliaras, J. B. D. Graaf, S. Inal, M. Saadaoui, *Flexible Printed Electron.* **2018**, *3*, 034004.
- [43] M. Wang, P. Baek, A. Akbarinejad, D. Barker, J. Trivas-Sejdic, *J. Mater. Chem. C* **2019**, *7*, 5534.
- [44] Z. Deng, H. Wang, P. X. Ma, B. Guo, *Nanoscale* **2020**, *12*, 1224.
- [45] T. Danker, M. Mazzanti, R. Tonini, A. Rakowska, H. Oberleithner, *Cell Biol. Int.* **1997**, *21*, 747.
- [46] M. Zhao, L. Chalmers, L. Cao, A. C. Vieira, M. Mannis, B. Reid, *Prog. Retinal Eye Res.* **2012**, *31*, 65.
- [47] R. Balint, N. J. Cassidy, S. H. Cartmell, *Tissue Eng., Part B: Rev.* **2013**, *19*, 48.

- [48] M. Levin, G. Pezzulo, J. M. Finkelstein, *Annu. Rev. Biomed. Eng.* **2017**, *19*, 353.
- [49] M. Levin, J. Selberg, M. Rolandi, *iScience* **2019**, *22*, 519.
- [50] M. Levin, *BioEssays* **2020**, *42*, 1900146.
- [51] K. A. McLaughlin, M. Levin, *Dev. Biol.* **2018**, *433*, 177.
- [52] M. Zhao, *Semin. Cell Dev. Biol.* **2009**, *20*, 674.
- [53] B. Sakmann, E. Neher, *Annu. Rev. Physiol.* **1984**, *46*, 455.
- [54] Y. Zhang, J. Clausmeyer, B. Babakinejad, A. López Córdoba, T. Ali, A. Shevchuk, Y. Takahashi, P. Novak, C. Edwards, M. Lab, S. Gopal, C. Chiappini, U. Anand, L. Magnani, R. C. Coombes, J. Gorelik, T. Matsue, W. Schuhmann, D. Klenerman, E. V. Sviderskaya, Y. Korchev, *ACS Nano* **2016**, *10*, 3214.
- [55] M. Jakešová, M. S. Ejneby, V. Đerek, T. Schmidt, M. Gryszel, J. Brask, R. Schindl, D. T. Simon, M. Berggren, F. Elinder, E. D. Głowacki, *Sci. Adv.* **2019**, *5*, eaav5265.
- [56] D. Ghezzi, M. R. Antognazza, R. Maccarone, S. Bellani, E. Lanzarini, N. Martino, M. Mete, G. Pertile, S. Bisti, G. Lanzani, F. Benfenati, *Nat. Photonics* **2013**, *7*, 400.
- [57] F. Amorini, I. Zironi, M. Marzocchi, I. Gualandi, M. Calienni, T. Cramer, B. Fraboni, G. Castellani, *ACS Appl. Mater. Interfaces* **2017**, *9*, 6679.
- [58] S. Y. Yeung, X. Gu, C. M. Tsang, S. W. Tsao, I. Hsing, *Sens. Actuators, A* **2019**, *287*, 185.
- [59] S. Inal, A. Hama, M. Ferro, C. Pitsalidis, J. Oziat, D. Iandolo, A.-M. Pappa, M. Hadida, M. Huerta, D. Marchat, P. Mailley, R. M. Owens, *Adv. Biosyst.* **2017**, *1*, 1700052.
- [60] D. Khodagholy, J. N. Gelinas, T. Thesen, W. Doyle, O. Devinsky, G. G. Malliaras, G. Buzsáki, *Nat. Neurosci.* **2015**, *18*, 310.
- [61] W. Lee, D. Kim, J. Rivnay, N. Matsuhisa, T. Lonjaret, T. Yokota, H. Yawo, M. Sekino, G. G. Malliaras, T. Someya, *Adv. Mater.* **2016**, *28*, 9722.
- [62] V. P. Pai, S. Aw, T. Shomrat, J. M. Lemire, M. Levin, *Development* **2012**, *139*, 313.
- [63] A. Accardi, *Science* **2015**, *349*, 789.
- [64] H. M. McNamara, R. Salegame, Z. A. Tanoury, H. Xu, S. Begum, G. Ortiz, O. Pourquie, A. E. Cohen, *Nat. Phys.* **2020**, *16*, 357.
- [65] C. D. McCaig, B. Song, A. M. Rajnicek, *J. Cell Sci.* **2009**, *122*, 4267.
- [66] M. Zhao, B. Song, J. Pu, T. Wada, B. Reid, G. Tai, F. Wang, A. Guo, P. Walczysko, Y. Gu, T. Sasaki, A. Suzuki, J. V. Forrester, H. R. Bourne, P. N. Devreotes, C. D. McCaig, J. M. Penninger, *Nature* **2006**, *442*, 457.
- [67] J. M. Khalifeh, Z. Zohny, M. MacEwan, M. Stephen, W. Johnston, P. Gamble, Y. Zeng, Y. Yan, W. Z. Ray, *IEEE Rev. Biomed. Eng.* **2018**, *11*, 217.
- [68] L. Leppik, K. M. C. Oliveira, M. B. Bhavsar, J. H. Barker, *Eur. J. Trauma Emerg. Surg.* **2020**, *46*, 231.
- [69] K. M. C. Oliveira, J. H. Barker, E. Berezikov, L. Pindur, S. Kynigopoulos, M. Eischen-Loges, Z. Han, M. B. Bhavsar, D. Henrich, L. Leppik, *Sci. Rep.* **2019**, *9*, 11433.
- [70] A. J. Heeger, *Chem. Soc. Rev.* **2010**, *39*, 2354.
- [71] A. J. Heeger, *Angew. Chem., Int. Ed.* **2001**, *40*, 2591.
- [72] M. Fahlman, S. Fabiano, V. Gueskine, D. Simon, M. Berggren, X. Crispin, *Nat. Rev. Mater.* **2019**, *4*, 627.
- [73] M. N. Gueye, A. Carella, J. Faure-Vincent, R. Demadrille, J.-P. Simonato, *Prog. Mater. Sci.* **2020**, *108*, 100616.
- [74] K. Kang, S. Watanabe, K. Broch, A. Sepe, A. Brown, I. Nasrallah, M. Nikolka, Z. Fei, M. Heeney, D. Matsumoto, K. Marumoto, H. Tanaka, S. Kuroda, H. Sirringhaus, *Nat. Mater.* **2016**, *15*, 896.
- [75] *Organic Electronics II: More Materials and Applications*, (Ed: H. Klauk), Wiley-VCH Verlag GmbH & Co. KGaA, Weinheim, Germany **2012**.
- [76] S. M. Sze, K. K. Ng, in *Physics of Semiconductor Devices*, John Wiley & Sons Ltd, Hoboken, NJ **2007**, pp. 7–75.
- [77] Y. Sui, Y. Deng, T. Du, Y. Shi, Y. Geng, *Mater. Chem. Front.* **2019**, *3*, 1932.
- [78] Z. Chen, H. Lemke, S. Albert-Seifried, M. Caironi, M. M. Nielsen, M. Heeney, W. Zhang, I. McCulloch, H. Sirringhaus, *Adv. Mater.* **2010**, *22*, 2371.
- [79] T. M. Swager, *Macromolecules* **2017**, *50*, 4867.
- [80] J. Rivnay, S. Inal, A. Salleo, R. M. Owens, M. Berggren, G. G. Malliaras, *Nat. Rev. Mater.* **2018**, *3*, 17086.
- [81] E.-G. Kim, J.-L. Brédas, *J. Am. Chem. Soc.* **2008**, *130*, 16880.
- [82] B. Kippelen, J.-L. Brédas, *Energy Environ. Sci.* **2009**, *2*, 251.
- [83] B. Yurash, D. X. Cao, V. V. Brus, D. Leifert, M. Wang, A. Dixon, M. Seifrid, A. E. Mansour, D. Lungwitz, T. Liu, P. J. Santiago, K. R. Graham, N. Koch, G. C. Bazan, T.-Q. Nguyen, *Nat. Mater.* **2019**, *18*, 1327.
- [84] M. Schwarze, C. Gaul, R. Scholz, F. Bussolotti, A. Hofacker, K. S. Schellhammer, B. Nell, B. D. Naab, Z. Bao, D. Spoltore, K. Vandewal, J. Widmer, S. Kera, N. Ueno, F. Ortman, K. Leo, *Nat. Mater.* **2019**, *18*, 242.
- [85] M. C. Gwinner, R. D. Pietro, Y. Vaynzof, K. J. Greenberg, P. K. H. Ho, R. H. Friend, H. Sirringhaus, *Adv. Funct. Mater.* **2011**, *21*, 1432.
- [86] K. Lee, S. Cho, S. H. Park, A. J. Heeger, C.-W. Lee, S.-H. Lee, *Nature* **2006**, *441*, 65.
- [87] O. Bubnova, Z. U. Khan, H. Wang, S. Braun, D. R. Evans, M. Fabretto, P. Hojati-Talemi, D. Dagnelund, J.-B. Arlin, Y. H. Geerts, S. Desbief, D. W. Breiby, J. W. Andreasen, R. Lazzaroni, W. M. Chen, I. Zozoulenko, M. Fahlman, P. J. Murphy, M. Berggren, X. Crispin, *Nat. Mater.* **2014**, *13*, 190.
- [88] I. Zozoulenko, A. Singh, S. K. Singh, V. Gueskine, X. Crispin, M. Berggren, *ACS Appl. Polym. Mater.* **2019**, *1*, 83.
- [89] K. Tybrandt, I. V. Zozoulenko, M. Berggren, *Sci. Adv.* **2017**, *3*, eaao3659.
- [90] V. Kaphle, P. R. Paudel, D. Dahal, R. K. Radha Krishnan, B. Lüssem, *Nat. Commun.* **2020**, *11*, 2515.
- [91] A. V. Volkov, K. Wijeratne, E. Mitraka, U. Ail, D. Zhao, K. Tybrandt, J. W. Andreasen, M. Berggren, X. Crispin, I. V. Zozoulenko, *Adv. Funct. Mater.* **2017**, *27*, 1700329.
- [92] C. M. Proctor, J. Rivnay, G. G. Malliaras, *J. Polym. Sci., Part B: Polym. Phys.* **2016**, *54*, 1433.
- [93] R. Noriega, J. Rivnay, K. Vandewal, F. P. V. Koch, N. Stingelin, P. Smith, M. F. Toney, A. Salleo, *Nat. Mater.* **2013**, *12*, 1038.
- [94] H. F. Haneef, A. M. Zeidell, O. D. Jurchescu, *J. Mater. Chem. C* **2020**, *8*, 759.
- [95] M. Nikolka, M. Hurhangee, A. Sadhanala, H. Chen, I. McCulloch, H. Sirringhaus, *Adv. Electron. Mater.* **2018**, *4*, 1700410.
- [96] N. Rolland, J. F. Franco-Gonzalez, R. Volpi, M. Linares, I. V. Zozoulenko, *Phys. Rev. Mater.* **2018**, *2*, 045605.
- [97] A. G. MacDiarmid, A. J. Epstein, *Synth. Met.* **1994**, *65*, 103.
- [98] M. Nikolka, G. Schweicher, J. Armitage, I. Nasrallah, C. Jellet, Z. Guo, M. Hurhangee, A. Sadhanala, I. McCulloch, C. B. Nielsen, H. Sirringhaus, *Adv. Mater.* **2018**, *30*, 1801874.
- [99] S. P. White, K. D. Dorfman, C. D. Frisbie, *J. Phys. Chem. C* **2016**, *120*, 108.
- [100] E. Macchia, R. A. Picca, K. Manoli, C. Di Franco, D. Blasi, L. Sarcina, N. Ditaranto, N. Cioffi, R. Österbacka, G. Scamarcio, F. Torricelli, L. Torsi, *Mater. Horiz.* **2020**, *7*, 999.
- [101] Z. S. Kim, S. C. Lim, S. H. Kim, Y. S. Yang, D. H. Hwang, *Sensors* **2012**, *12*, 11238.
- [102] R. A. Picca, K. Manoli, E. Macchia, L. Sarcina, C. Di Franco, N. Cioffi, D. Blasi, R. Österbacka, F. Torricelli, G. Scamarcio, L. Torsi, *Adv. Funct. Mater.* **2019**, *30*, 1904513.
- [103] M. Y. Mulla, P. Seshadri, L. Torsi, K. Manoli, A. Mallardi, N. Ditaranto, M. V. Santacroce, C. Di Franco, G. Scamarcio, M. Magliulo, *J. Mater. Chem. B* **2015**, *3*, 5049.
- [104] X. Strakosas, B. Wei, D. C. Martin, R. M. Owens, *J. Mater. Chem. B* **2016**, *4*, 4952.
- [105] P. Didier, N. Lobato-Dauzier, N. Clément, A. J. Genot, Y. Sasaki, É. Leclerc, T. Minamiki, Y. Sakai, T. Fujii, T. Minami, *ChemElectroChem* **2020**, *7*, 1332.

- [106] E. Macchia, P. Romele, K. Manoli, M. Ghittorelli, M. Magliulo, Z. M. Kovács-Vajna, F. Torricelli, L. Torsi, *Flexible Printed Electron.* **2018**, *3*, 034002.
- [107] J. Song, J. Dailey, H. Li, H.-J. Jang, P. Zhang, J. T.-H. Wang, A. D. Everett, H. E. Katz, *Adv. Funct. Mater.* **2017**, *27*, 1606506.
- [108] S. Casalini, A. C. Dumitru, F. Leonardi, C. A. Bortolotti, E. T. Herruzo, A. Campana, R. F. de Oliveira, T. Cramer, R. Garcia, F. Biscarini, *ACS Nano* **2015**, *9*, 5051.
- [109] D.-J. Kim, N.-E. Lee, J.-S. Park, I.-J. Park, J.-G. Kim, H. J. Cho, *Biosens. Bioelectron.* **2010**, *25*, 2477.
- [110] C. Napoli, S. Lai, A. Giannetti, S. Tombelli, F. Baldini, M. Barbaro, A. Bonfiglio, *Sensors* **2018**, *18*, 990.
- [111] S. P. White, K. D. Dorfman, C. D. Frisbie, *Anal. Chem.* **2015**, *87*, 1861.
- [112] A. M. Pappa, V. F. Curto, M. Braendlein, X. Strakosas, M. J. Donahue, M. Fiocchi, G. G. Malliaras, R. M. Owens, *Adv. Healthcare Mater.* **2016**, *5*, 2295.
- [113] E. Tan, A.-M. Pappa, C. Pitsalidis, J. Nightingale, S. Wood, F. A. Castro, R. M. Owens, J.-S. Kim, *Biotechnol. Bioeng.* **2020**, *117*, 291.
- [114] M. Braendlein, A.-M. Pappa, M. Ferro, A. Lopresti, C. Acquaviva, E. Mamessier, G. G. Malliaras, R. M. Owens, *Adv. Mater.* **2017**, *29*, 1605744.
- [115] A. M. Pappa, O. Parlak, G. Scheiblin, P. Mailley, A. Salleo, R. M. Owens, *Trends Biotechnol.* **2018**, *36*, 45.
- [116] J. T. Friedlein, R. R. McLeod, J. Rivnay, *Org. Electron.* **2018**, *63*, 398.
- [117] J. Borges-González, C. J. Kousseff, C. B. Nielsen, *J. Mater. Chem. C* **2019**, *7*, 1111.
- [118] M. Berggren, G. G. Malliaras, *Science* **2019**, *364*, 233.
- [119] E. S. Place, N. D. Evans, M. M. Stevens, *Nat. Mater.* **2009**, *8*, 457.
- [120] L. Chen, C. Yan, Z. Zheng, *Mater. Today* **2018**, *21*, 38.
- [121] J. T. Parsons, A. R. Horwitz, M. A. Schwartz, *Nat. Rev. Mol. Cell Biol.* **2010**, *11*, 633.
- [122] J. Z. Kechagia, J. Ivaska, P. Roca-Cusachs, *Nat. Rev. Mol. Cell Biol.* **2019**, *20*, 457.
- [123] N. Wang, J. D. Tytell, D. E. Ingber, *Nat. Rev. Mol. Cell Biol.* **2009**, *10*, 75.
- [124] L. Ghasemi-Mobarakeh, M. P. Prabhakaran, M. Morshed, M. H. Nasr-Esfahani, H. Baharvand, S. Kiani, S. S. Al-Deyab, S. Ramakrishna, *J. Tissue Eng. Regener. Med.* **2011**, *5*, e17.
- [125] U. Hersel, C. Dahmen, H. Kessler, *Biomaterials* **2003**, *24*, 4385.
- [126] G. Oyman, C. Geyik, R. Ayranci, M. Ak, D. O. Demirkol, S. Timur, H. Coskunol, *RSC Adv.* **2014**, *4*, 53411.
- [127] E. W. C. Chan, D. Bennet, P. Baek, D. Barker, S. Kim, J. Travas-Sejdic, *Biomacromolecules* **2018**, *19*, 1456.
- [128] W. Du, D. Ohayon, C. Combe, L. Mottier, I. P. Maria, R. S. Ashraf, H. Fiumelli, S. Inal, I. McCulloch, *Chem. Mater.* **2018**, *30*, 6164.
- [129] A. Venturato, G. MacFarlane, J. Geng, M. Bradley, *Macromol. Biosci.* **2016**, *16*, 1864.
- [130] F. Pires, Q. Ferreira, C. A. V. Rodrigues, J. Morgado, F. C. Ferreira, *Biochim. Biophys. Acta, Gen. Subj.* **2015**, *1850*, 1158.
- [131] X. Zhou, A. Yang, Z. Huang, G. Yin, X. Pu, J. Jin, *Colloids Surf., B* **2017**, *149*, 217.
- [132] M. Schroepfer, F. Junghans, D. Voigt, M. Meyer, A. Breier, G. Schulze-Tanzil, I. Prade, *ACS Omega* **2020**, *5*, 5498.
- [133] A. J. Hackett, J. Malmström, J. Travas-Sejdic, *Prog. Polym. Sci.* **2017**, *70*, 18.
- [134] C. Pitsalidis, M. P. Ferro, D. Iandolo, L. Tzounis, S. Inal, R. M. Owens, *Sci. Adv.* **2018**, *4*, 4253.
- [135] D. Mawad, C. Mansfield, A. Lauto, F. Perbellini, G. W. Nelson, J. Tonkin, S. O. Bello, D. J. Carrad, A. P. Micolich, M. M. Mahat, J. Furman, D. Payne, A. R. Lyon, J. J. Gooding, S. E. Harding, C. M. Terracciano, M. M. Stevens, *Sci. Adv.* **2016**, *2*, e1601007.
- [136] C. Uhler, G. V. Shivashankar, *Nat. Rev. Mol. Cell Biol.* **2017**, *18*, 717.
- [137] A. Blau, *Curr. Opin. Colloid Interface Sci.* **2013**, *18*, 481.
- [138] J. Y. Wong, R. Langer, D. E. Ingber, *Proc. Natl. Acad. Sci. USA* **1994**, *91*, 3201.
- [139] A. M.-D. Wan, S. Inal, T. Williams, K. Wang, P. Leleux, L. Estevez, E. P. Giannelis, C. Fischbach, G. G. Malliaras, D. Gourdon, *J. Mater. Chem. B* **2015**, *3*, 5040.
- [140] A. M. D. Wan, D. J. Brooks, A. Gumus, C. Fischbach, G. G. Malliaras, *Chem. Commun.* **2009**, 5278.
- [141] M. Marzocchi, I. Gualandi, M. Calienni, I. Zironi, E. Scavetta, G. Castellani, B. Fraboni, *ACS Appl. Mater. Interfaces* **2015**, *7*, 17993.
- [142] C. Saltó, E. Saindon, M. Bolin, A. Kancierzewska, M. Fahlman, E. W. H. Jager, P. Tengvall, E. Arenas, M. Berggren, *Langmuir* **2008**, *24*, 14133.
- [143] P. J. Molino, M. J. Higgins, P. C. Innis, R. M. I. Kapsa, G. G. Wallace, *Langmuir* **2012**, *28*, 8433.
- [144] F. Lotti, F. Ranieri, G. Vadalà, L. Zollo, G. Di Pino, *Front. Neurosci.* **2017**, *11*, 497.
- [145] M. Kapnisi, C. Mansfield, C. Marijon, A. G. Guex, F. Perbellini, I. Bardi, E. J. Humphrey, J. L. Puetzer, D. Mawad, D. C. Koutsogeorgis, D. J. Stuckey, C. M. Terracciano, S. E. Harding, M. M. Stevens, *Adv. Funct. Mater.* **2018**, *28*, 1800618.
- [146] A. Prasad, Q.-S. Xue, V. Sankar, T. Nishida, G. Shaw, W. J. Streit, J. C. Sanchez, *J. Neural Eng.* **2012**, *9*, 056015.
- [147] L. Ouyang, C. L. Shaw, C. Kuo, A. L. Griffin, D. C. Martin, *J. Neural Eng.* **2014**, *11*, 026005.
- [148] D. C. Martin, *MRS Commun.* **2015**, *5*, 131.
- [149] H. Yuk, B. Lu, X. Zhao, *Chem. Soc. Rev.* **2019**, *48*, 1642.
- [150] A. Gelmi, A. Cieslar-Pobuda, E. de Muinck, M. Los, M. Rafat, E. W. H. Jager, *Adv. Healthcare Mater.* **2016**, *5*, 1471.
- [151] B. Guo, P. X. Ma, *Biomacromolecules* **2018**, *19*, 1764.
- [152] U. Ail, M. J. Jafari, H. Wang, T. Ederth, M. Berggren, X. Crispin, *Adv. Funct. Mater.* **2016**, *26*, 6288.
- [153] A. M. Pappa, D. Ohayon, A. Giovannitti, I. P. Maria, A. Savva, I. Uguz, J. Rivnay, I. McCulloch, R. M. Owens, S. Inal, *Sci. Adv.* **2018**, *4*, 0911.
- [154] C. E. Schmidt, V. R. Shastri, J. P. Vacanti, R. Langer, *Proc. Natl. Acad. Sci. USA* **1997**, *94*, 8948.
- [155] A. S. Rowlands, J. J. Cooper-White, *Biomaterials* **2008**, *29*, 4510.
- [156] B. C. Thompson, R. T. Richardson, S. E. Moulton, A. J. Evans, S. O'Leary, G. M. Clark, G. G. Wallace, *J. Controlled Release* **2010**, *141*, 161.
- [157] S. Meng, Z. Zhang, M. Rouabhia, *J. Bone Miner. Metab.* **2011**, *29*, 535.
- [158] R. Saigal, E. Cimetta, N. Tandon, J. Zhou, R. Langer, M. Young, G. Vunjak-Novakovic, S. Redenti, in *2013 35th Annual Int. Conf. of the IEEE Engineering in Medicine and Biology Society (EMBC)*, IEEE, Piscataway, NJ **2013**, pp. 1627–1631.
- [159] Q. Zhang, D. Esrafilzadeh, J. M. Crook, R. Kapsa, E. M. Stewart, E. Tomaskovic-Crook, G. G. Wallace, X.-F. Huang, *Sci. Rep.* **2017**, *7*, 42525.
- [160] H. Zhang, G. G. Wallace, M. J. Higgins, *Biointerphases* **2019**, *14*, 021003.
- [161] B. Zhang, A. R. Nagle, G. G. Wallace, T. W. Hanks, P. J. Molino, *Biofouling* **2015**, *31*, 493.
- [162] R. T. Richardson, A. K. Wise, B. C. Thompson, B. O. Flynn, P. J. Atkinson, N. J. Fretwell, J. B. Fallon, G. G. Wallace, R. K. Shepherd, G. M. Clark, S. J. O'Leary, *Biomaterials* **2009**, *30*, 2614.
- [163] B. S. Spearman, A. J. Hodge, J. L. Porter, J. G. Hardy, Z. D. Davis, T. Xu, X. Zhang, C. E. Schmidt, M. C. Hamilton, E. A. Lipke, *Acta Biomater.* **2015**, *28*, 109.
- [164] M. P. Prabhakaran, L. Ghasemi-Mobarakeh, G. Jin, S. Ramakrishna, *J. Biosci. Bioeng.* **2011**, *112*, 501.
- [165] M. Kaisti, Z. Boeva, J. Koskinen, S. Nieminen, J. Bobacka, K. Levon, *ACS Sens.* **2016**, *1*, 1423.

- [166] C.-W. Hsiao, M.-Y. Bai, Y. Chang, M.-F. Chung, T.-Y. Lee, C.-T. Wu, B. Maiti, Z.-X. Liao, R.-K. Li, H.-W. Sung, *Biomaterials* **2013**, *34*, 1063.
- [167] T. H. Qazi, R. Rai, A. R. Boccaccini, *Biomaterials* **2014**, *35*, 9068.
- [168] Y. Fan, X. Chen, A. D. Trigg, C. Tung, J. Kong, Z. Gao, *J. Am. Chem. Soc.* **2007**, *129*, 5437.
- [169] K. S. Nalwa, Y. Cai, A. L. Thoeming, J. Shinar, R. Shinar, S. Chaudhary, *Adv. Mater.* **2010**, *22*, 4157.
- [170] N. Martino, P. Feyen, M. Porro, C. Bossio, E. Zucchetti, D. Ghezzi, F. Benfenati, G. Lanzani, M. R. Antognazza, *Sci. Rep.* **2015**, *5*, 8911.
- [171] Y. Wu, Y. Peng, H. Bohra, J. Zou, V. D. Ranjan, Y. Zhang, Q. Zhang, M. Wang, *ACS Appl. Mater. Interfaces* **2019**, *11*, 4833.
- [172] M. Magliulo, D. De Tullio, I. Vikholm-Lundin, W. M. Albers, T. Munter, K. Manoli, G. Palazzo, L. Torsi, *Anal. Bioanal. Chem.* **2016**, *408*, 3943.
- [173] R. A. Picca, K. Manoli, A. Luciano, M. C. Sportelli, G. Palazzo, L. Torsi, N. Cioffi, *Sens. Actuators, B* **2018**, *274*, 210.
- [174] P. Seshadri, K. Manoli, N. Schneiderhan-Marra, U. Anthes, P. Wierzychowiec, K. Bonrad, C. Di Franco, L. Torsi, *Biosens. Bioelectron.* **2018**, *104*, 113.
- [175] S. Casalini, F. Leonardi, T. Cramer, F. Biscarini, *Org. Electron.* **2013**, *14*, 156.
- [176] K. Schmoltner, J. Kofler, A. Klug, E. J. W. List-Kratochvil, *Adv. Mater.* **2013**, *25*, 6895.
- [177] P. Cavassin, A.-M. Pappa, C. Pitsalidis, H. F. P. Barbosa, R. Colucci, J. Saez, Y. Tuchman, A. Salleo, G. C. Faria, R. M. Owens, *Adv. Mater. Technol.* **2020**, *5*, 1900680.
- [178] Y. Zhang, S. Wustoni, A. Savva, A. Giovannitti, I. McCulloch, S. Inal, *J. Mater. Chem. C* **2018**, *6*, 5218.
- [179] E. Zeglio, O. Inganäs, *Adv. Mater.* **2018**, *30*, 1800941.
- [180] M. Moser, J. F. Ponder Jr., A. Wadsworth, A. Giovannitti, I. McCulloch, *Adv. Funct. Mater.* **2019**, *29*, 1807033.
- [181] M. J. Donahue, A. Sanchez-Sanchez, S. Inal, J. Qu, R. M. Owens, D. Mecerreyes, G. G. Malliaras, D. C. Martin, *Mater. Sci. Eng., R* **2020**, *140*, 100546.
- [182] W. Lövenich, *Polym. Sci., Ser. C* **2014**, *56*, 135.
- [183] A. Al Baroot, A. Alshammari, M. Grell, *Thin Solid Films* **2019**, *669*, 665.
- [184] D. Zhao, L. Li, W. Niu, S. Chen, *Sens. Actuators, B* **2017**, *243*, 380.
- [185] E. Lim, K. A. Peterson, G. M. Su, M. L. Chabiny, *Chem. Mater.* **2018**, *30*, 998.
- [186] X. Wang, X. Zhang, L. Sun, D. Lee, S. Lee, M. Wang, J. Zhao, Y. Shao-Horn, M. Dincă, T. Palacios, K. K. Gleason, *Sci. Adv.* **2018**, *4*, 5780.
- [187] A. Savva, D. Ohayon, J. Surgailis, A. F. Paterson, T. C. Hidalgo, X. Chen, I. P. Maria, B. D. Paulsen, A. J. Petty, J. Rivnay, I. McCulloch, S. Inal, *Adv. Electron. Mater.* **2019**, *5*, 1900249.
- [188] C. B. Nielsen, A. Giovannitti, D.-T. Sbircea, E. Bandiello, M. R. Niazi, D. A. Hanifi, M. Sessolo, A. Amassian, G. G. Malliaras, J. Rivnay, I. McCulloch, *J. Am. Chem. Soc.* **2016**, *138*, 10252.
- [189] A. Giovannitti, D.-T. Sbircea, S. Inal, C. B. Nielsen, E. Bandiello, D. A. Hanifi, M. Sessolo, G. G. Malliaras, I. McCulloch, J. Rivnay, *Proc. Natl. Acad. Sci. USA* **2016**, *113*, 12017.
- [190] Z. S. Parr, R. Halaksa, P. A. Finn, R. B. Rashid, A. Kovalenko, M. Weiter, J. Rivnay, J. Krajčovič, C. B. Nielsen, *ChemPlusChem* **2019**, *84*, 1384.
- [191] V. Venkatraman, J. T. Friedlein, A. Giovannitti, I. P. Maria, I. McCulloch, R. R. McLeod, J. Rivnay, *Adv. Sci.* **2018**, *5*, 1800453.
- [192] S. Wustoni, C. Combe, D. Ohayon, M. H. Akhtar, I. McCulloch, S. Inal, *Adv. Funct. Mater.* **2019**, *29*, 1904403.
- [193] A. Giovannitti, C. B. Nielsen, J. Rivnay, M. Kirkus, D. J. Harkin, A. J. P. White, H. Sirringhaus, G. G. Malliaras, I. McCulloch, *Adv. Funct. Mater.* **2016**, *26*, 514.
- [194] R. B. Dabke, G. D. Singh, A. Dhanabalan, R. Lal, A. Q. Contractor, *Anal. Chem.* **1997**, *69*, 724.
- [195] S. T. Keene, D. Fogarty, R. Cooke, C. D. Casadevall, A. Salleo, O. Parlak, *Adv. Healthcare Mater.* **2019**, *8*, 1901321.
- [196] N. Coppedè, M. Giannetto, M. Villani, V. Lucchini, E. Battista, M. Careri, A. Zappettini, *Org. Electron.* **2020**, *78*, 105579.
- [197] L. Groenendaal, F. Jonas, D. Freitag, H. Pielartzik, J. R. Reynolds, *Adv. Mater.* **2000**, *12*, 481.
- [198] J. F. Ponder, A. M. Österholm, J. R. Reynolds, *Macromolecules* **2016**, *49*, 2106.
- [199] J. L. Brédas, F. Wudl, A. J. Heeger, *Solid State Commun.* **1987**, *63*, 577.
- [200] R. A. Matula, *J. Phys. Chem. Ref. Data* **1979**, *8*, 1147.
- [201] H. Yano, K. Kudo, K. Marumo, H. Okuzaki, *Sci. Adv.* **2019**, *5*, 9492.
- [202] X. Crispin, F. L. E. Jakobsson, A. Crispin, P. C. M. Grim, P. Andersson, A. Volodin, C. van Haesendonck, M. Van der Auweraer, W. R. Salaneck, M. Berggren, *Chem. Mater.* **2006**, *18*, 4354.
- [203] R. H. Karlsson, A. Herland, M. Hamed, J. A. Wigenius, A. Åslund, X. Liu, M. Fahlman, O. Inganäs, P. Konradsson, *Chem. Mater.* **2009**, *21*, 1815.
- [204] B. Guo, Q. Yin, J. Zhou, W. Li, K. Zhang, Y. Li, *ACS Sustainable Chem. Eng.* **2019**, *7*, 8206.
- [205] S. T. Larsen, R. F. Vreeland, M. L. Heien, R. Taboryski, *Analyst* **2012**, *137*, 1831.
- [206] S. Inal, J. Rivnay, A. I. Hofmann, I. Uguz, M. Mumtaz, D. Katsigiannopoulos, C. Brochon, E. Cloutet, G. Hadziioannou, G. G. Malliaras, *J. Polym. Sci., Part B: Polym. Phys.* **2016**, *54*, 147.
- [207] P. J. Molino, Z. Yue, B. Zhang, A. Tibbens, X. Liu, R. M. I. Kapsa, M. J. Higgins, G. G. Wallace, *Adv. Mater. Interfaces* **2014**, *1*, 1300122.
- [208] S. Tekoglu, D. Wielend, M. C. Scharber, N. S. Sariciftci, C. Yumusak, *Adv. Mater. Technol.* **2020**, *5*, 1900699.
- [209] H. Shi, C. Liu, Q. Jiang, J. Xu, *Adv. Electron. Mater.* **2015**, *1*, 1500017.
- [210] E. Zeglio, M. Vagin, C. Musumeci, F. N. Ajjan, R. Gabriellsson, X. T. Trinh, N. T. Son, A. Maziz, N. Solin, O. Inganäs, *Chem. Mater.* **2015**, *27*, 6385.
- [211] K. M. Persson, R. Karlsson, K. Svennersten, S. Löffler, E. W. H. Jager, A. Richter-Dahlfors, P. Konradsson, M. Berggren, *Adv. Mater.* **2011**, *23*, 4403.
- [212] S. Inal, J. Rivnay, P. Leleux, M. Ferro, M. Ramuz, J. C. Brendel, M. M. Schmidt, M. Thelakkat, G. G. Malliaras, *Adv. Mater.* **2014**, *26*, 7450.
- [213] Y. Wang, C. Zhu, R. Pfattner, H. Yan, L. Jin, S. Chen, F. Molina-Lopez, F. Lissel, J. Liu, N. I. Rabiah, Z. Chen, J. W. Chung, C. Linder, M. F. Toney, B. Murmann, Z. Bao, *Sci. Adv.* **2017**, *3*, 1602076.
- [214] J. Y. Oh, S. Rondeau-Gagné, Y.-C. Chiu, A. Chortos, F. Lissel, G.-J. N. Wang, B. C. Schroeder, T. Kurosawa, J. Lopez, T. Katsumata, J. Xu, C. Zhu, X. Gu, W.-G. Bae, Y. Kim, L. Jin, J. W. Chung, J. B.-H. Tok, Z. Bao, *Nature* **2016**, *539*, 411.
- [215] M. Ashizawa, Y. Zheng, H. Tran, Z. Bao, *Prog. Polym. Sci.* **2020**, *100*, 101181.
- [216] F. Decataldo, T. Cramer, D. Martelli, I. Gualandi, W. S. Korim, S. T. Yao, M. Tassarolo, M. Murgia, E. Scavetta, R. Amici, B. Fraboni, *Sci. Rep.* **2019**, *9*, 10598.
- [217] M. Sasaki, B. C. Karikkineth, K. Nagamine, H. Kaji, K. Torimitsu, M. Nishizawa, *Adv. Healthcare Mater.* **2014**, *3*, 1919.
- [218] E. Cuttaz, J. Goding, C. Valles-Giraldo, U. Aregueta-Robles, N. Lovell, D. Ghezzi, R. A. Green, *Biomater. Sci.* **2019**, *7*, 1372.
- [219] D. Mawad, A. Artzy-Schnirman, J. Tonkin, J. Ramos, S. Inal, M. M. Mahat, N. Darwish, L. Zwi-Dantsis, G. G. Malliaras, J. J. Gooding, A. Lauto, M. M. Stevens, *Chem. Mater.* **2016**, *28*, 6080.
- [220] D.-H. Kim, N. Lu, R. Ma, Y.-S. Kim, R.-H. Kim, S. Wang, J. Wu, S. M. Won, H. Tao, A. Islam, K. J. Yu, T. Kim, R. Chowdhury, M. Ying, L. Xu, M. Li, H.-J. Chung, H. Keum, M. McCormick,

- P. Liu, Y.-W. Zhang, F. G. Omenetto, Y. Huang, T. Coleman, J. A. Rogers, *Science* **2011**, 333, 838.
- [221] V. R. Feig, H. Tran, Z. Bao, *ACS Cent. Sci.* **2018**, 4, 337.
- [222] C. J. Bettinger, Z. Bao, *Adv. Mater.* **2010**, 22, 651.
- [223] M. Jia, M. Rolandi, *Adv. Healthcare Mater.* **2020**, 9, 1901372.
- [224] L. V. Kayser, D. J. Lipomi, *Adv. Mater.* **2019**, 31, 1806133.
- [225] D. Khodagholy, J. N. Gelinias, G. Buzsáki, *Science* **2017**, 358, 369.
- [226] J. Pas, C. Pitsalidis, D. A. Koutsouras, P. P. Quilichini, F. Santoro, B. Cui, L. Gallais, R. P. O'Connor, G. G. Malliaras, R. M. Owens, *Adv. Biosyst.* **2018**, 2, 1700164.
- [227] A. Schander, T. Teßmann, S. Strokov, H. Stemmann, A. K. Kreiter, W. Lang, in *2016 38th Annual Int. Conf. of the IEEE Engineering in Medicine and Biology Society (EMBC)*, IEEE, Piscataway, NJ **2016**, pp. 6174–6177.
- [228] B. Zhu, S.-C. Luo, H. Zhao, H.-A. Lin, J. Sekine, A. Nakao, C. Chen, Y. Yamashita, H. Yu, *Nat. Commun.* **2014**, 5, 4523.
- [229] A. S. Karimullah, D. R. S. Cumming, M. Riehle, N. Gadegaard, *Sens. Actuators, B* **2013**, 176, 667.
- [230] W.-W. Hu, T.-C. Chen, C.-W. Tsao, Y.-C. Cheng, *J. Biomed. Mater. Res., Part B* **2019**, 107, 1607.
- [231] D. A. Koutsouras, L. V. Lingstedt, K. Lieberth, J. Reinholz, V. Mailänder, P. W. M. Blom, P. Gkoupidenis, *Adv. Healthcare Mater.* **2019**, 8, 1901215.
- [232] L. Kergoat, G. Dieuset, V. Le Rolle, G. G. Malliaras, B. Martin, C. Bernard, A. I. Hernández, in *2018 40th Annual Int. Conf. of the IEEE Engineering in Medicine and Biology Society (EMBC)*, IEEE, Piscataway, NJ **2018**, pp. 4760–4763.
- [233] M. Ganji, E. Kaestner, J. Hermiz, N. Rogers, A. Tanaka, D. Cleary, S. H. Lee, J. Snider, M. Halgren, G. R. Cosgrove, B. S. Carter, D. Barba, I. Uguz, G. G. Malliaras, S. S. Cash, V. Gilja, E. Halgren, S. A. Dayeh, *Adv. Funct. Mater.* **2018**, 28, 1700232.
- [234] G. D. Spyropoulos, J. Savarin, E. F. Gomez, D. T. Simon, M. Berggren, J. N. Gelinias, E. Stavrinidou, D. Khodagholy, *Adv. Mater. Technol.* **2020**, 5, 1900652.
- [235] K. Qu, S. M. Kondengaden, J. Li, X. Wang, M. D. Sevilla, L. Li, X. Zeng, *Appl. Surf. Sci.* **2019**, 486, 561.
- [236] C. Kigure, H. Naganuma, Y. Sasaki, H. Kino, H. Tomita, T. Tanaka, *Jpn. J. Appl. Phys.* **2013**, 52, 04CL03.
- [237] Y. Zhang, Y. Chen, Y. Qi, D. Huang, M. Yang, X. Yu, Y. Hu, Z. Li, *Sens. Actuators, B* **2016**, 237, 1007.
- [238] S. M. Richardson-Burns, J. L. Hendricks, B. Foster, L. K. Povlich, D.-H. Kim, D. C. Martin, *Biomaterials* **2007**, 28, 1539.
- [239] L. M. Ferrari, S. Sudha, S. Tarantino, R. Esposti, F. Bolzoni, P. Cavallari, C. Cipriani, V. Mattoli, F. Greco, *Adv. Sci.* **2018**, 5, 1700771.
- [240] N. V. de Camp, G. Kalinka, J. Bergeler, *Sci. Rep.* **2018**, 8, 14041.
- [241] A. Zucca, C. Cipriani, Sudha, S. Tarantino, D. Ricci, V. Mattoli, F. Greco, *Adv. Healthcare Mater.* **2015**, 4, 983.
- [242] P. Leleux, J.-M. Badier, J. Rivnay, C. Bénar, T. Hervé, P. Chauvel, G. G. Malliaras, *Adv. Healthcare Mater.* **2014**, 3, 490.
- [243] H.-C. Tian, J.-Q. Liu, X.-Y. Kang, Q. He, B. Yang, X. Chen, C.-S. Yang, *Sens. Actuators, A* **2015**, 228, 28.
- [244] J. A. Chikar, J. L. Hendricks, S. M. Richardson-Burns, Y. Raphael, B. E. Pflingst, D. C. Martin, *Biomaterials* **2012**, 33, 1982.
- [245] T. D. Y. Kozai, K. Catt, Z. Du, K. Na, O. Srivannavit, R. M. Haque, J. Seymour, K. D. Wise, E. Yoon, X. T. Cui, *IEEE Trans. Biomed. Eng.* **2016**, 63, 111.
- [246] L. Zhou, L. Fan, X. Yi, Z. Zhou, C. Liu, R. Fu, C. Dai, Z. Wang, X. Chen, P. Yu, D. Chen, G. Tan, Q. Wang, C. Ning, *ACS Nano* **2018**, 12, 10957.
- [247] A. Mihic, Z. Cui, J. Wu, G. Vlacic, Y. Miyagi, S.-H. Li, S. Lu, H.-W. Sung, R. D. Weisel, R.-K. Li, *Circulation* **2015**, 132, 772.
- [248] Z. Cui, N. C. Ni, J. Wu, G.-Q. Du, S. He, T. M. Yau, R. D. Weisel, H.-W. Sung, R.-K. Li, *Theranostics* **2018**, 8, 2752.
- [249] S. Liang, Y. Zhang, H. Wang, Z. Xu, J. Chen, R. Bao, B. Tan, Y. Cui, G. Fan, W. Wang, W. Liu, *Adv. Mater.* **2018**, 30, 1704235.
- [250] C. Cui, N. Faraji, A. Lauto, L. Travaglini, J. Tonkin, D. Mahns, E. Humphrey, C. Terracciano, J. J. Gooding, J. Seidel, D. Mawad, *Biomater. Sci.* **2018**, 6, 493.
- [251] X. Strakosas, M. Sessolo, A. Hama, J. Rivnay, E. Stavrinidou, G. G. Malliaras, R. M. Owens, *J. Mater. Chem. B* **2014**, 2, 2537.
- [252] A. G. Guex, C. D. Spicer, A. Armgarth, A. Gelmi, E. J. Humphrey, C. M. Terracciano, S. E. Harding, M. M. Stevens, *MRS Commun.* **2017**, 7, 375.
- [253] Y. Min, Y. Liu, Y. Poojari, J.-C. Wu, B. E. Hildreth III, T. J. Rosol, A. J. Epstein, *Synth. Met.* **2014**, 198, 308.
- [254] A. G. Guex, J. L. Puetzer, A. Armgarth, E. Littmann, E. Stavrinidou, E. P. Giannelis, G. G. Malliaras, M. M. Stevens, *Acta Biomater.* **2017**, 62, 91.
- [255] L. Tayebi, A. Shahini, M. Yazdimamaghani, K. J. Walker, M. Eastman, H. Hatami-Marbini, B. Smith, J. L. Ricci, S. Madhally, D. Vashaea, *Int. J. Nanomed.* **2013**, 9, 167.
- [256] S. Tsukada, H. Nakashima, K. Torimitsu, *PLoS One* **2012**, 7, e33689.
- [257] Y. Kim, T. Lim, C.-H. Kim, C. S. Yeo, K. Seo, S.-M. Kim, J. Kim, S. Y. Park, S. Ju, M.-H. Yoon, *NPG Asia Mater* **2018**, 10, 1086.
- [258] L. H. Jimison, S. A. Tria, D. Khodagholy, M. Gurfinkel, E. Lanzarini, A. Hama, G. G. Malliaras, R. M. Owens, *Adv. Mater.* **2012**, 24, 5919.
- [259] J. Rivnay, M. Ramuz, P. Leleux, A. Hama, M. Huerta, R. M. Owens, *Appl. Phys. Lett.* **2015**, 106, 043301.
- [260] S. Tria, L. H. Jimison, A. Hama, M. Bongo, R. M. Owens, *Biosensors* **2013**, 3, 44.
- [261] D. Gentili, P. D'Angelo, F. Militano, R. Mazzei, T. Poerio, M. Bruciale, G. Tarabella, S. Bonetti, S. L. Marasso, M. Cocuzza, L. Giorno, S. Iannotta, M. Civalini, *J. Mater. Chem. B* **2018**, 6, 5400.
- [262] P. Leleux, J. Rivnay, T. Lonjaret, J.-M. Badier, C. Bénar, T. Hervé, P. Chauvel, G. G. Malliaras, *Adv. Healthcare Mater.* **2015**, 4, 142.
- [263] A. Campana, T. Cramer, D. T. Simon, M. Berggren, F. Biscarini, *Adv. Mater.* **2014**, 26, 3874.
- [264] H. Lee, S. Lee, W. Lee, T. Yokota, K. Fukuda, T. Someya, *Adv. Funct. Mater.* **2019**, 29, 1906982.
- [265] O. Parlak, S. T. Keene, A. Marais, V. F. Curto, A. Salleo, *Sci. Adv.* **2018**, 4, 2904.
- [266] E. Bihar, Y. Deng, T. Miyake, M. Saadaoui, G. G. Malliaras, M. Rolandi, *Sci. Rep.* **2016**, 6, 27582.
- [267] M. Berto, C. Diacchi, L. Theuer, M. D. Lauro, D. T. Simon, M. Berggren, F. Biscarini, V. Beni, C. A. Bortolotti, *Flexible Printed Electron.* **2018**, 3, 024001.
- [268] L. Chen, Y. Fu, N. Wang, A. Yang, Y. Li, J. Wu, H. Ju, F. Yan, *ACS Appl. Mater. Interfaces* **2018**, 10, 18470.
- [269] Y. Fu, N. Wang, A. Yang, H. K. Law, L. Li, F. Yan, *Adv. Mater.* **2017**, 29, 1703787.
- [270] M. Ramuz, A. Hama, J. Rivnay, P. Leleux, R. M. Owens, *J. Mater. Chem. B* **2015**, 3, 5971.
- [271] V. F. Curto, B. Marchiori, A. Hama, A.-M. Pappa, M. P. Ferro, M. Braendlein, J. Rivnay, M. Fiocchi, G. G. Malliaras, M. Ramuz, R. M. Owens, *Microsyst. Nanoeng.* **2017**, 3, 17028.
- [272] D. Khodagholy, J. Rivnay, M. Sessolo, M. Gurfinkel, P. Leleux, L. H. Jimison, E. Stavrinidou, T. Herve, S. Sanaur, R. M. Owens, G. G. Malliaras, *Nat. Commun.* **2013**, 4, 2133.
- [273] K. Xie, N. Wang, X. Lin, Z. Wang, X. Zhao, P. Fang, H. Yue, J. Kim, J. Luo, S. Cui, F. Yan, P. Shi, *eLife* **2020**, 9, e50345.
- [274] E. Macchia, K. Manoli, B. Holzer, C. Di Franco, R. A. Picca, N. Cioffi, G. Scamarcio, G. Palazzo, L. Torsi, *Anal. Bioanal. Chem.* **2019**, 411, 4899.
- [275] C. Diacchi, M. Berto, M. Di Lauro, E. Bianchini, M. Pinti, D. T. Simon, F. Biscarini, C. A. Bortolotti, *Biointerphases* **2017**, 12, 05F401.

- [276] E. Macchia, L. Sarcina, R. A. Picca, K. Manoli, C. Di Franco, G. Scamarcio, L. Torsi, *Anal. Bioanal. Chem.* **2020**, 412, 811.
- [277] S. K. Sailapu, E. Macchia, I. Merino-Jimenez, J. P. Esquivel, L. Sarcina, G. Scamarcio, S. D. Munteer, L. Torsi, N. Sabaté, *Biosens. Bioelectron.* **2020**, 156, 112103.
- [278] G. Palazzo, D. D. Tullio, M. Magliulo, A. Mallardi, F. Intranuovo, M. Y. Mulla, P. Favia, I. Vikholm-Lundin, L. Torsi, *Adv. Mater.* **2015**, 27, 911.
- [279] K. Manoli, G. Palazzo, E. Macchia, A. Tiwari, C. D. Franco, G. Scamarcio, P. Favia, A. Mallardi, L. Torsi, *Organic Sensors and Bioelectronics X*, SPIE, Bellingham, Washington USA, Vol. 10364 **2017**.
- [280] T. Cramer, B. Chelli, M. Murgia, M. Barbalinardo, E. Bystrenova, D. M. de Leeuw, F. Biscarini, *Phys. Chem. Chem. Phys.* **2013**, 15, 3897.
- [281] K. Nagamine, T. Mano, R. Shiwaku, H. Furusawa, H. Matsui, D. Kumaki, S. Tokito, *Sens. Mater.* **2019**, 31, 1205.
- [282] Y. Jang, M. Jang, H. Kim, S. J. Lee, E. Jin, J. Y. Koo, I.-C. Hwang, Y. Kim, Y. H. Ko, I. Hwang, J. H. Oh, K. Kim, *Chem* **2017**, 3, 641.
- [283] A. Williamson, M. Ferro, P. Leleux, E. Ismailova, A. Kaszas, T. Doublet, P. Quilichini, J. Rivnay, B. Rözsa, G. Katona, C. Bernard, G. G. Malliaras, *Adv. Mater.* **2015**, 27, 4405.
- [284] D. T. Simon, S. Kurup, K. C. Larsson, R. Hori, K. Tybrandt, M. Goiny, E. W. H. Jager, M. Berggren, B. Canlon, A. Richter-Dahlfors, *Nat. Mater.* **2009**, 8, 742.
- [285] A. Williamson, J. Rivnay, L. Kergoat, A. Jonsson, S. Inal, I. Uguz, M. Ferro, A. Ivanov, T. A. Sjöström, D. T. Simon, M. Berggren, G. G. Malliaras, C. Bernard, *Adv. Mater.* **2015**, 27, 3138.
- [286] A. Jonsson, S. Inal, I. Uguz, A. J. Williamson, L. Kergoat, J. Rivnay, D. Khodagholy, M. Berggren, C. Bernard, G. G. Malliaras, D. T. Simon, *Proc. Natl. Acad. Sci. USA* **2016**, 113, 9440.
- [287] K. Tybrandt, K. C. Larsson, S. Kurup, D. T. Simon, P. Kjäll, J. Isaksson, M. Sandberg, E. W. H. Jager, A. Richter-Dahlfors, M. Berggren, *Adv. Mater.* **2009**, 21, 4442.
- [288] E. O. Gabrielsson, A. Armgarth, P. Hammarström, K. P. R. Nilsson, M. Berggren, *Macromol. Mater. Eng.* **2016**, 301, 359.
- [289] D. J. Poxson, E. O. Gabrielsson, A. Bonisoli, U. Linderhed, T. Abrahamsson, I. Matthiesen, K. Tybrandt, M. Berggren, D. T. Simon, *ACS Appl. Mater. Interfaces* **2019**, 11, 14200.
- [290] A. Jonsson, T. A. Sjöström, K. Tybrandt, M. Berggren, D. T. Simon, *Sci. Adv.* **2016**, 2, 1601340.
- [291] K. Tybrandt, *Soft Matter* **2017**, 13, 8171.
- [292] C. M. Proctor, I. Uguz, A. Slezia, V. Curto, S. Inal, A. Williamson, G. G. Malliaras, *Adv. Biosyst.* **2019**, 3, 1800270.
- [293] V. Benfenati, N. Martino, M. R. Antognazza, A. Pistone, S. Toffanin, S. Ferroni, G. Lanzani, M. Muccini, *Adv. Healthcare Mater.* **2014**, 3, 392.
- [294] M. S. Ejneby, L. Migliaccio, M. Gicevičius, V. Đerek, M. Jakešová, F. Elinder, E. D. Głowacki, *Adv. Mater. Technol.* **2020**, 5, 1900860.
- [295] P. Feyen, E. Colombo, D. Endeman, M. Nova, L. Laudato, N. Martino, M. R. Antognazza, G. Lanzani, F. Benfenati, D. Ghezzi, *Sci. Rep.* **2016**, 6, 22718.
- [296] L. Ferlauto, M. J. I. A. Leccardi, N. A. L. Chenais, S. C. A. Gilliéron, P. Vagni, M. Bevilacqua, T. J. Wolfensberger, K. Sivula, D. Ghezzi, *Nat. Commun.* **2018**, 9, 992.
- [297] M. R. Antognazza, M. D. Paolo, D. Ghezzi, M. Mete, S. D. Marco, J. F. Maya-Vetencourt, R. Maccarone, A. Desii, F. D. Fonzo, M. Bramini, A. Russo, L. Laudato, I. Donelli, M. Cilli, G. Freddi, G. Pertile, G. Lanzani, S. Bisti, F. Benfenati, *Adv. Healthcare Mater.* **2016**, 5, 2271.
- [298] K. Myny, E. van Veenendaal, G. H. Gelinck, J. Genoe, W. Dehaene, P. Heremans, *IEEE J. Solid-State Circuits* **2012**, 47, 284.
- [299] D. Khodagholy, M. Gurfinkel, E. Stavrinidou, P. Leleux, T. Herve, S. Sanaur, G. G. Malliaras, *Appl. Phys. Lett.* **2011**, 99, 163304.
- [300] T. Someya, T. Sekitani, S. Iba, Y. Kato, H. Kawaguchi, T. Sakurai, *Proc. Natl. Acad. Sci. USA* **2004**, 101, 9966.
- [301] C. Dincer, R. Bruch, A. Kling, S. Dittrich, G. A. Urban, *Trends Biotechnol.* **2017**, 35, 728.
- [302] D. T. Simon, E. O. Gabrielsson, K. Tybrandt, M. Berggren, *Chem. Rev.* **2016**, 116, 13009.
- [303] L. Kergoat, L. Herlogsson, D. Braga, B. Piro, M. C. Pham, X. Crispin, M. Berggren, G. Horowitz, *Adv. Mater.* **2010**, 22, 2565.
- [304] L. Kergoat, B. Piro, M. Berggren, G. Horowitz, M.-C. Pham, *Anal. Bioanal. Chem.* **2012**, 402, 1813.
- [305] D. Wang, V. Noël, B. Piro, *Electronics* **2016**, 5, 9.
- [306] B. Nketia-Yawson, Y.-Y. Noh, *Adv. Funct. Mater.* **2018**, 28, 1802201.
- [307] M. L. Hammock, O. Knopfmacher, B. D. Naab, J. B.-H. Tok, Z. Bao, *ACS Nano* **2013**, 7, 3970.
- [308] T. Arbring Sjöström, M. Berggren, E. O. Gabrielsson, P. Janson, D. J. Poxson, M. Seitanidou, D. T. Simon, *Adv. Mater. Technol.* **2018**, 3, 1700360.
- [309] J. Isaksson, P. Kjäll, D. Nilsson, N. Robinson, M. Berggren, A. Richter-Dahlfors, *Nat. Mater.* **2007**, 6, 673.
- [310] D. T. Simon, E. W. H. Jager, K. Tybrandt, K. C. Larsson, S. Kurup, A. Richter-Dahlfors, M. Berggren, *TRANSDUCERS 2009—2009 Int. Conf. on Solid-State Sensors, Actuators, and Microsystems*, IEEE, Denver, CO, USA **2009**, pp. 1790–1793.
- [311] T. A. Sjöström, A. Jonsson, E. O. Gabrielsson, M. Berggren, D. T. Simon, K. Tybrandt, *Adv. Mater. Technol.* **2020**, 5, 1900750.
- [312] L. Zhou, K. Wang, H. Sun, S. Zhao, X. Chen, D. Qian, H. Mao, J. Zhao, *Nano-Micro Lett.* **2019**, 11, 20.
- [313] I. Uguz, M. Ganji, A. Hama, A. Tanaka, S. Inal, A. Youssef, R. M. Owens, P. P. Quilichini, A. Ghestem, C. Bernard, S. A. Dayeh, G. G. Malliaras, *Adv. Healthcare Mater.* **2016**, 5, 3094.
- [314] S. Kim, J.-O. Jeong, S. Lee, J.-S. Park, H.-J. Gwon, S. I. Jeong, J. G. Hardy, Y.-M. Lim, J. Y. Lee, *Sci. Rep.* **2018**, 8, 3721.
- [315] P. Leleux, C. Johnson, X. Strakosas, J. Rivnay, T. Hervé, R. M. Owens, G. G. Malliaras, *Adv. Healthcare Mater.* **2014**, 3, 1377.
- [316] J. Rivnay, P. Leleux, M. Ferro, M. Sessolo, A. Williamson, D. A. Koutsouras, D. Khodagholy, M. Ramuz, X. Strakosas, R. M. Owens, C. Benar, J.-M. Badier, C. Bernard, G. G. Malliaras, *Sci. Adv.* **2015**, 1, 1400251.
- [317] A. J. Casson, *Biomed. Eng. Lett.* **2019**, 9, 53.
- [318] Y. N. Kalia, A. Naik, J. Garrison, R. H. Guy, *Adv. Drug Delivery Rev.* **2004**, 56, 619.
- [319] Y. Ogawa, K. Kato, T. Miyake, K. Nagamine, T. Ofuji, S. Yoshino, M. Nishizawa, *Adv. Healthcare Mater.* **2015**, 4, 506.
- [320] N. G. Hatsopoulos, J. P. Donoghue, *Annu. Rev. Neurosci.* **2009**, 32, 249.
- [321] D. R. Merrill, M. Bikson, J. G. R. Jefferys, *J. Neurosci. Methods* **2005**, 141, 171.
- [322] S. F. Cogan, *Annu. Rev. Biomed. Eng.* **2008**, 10, 275.
- [323] M. Sessolo, D. Khodagholy, J. Rivnay, F. Maddalena, M. Gleyzes, E. Steidl, B. Buisson, G. G. Malliaras, *Adv. Mater.* **2013**, 25, 2135.
- [324] R. Green, M. R. Abidian, *Adv. Mater.* **2015**, 27, 7620.
- [325] S. E. Moulton, M. J. Higgins, R. M. I. Kapsa, G. G. Wallace, *Adv. Funct. Mater.* **2012**, 22, 2003.
- [326] A. E. Rochford, A. Carnicer-Lombarte, V. F. Curto, G. G. Malliaras, D. G. Barone, *Adv. Mater.* **2020**, 32, 1903182.
- [327] D. Khodagholy, T. Doublet, M. Gurfinkel, P. Quilichini, E. Ismailova, P. Leleux, T. Herve, S. Sanaur, C. Bernard, G. G. Malliaras, *Adv. Mater.* **2011**, 23, H268.
- [328] D. Khodagholy, T. Doublet, P. Quilichini, M. Gurfinkel, P. Leleux, A. Ghestem, E. Ismailova, T. Hervé, S. Sanaur, C. Bernard, G. G. Malliaras, *Nat. Commun.* **2013**, 4, 1575.
- [329] A. Jonsson, Z. Song, D. Nilsson, B. A. Meyerson, D. T. Simon, B. Linderth, M. Berggren, *Sci. Adv.* **2015**, 1, e1500039.

- [330] C. M. Proctor, A. Slézia, A. Kaszas, A. Ghestem, I. del Agua, A. M. Pappa, C. Bernard, A. Williamson, G. G. Malliaras, *Sci. Adv.* **2018**, *4*, 1291.
- [331] X. Navarro, T. B. Krueger, N. Lago, S. Micera, T. Stieglitz, P. Dario, *J. Peripher. Nerv. Syst.* **2005**, *10*, 229.
- [332] K. Birmingham, V. Gradinaru, P. Anikeeva, W. M. Grill, V. Pikov, B. McLaughlin, P. Pasricha, D. Weber, K. Ludwig, K. Famm, *Nat. Rev. Drug Discovery* **2014**, *13*, 399.
- [333] V. Giagka, W. A. Serdijn, *Bioelectron. Med.* **2018**, *4*, 8.
- [334] P. Sanjuan-Alberte, F. J. Rawson, *Ther. Delivery* **2019**, *10*, 139.
- [335] M. K. Kwan, E. J. Wall, J. Massie, S. R. Garfin, *Acta Orthop. Scand.* **1992**, *63*, 267.
- [336] C. E. Larson, E. Meng, *J. Neurosci. Methods* **2020**, *332*, 108523.
- [337] B. S. Spearman, V. H. Desai, S. Mobini, M. D. McDermott, J. B. Graham, K. J. Otto, J. W. Judy, C. E. Schmidt, *Adv. Funct. Mater.* **2018**, *28*, 1701713.
- [338] P. Schönle, F. Michoud, N. Brun, A. Guex, S. P. Lacour, Q. Wang, Q. Huang, *2016 38th Annual Int. Conf. of the IEEE Engineering in Medicine and Biology Society (EMBC)*, IEEE, Piscataway, NJ **2016**, pp. 4439–4442.
- [339] C. A. R. Chapman, K. Aristovich, M. Donega, C. T. Fjordbakk, T.-R. Stathopoulou, J. Viscasillas, J. Avery, J. D. Perkins, D. Holder, *J. Neural Eng.* **2019**, *16*, 016001.
- [340] A. Barriga-Rivera, L. Bareket, J. Goding, U. A. Aregueta-Robles, G. J. Suaning, *Front. Neurosci.* **2017**, *11*, 620.
- [341] N. Barnes, A. F. Scott, P. Lieby, M. A. Petoe, C. McCarthy, A. Stacey, L. N. Ayton, N. C. Sinclair, M. N. Shivdasani, N. H. Lovell, H. J. McDermott, J. G. W. and, *J. Neural Eng.* **2016**, *13*, 036013.
- [342] R. A. Green, P. B. Matteucci, R. T. Hassarati, B. Giraud, C. W. D. Dodds, S. Chen, P. J. Byrnes-Preston, G. J. Suaning, L. A. Poole-Warren, N. H. Lovell, *J. Neural Eng.* **2013**, *10*, 016009.
- [343] N. Martino, D. Ghezzi, F. Benfenati, G. Lanzani, M. R. Antognazza, *J. Mater. Chem. B* **2013**, *1*, 3768.
- [344] J. F. Maya-Vetencourt, D. Ghezzi, M. R. Antognazza, E. Colombo, M. Mete, P. Feyen, A. Desii, A. Buschiazio, M. Di Paolo, S. Di Marco, F. Ticconi, L. Emionite, D. Shmal, C. Marini, I. Donelli, G. Freddi, R. Maccarone, S. Bisti, G. Sambuceti, G. Pertile, G. Lanzani, F. Benfenati, *Nat. Mater.* **2017**, *16*, 681.
- [345] M. J. Foggia, R. V. Quevedo, M. R. Hansen, *Laryngoscope Invest. Otolaryngol.* **2019**, *4*, 678.
- [346] Q. Zhang, S. Beirne, K. Shu, D. Esrafilzadeh, X.-F. Huang, G. G. Wallace, *Sci. Rep.* **2018**, *8*, 9855.
- [347] S.-M. Kim, N. Kim, Y. Kim, M.-S. Baik, M. Yoo, D. Kim, W.-J. Lee, D.-H. Kang, S. Kim, K. Lee, M.-H. Yoon, *NPG Asia Mater* **2018**, *10*, 255.
- [348] Z. Liu, L. Dong, L. Wang, X. Wang, K. Cheng, Z. Luo, W. Weng, *Sci. Rep.* **2017**, *7*, 17926.
- [349] F. Lodola, V. Rosti, G. Tullii, A. Desii, L. Tapella, P. Catarsi, D. Lim, F. Moccia, M. R. Antognazza, *Sci. Adv.* **2019**, *5*, 4620.
- [350] M. Sytnyk, M. Jakešová, M. Litviňuková, O. Mashkov, D. Kriegner, J. Stangl, J. Nebesářová, F. W. Fecher, W. Schöfberger, N. S. Sariciftci, R. Schindl, W. Heiss, E. D. Głowacki, *Nat. Commun.* **2017**, *8*, 91.
- [351] C. Dai, B. Liu, *Energy Environ. Sci.* **2020**, *13*, 24.
- [352] B. Srinivasan, A. R. Kolli, M. B. Esch, H. E. Abaci, M. L. Shuler, J. J. Hickman, *J. Lab. Autom.* **2015**, *20*, 107.
- [353] X. Strakosas, M. Huerta, M. J. Donahue, A. Hama, A.-M. Pappa, M. Ferro, M. Ramuz, J. Rivnay, R. M. Owens, *J. Appl. Polym. Sci.* **2017**, *134*, 44483.
- [354] D. A. Koutsouras, P. Gkoupidenis, C. Stolz, V. Subramanian, G. G. Malliaras, D. C. Martin, *ChemElectroChem* **2017**, *4*, 2321.
- [355] Y. Zhang, J. Li, R. Li, D.-T. Sbircea, A. Giovannitti, J. Xu, H. Xu, G. Zhou, L. Bian, I. McCulloch, N. Zhao, *ACS Appl. Mater. Interfaces* **2017**, *9*, 38687.
- [356] S. N. Bhatia, D. E. Ingber, *Nat. Biotechnol.* **2014**, *32*, 760.
- [357] E. Macchia, K. Manoli, B. Holzer, C. Di Franco, M. Ghittorelli, F. Torricelli, D. Alberga, G. F. Mangiatordi, G. Palazzo, G. Scamarcio, L. Torsi, *Nat. Commun.* **2018**, *9*, 3223.
- [358] R. S. Khan, Z. Khurshid, F. Yahya Ibrahim Asiri, *Diagnostics* **2017**, *7*, 39.
- [359] H. Mashir, R. A. Dweik, *Adv. Powder Technol.* **2009**, *20*, 420.
- [360] J. Freudenberg, F. Hinkel, D. Jänsch, U. H. F. Bunz, *Top. Curr. Chem.* **2017**, *375*, 67.
- [361] A. Babayan, K. Pantel, *Genome Med* **2018**, *10*, 21.
- [362] A. Bardelli, K. Pantel, *Cancer Cell* **2017**, *31*, 172.
- [363] J. Kaiser, *Science* **2018**, *359*, 259.
- [364] S. Alimirzaie, M. Bagherzadeh, M. R. Akbari, *Clin. Genet.* **2019**, *95*, 643.
- [365] M. Giordani, M. Berto, M. Di Lauro, C. A. Bortolotti, M. Zoli, F. Biscarini, *ACS Sens.* **2017**, *2*, 1756.
- [366] H. U. Khan, M. E. Roberts, O. Johnson, R. Förch, W. Knoll, Z. Bao, *Adv. Mater.* **2010**, *22*, 4452.
- [367] P. Lin, X. Luo, I.-M. Hsing, F. Yan, *Adv. Mater.* **2011**, *23*, 4035.
- [368] L. Jagannathan, V. Subramanian, *Biosens. Bioelectron.* **2009**, *25*, 288.
- [369] Q. Zhang, V. Subramanian, *2007 IEEE Int. Electron Devices Meeting*, IEEE, Piscataway, New Jersey, US **2007**.
- [370] G. Dijk, A. L. Rutz, G. G. Malliaras, *Adv. Mater. Technol.* **2020**, *5*, 1900662.
- [371] H. Bronstein, Z. Chen, R. S. Ashraf, W. Zhang, J. Du, J. R. Durrant, P. Shakya Tuladhar, K. Song, S. E. Watkins, Y. Geerts, M. M. Wienk, R. A. J. Janssen, T. Anthopoulos, H. Sirringhaus, M. Heeney, I. McCulloch, *J. Am. Chem. Soc.* **2011**, *133*, 3272.
- [372] J. P. K. Armstrong, M. M. Stevens, *Tissue Eng., Part A* **2019**, *25*, 688.
- [373] K. Tybrandt, R. Forchheimer, M. Berggren, *Nat. Commun.* **2012**, *3*, 871.
- [374] C. M. Boutry, L. Beker, Y. Kaizawa, C. Vassos, H. Tran, A. C. Hinckley, R. Pfattner, S. Niu, J. Li, J. Claverie, Z. Wang, J. Chang, P. M. Fox, Z. Bao, *Nat. Biomed. Eng.* **2019**, *3*, 47.
- [375] S. Gupta, W. T. Navaraj, L. Lorenzelli, R. Dahiya, *Npj Flexible Electron.* **2018**, *2*, 8.
- [376] H. Fang, K. J. Yu, C. Gloschat, Z. Yang, E. Song, C.-H. Chiang, J. Zhao, S. M. Won, S. Xu, M. Trumpis, Y. Zhong, S. W. Han, Y. Xue, D. Xu, S. W. Choi, G. Cauwenberghs, M. Kay, Y. Huang, J. Viventi, I. R. Efimov, J. A. Rogers, *Nat. Biomed. Eng.* **2017**, *1*, 0038.
- [377] Y. Choi, J. Koo, J. A. Rogers, *MRS Bull.* **2020**, *45*, 103.
- [378] L. Yang, Y. Li, Y. Fang, *Adv. Mater.* **2013**, *25*, 3881.
- [379] S. G. Higgins, M. Becce, A. Belessiotis-Richards, H. Seong, J. E. Sero, M. M. Stevens, *Adv. Mater.* **2020**, *32*, 1903862.
- [380] S. M. Wellman, J. R. Eles, K. A. Ludwig, J. P. Seymour, N. J. Michelson, W. E. McFadden, A. L. Vazquez, T. D. Y. Kozai, *Adv. Funct. Mater.* **2018**, *28*, 1701269.
- [381] C. F. Guimarães, L. Gasperini, A. P. Marques, R. L. Reis, *Nat. Rev. Mater.* **2020**, *5*, 351.
- [382] I. Sahalianov, S. K. Singh, K. Tybrandt, M. Berggren, I. Zozoulenko, *RSC Adv.* **2019**, *9*, 42498.
- [383] C. Boehler, Z. Aqrave, M. Asplund, *Bioelectron. Med.* **2019**, *2*, 89.
- [384] C. S. Wood, M. R. Thomas, J. Budd, T. P. Mashamba-Thompson, K. Herbst, D. Pillay, R. W. Peeling, A. M. Johnson, R. A. McKendry, M. M. Stevens, *Nature* **2019**, *566*, 467.



Stuart G. Higgins received his Ph.D. degree in experimental solid-state physics from Imperial College London in 2014. He worked as a Research Associate in the Optoelectronics Group at the Cavendish Laboratory, University of Cambridge from 2015 to 2016. Since 2016 he has been a Research Associate in the Stevens Group at Imperial College London. His current research interests include the microfabrication of biomaterials for biointerfacing applications, and the development of organic semiconductor-based bioelectronic systems.



Molly M. Stevens is Professor of Biomedical Materials and Regenerative Medicine at Imperial College London and Research Director for Biomedical Material Sciences in the Institute of Biomedical Engineering. She is a Foreign Member of the US National Academy of Engineering and a Fellow of eight UK academies, including the Royal Society and the Royal Society of Chemistry where she is President of the Division of Materials Chemistry.